UNIVERSITY OF THESSALY

SCHOOL OF ENGINEERING
DEPARTMENT OF MECHANICAL ENGINEERING

EXPERIMENTAL DETERMINATION OF ELASTIC LIMIT UNDER SHEAR LOADING IN CELLULAR ALUMINUM STRUCTURES

DIMITRIOS TSOGIAS

Supervisor: **Dr. Alexis Kermanidis**

Submitted in partial fulfillment of the requirements for the degree of Diploma in Mechanical Engineering at the University of Thessaly

Volos,2022

Approved by the Committee on Final Examination:

Advisor	**Dr. Alexis Kermanidis**, Associate Professor of Mechanical Behavior of Metallic Materials, Department of Mechanical Engineering, University of Thessaly
Member	**Dr. Nikolaos Aravas**, Professor of Computational Mechanics of Structures, Department of Mechanical Engineering, University of Thessaly
Member	**Dr. Gregory Haidemenopoulos**, Professor of Physical Metallurgy, Department of Mechanical Engineering, University of Thessaly

Acknowledgements

First and foremost, I would like to thank my family for their wise counsels and for supporting me all these years throughout my studies. It would not have been possible to pursue engineering without their continuous support and encouragement.

I express my sincere gratitude to my supervisor Dr. Alexis Kermanidis who patiently assisted me with every problem that I encountered working on this thesis and – with his lectures inspired me to choose this field of engineering and it is important to acknowledge that without his constant support and guidance, I would be lost.

I would also like to thank the members of the committee Dr. Nikolaos Aravas and Dr. Gregory Haidemenopoulos for their time and valuable feedback on this work.

Finally, I must thank my good friends Filippos Katsimalis, Dimitris Petrolekas, Orestis Pliakis and Dimitris Sdrolias who stood by me in times of difficulty from the very beginning of my studies. They gave me extra strength and motivation to keep going and also, they helped me become a better version of myself. For this reason, this thesis is dedicated to them.

EXPERIMENTAL DETERMINATION OF ELASTIC LIMIT UNDER SHEAR LOADING IN CELLULAR ALUMINUM STRUCTURES

Dimitrios Tsogias
Department of Mechanical Engineering, University of Thessaly

Supervisor: **Dr. Alexis Kermanidis**
Associate Professor of Mechanical Behavior of Metallic Materials, Department of Mechanical Engineering, University of Thessaly

Abstract

Hexagonal aluminum honeycomb (cellular aluminum structures) is a hexagonal core product similar to a bee cell. It is often used as a core for "sandwich" composites with many applications in the modern world, such as: Jet aircraft and rocket substructure, electric shielding enclosures, wind turbine blades, energy absorption protective structures, exterior architectural wall panels, boat constructions, automobile and civil structures. It is noticeable that the main fields of its applications are in aerospace, automotive, woodworking industries but it can be found in many other fields as well, from packaging materials to sporting goods like skis and snowboards.

An apt and common question is what are the benefits of using honeycomb structures and why is it widely used in engineering and scientific applications. The main reason and the interesting part are that a honeycomb shaped structure provides a material with minimal density and relatively high compression properties and shear properties. Also, honeycomb's core has several significant advantages, such as: it is lightweight (which implies low cost of production compared to other structures), resistance to stiffness, good fire reaction, corrosion resistance and good energy absorption properties at dynamic collisions.

In this work, shear tests were conducted on honeycomb core specimens of aluminum 5052 for the study and further understanding of its mechanical behavior within the ASTM C273 specification. More specifically, the conditions and the parameters were explored under which the specimen is having an elastic behavior and the critical point-force where the specimen starts to present plastic behavior.

Key words: honeycomb core, sandwich structure, shear stress, elastic behavior, plastic behavior

ΠΕΙΡΑΜΑΤΙΚΗ ΔΙΕΡΕΥΝΗΣΗ ΤΟΥ ΟΡΙΟΥ ΕΛΑΣΤΙΚΟΤΗΤΑΣ ΣΕ ΔΙΑΤΜΗΣΗ ΚΥΨΕΛΟΕΙΔΩΝ ΔΟΜΩΝ ΑΛΟΥΜΙΝΙΟΥ

Δημήτριος Τσόγιας
Τμήμα Μηχανολόγων Μηχανικών, Πανεπιστήμιο Θεσσαλίας

Επιβλέπων: **Δρ. Αλέξης Κερμανίδης**
Αναπληρωτής καθηγητής Μηχανικής Συμπεριφοράς Μεταλλικών Υλικών,
Πανεπιστήμιο Θεσσαλίας

Περίληψη

Η εξαγωνική κυψελοειδής δομή (honeycomb) είναι ένα προιόν εξαγωνικού πυρήνα παρόμοιο με ένα κελί μέλισσας. Συχνά χρησιμοποιείται ως πυρήνας για σύνθετα υλικά τύπου “sandwich” με πολλές εφαρμογές στο σύγχρονο κόσμο, όπως: υποδομές αεριωθούμενων αεροσκάφων και πυραύλων, ηλεκτρικά περιβλήματα θωράκισης, πτερύγια ανεμογεννήτριων, προστατευτικές δομές απορρόφησης ενέργειας, εξωτερικά αρχιτεκτονικά πάνελ τοίχων, κατασκευές σκαφών και αυτοκινήτων και πολεοδομικών δομών. Παρατηρείται οτι τα κύρια πεδία εφαρμογών του ειναι στην αεροδιαστημική, αυτοκινηστική, ξυλουργική βιομηχανία αλλά μπορεί να βρεθεί και σε πολλούς άλλους τομείς, από υλικά συσκευασίας έως αθλητικά είδη όπως ski και snowboard.

Μία εύστοχη και συχνή ερώτηση ειναι ποια ειναι τα οφέλη από τη χρήση κυψελοειδών δομών και γιατί χρησιμοποιούνται ευρέως στη μηχανική και σε επιστημονικές εφαρμογές. Ο κύριος λόγος και το ενδιαφέρον μέρος είναι ότι μια honeycomb δομή παρέχει ένα υλικό με ελάχιστη πυκνότητα και σχετικά υψηλές ιδιότητες σε συμπίεση και ιδιότητες σε διάτμηση. Επίσης, ο πυρήνας του honeycomb έχει αρκετά σημαντικά πλεονεκτήματα, όπως: είναι ελαφρύς (πράγμα που συνεπάγεται χαμηλό κόστος παραγωγής σε σύγκριση με άλλες δομές), αντοχή στη δυσκαμψία, καλή αντίδραση σε εύφλεκτα περιβάλλοντα, αντοχή σε διάβρωση και καλές ιδιοτητες απορρόφησης ενέργειας σε δυναμικές κρούσεις.

Σε αυτή την διπλωματική εργασία, πραγματοποιήθηκαν πειράματα διάτμησης σε δοκίμια με πυρήνα honeycomb από αλουμίνιο σειράς 5052 για τη μελέτη και την περαιτέρω κατανόηση της μηχανικής συμπεριφοράς του, σύμφωνα με τις προδιαγραφές ASTM C273. Ειδικότερα, διερευνήθηκαν οι συνθήκες και οι παράμετροι κάτω από τις οποίες το δοκίμιο έχει ελαστική συμπεριφορά και το κρίσιμο σημείο δύναμης όπου αρχίζει να παρουσιάζει πλαστική συμπεριφορά.

Λέξεις-κλειδιά: πυρήνας honeycomb, δομές sandwich, διατμητικές τάσεις, ελαστική συμπεριφορά, πλαστική συμπεριφορά

Table of Contents

List of Figures

List of Plots

List of Tables

Chapter 1. INTRODUCTION

1.1 Problem description and Research methodology

A common objective in engineering and material science is to create materials with the biggest strength and the minimum weight and minimum amount of materials (minimum cost). Honeycomb sandwich structures are frequently used to achieve these outcomes and over time they are used more and more in mechanical-scientific applications, due to the high stiffness, good resistance and the lightweight structure that they provide. A honeycomb structure material is produced using an array of hollow tubes or cells (honeycomb core) "sandwiched" between two face sheets (solid plates), which most commonly are made of aluminum or carbon fiber reinforced polymer and the adhesive that bonds them together (figure 1.1).

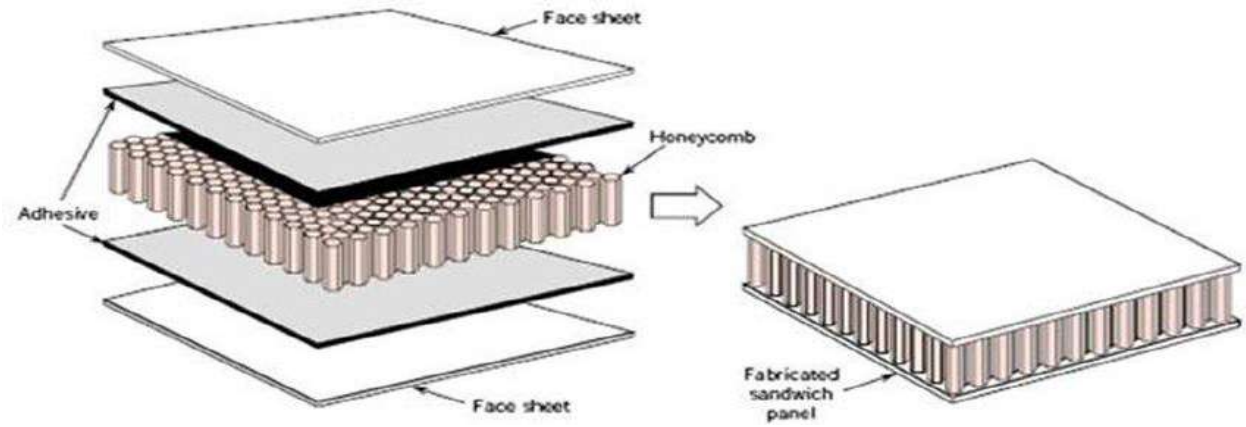

Figure 1.1: Honeycomb sandwich panel construction [1]

The solid plates are designed to carry the bulk of the bending load and honeycomb's core provide resistance in shear loads. With this combination of properties and in a field that is still not fully investigated, it is really interesting to study and understand more about the mechanical behavior of these materials, with the aim of being able to be applied in more technological applications.

The contribution of this thesis work is the experimental study of cellular structures of aluminum series 5052 with loading – unloading stress tests and tests with more cycles in pure shear and providing results about the mechanical behavior of them. The method chosen for these tests was consistent with ASTM specification, and with the help of RWTH Aachen University (comparison of results in different specimens) it was concluded that the experimental results are adequate and accurate, as will be discussed in the following chapters.

Chapter 2. BIBLIOGRAPHIC RESEARCH

2.1 Types of cellular structures

The most common materials, for sandwich panels, for the production of the solid plates are aluminum or carbon fiber reinforced polymer. The core is usually made of foam or honeycomb structures made of aramid paper (e.g., Nomex) or aluminum. The aramid material is a subcategory of heat-resistant and synthetic fiber materials with a hard body. According to investigational experiments and studies (e.g., Aktay, Johnson and Kröplin [2]) Aramid is preferred to be used rather than aluminum because the latter has high susceptibility to corrosion if there is an inflow of moisture.

In this work, aluminum solid plates and aluminum core is used for the experimental tests, but it is advantageous to make a brief reference to the main types of honeycombs composites.

- ALUMINUM HONEYCOMBS
- NOMEX HONEYCOMBS
- THERMOPLASTIC HONEYCOMBS
- STAINLESS STEEL HONEYCOMBS
- FOAM HONEYCOMBS

Figure 2.1: Aluminum honeycomb core

Aluminum honeycombs possess the highest strength and weight ratio and have a mixture of geometric cell shapes and by foil thickness and cell size.

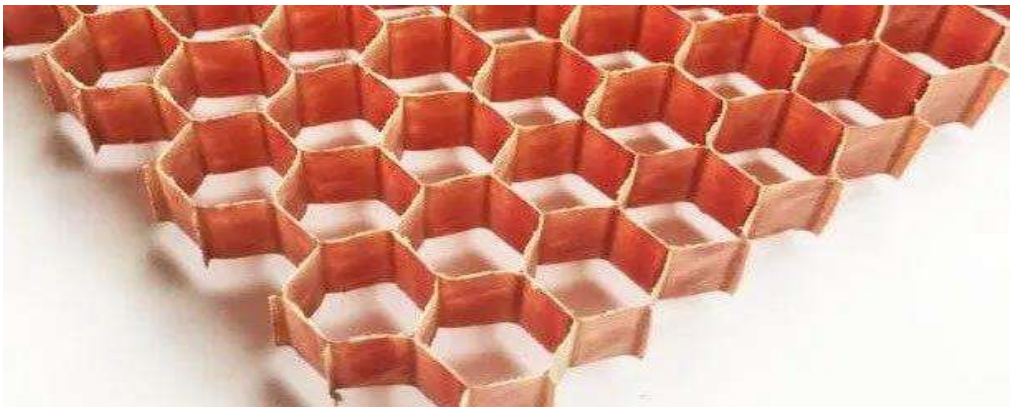

Figure 2.2: Nomex honeycomb core

Nomex honeycombs are manufactured by a type of paper-based on Kevlar fibers which is known as Nomex paper with fire-resistant properties. High strength, solid stability, and low density are the main properties of these cores, nevertheless, compared to other materials they are more expensive.

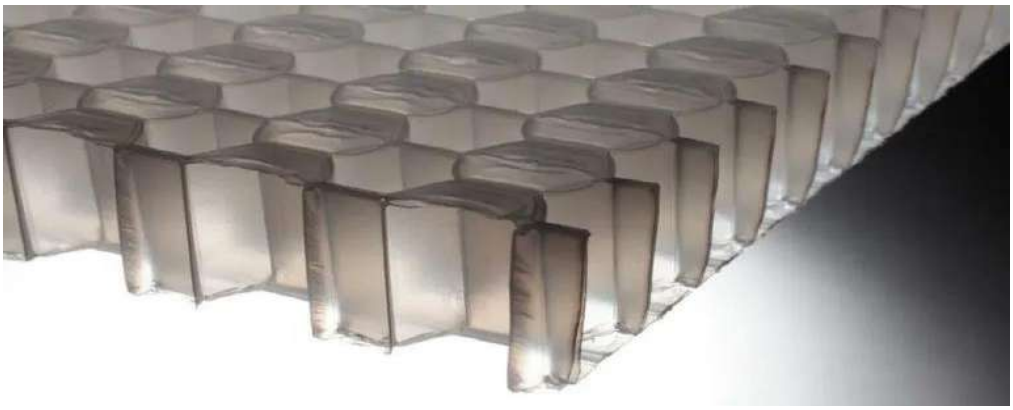

Figure 2.3: Thermoplastic honeycomb core

These cores are recyclable and are lightweight and there are several types of these honeycombs such as;

1.Abs (Acrylonitrile Butadiene Styrene) that offers surface hardness, toughness, rigid structure, dimensional stability and impact resistance.

2. Polycarbonate offers good light transmission, self-extinguishing properties and robust heat resistance.

3.Propylene provides noteworthy chemical resistance.

Figure 2.4: Stainless steel honeycomb core

Stainless steel honeycombs are attributed with perfect moisture and corrosion resistance, fire resistance, fungi resistance. They are used where honeycomb is subjected to hostile environments like bulkheads, train doors and floors i.e.

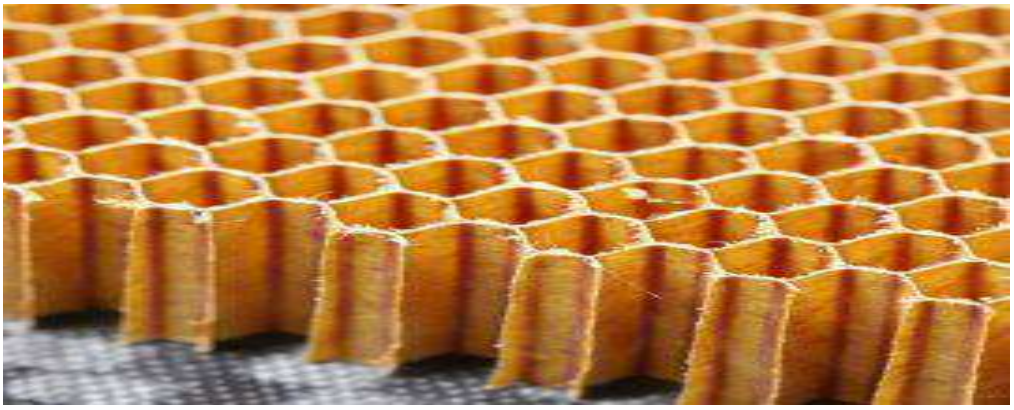

Figure 2.5: Foam honeycomb core

Foams are one of the most common forms of core material. They can be manufactured from a variety of synthetic polymers including polyvinyl chloride (PVC), polystyrene (PS), polyurethane (PU), polymethacrylamide and polyetherimide (PEI), with densities being in the range of 30 $\mathrm{kg/m^3}$ to 300 $\mathrm{kg/m^3}$.

It is also important to mention that depending on the results required and the conditions, there are different cell geometries that are being selected. Some of these geometries are shown in the figure below.

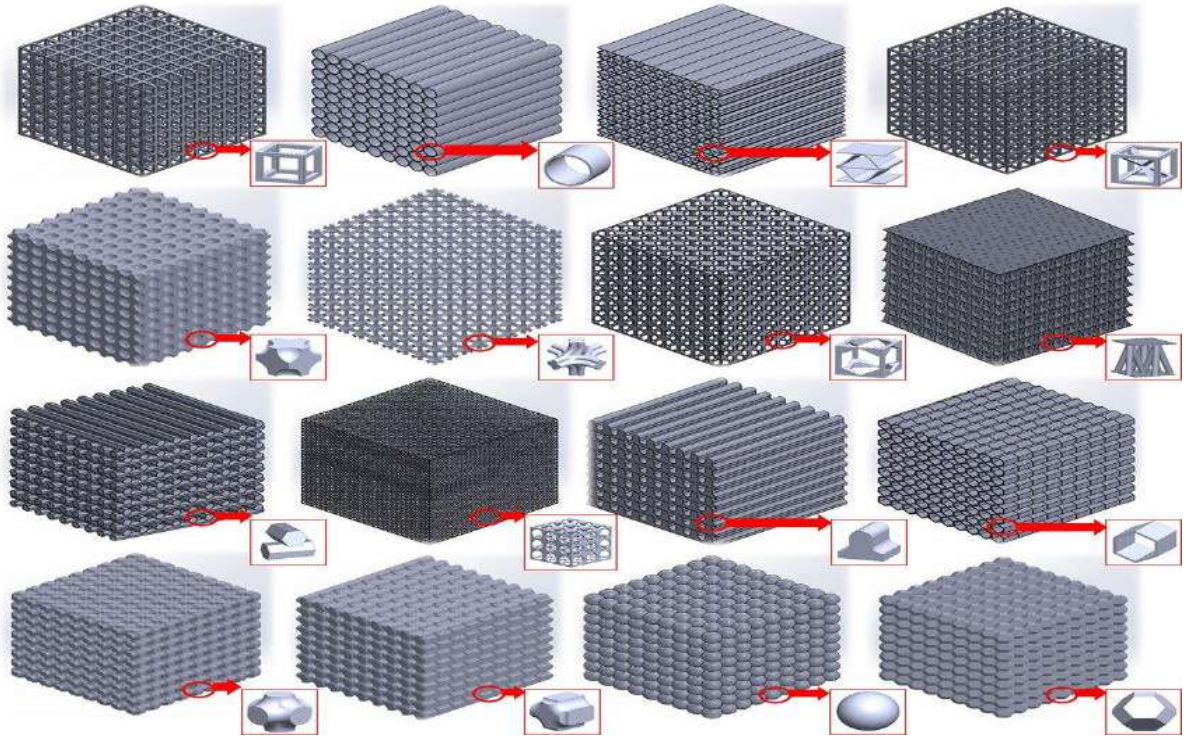

Figure 2.6: Initial sixteen bio-inspired periodic cubic of cellular structures [3]

2.2 Methods of production of aluminum cellular structures

The manufacturing of a honeycomb can be divided in the following five ways: adhesive bonding, resistance welding, brazing, diffusion bonding and thermal fusion. From the aforementioned five ways the most common manufacturing method is adhesive bonding. Adhesive bonding can be achieved with the use of either one of the following methods.

1.Expansion Method

The steps of this method are:
1) Aluminum honeycomb manufacturing begins life as a roll of foil with the required thickness.
2) Foil is passed through a printer for adhesive lines to be printed.
3) Once the lines are printed, the foil is cut to size and stacked into piles using a stacking machine.

4) These stacked sheets are pressed using a heated press to allow the adhesive to cure and bond the sheets of foil together to form a block of honeycomb.
5) The block of honeycomb can be cut into slices with the thickness of the slices being tailored to each customer's individual requirements.
6) Finally, the honeycomb is expanded, which completes the manufacturing process.

The expansion process for honeycomb core manufacturing is depicted in figure 2.7.

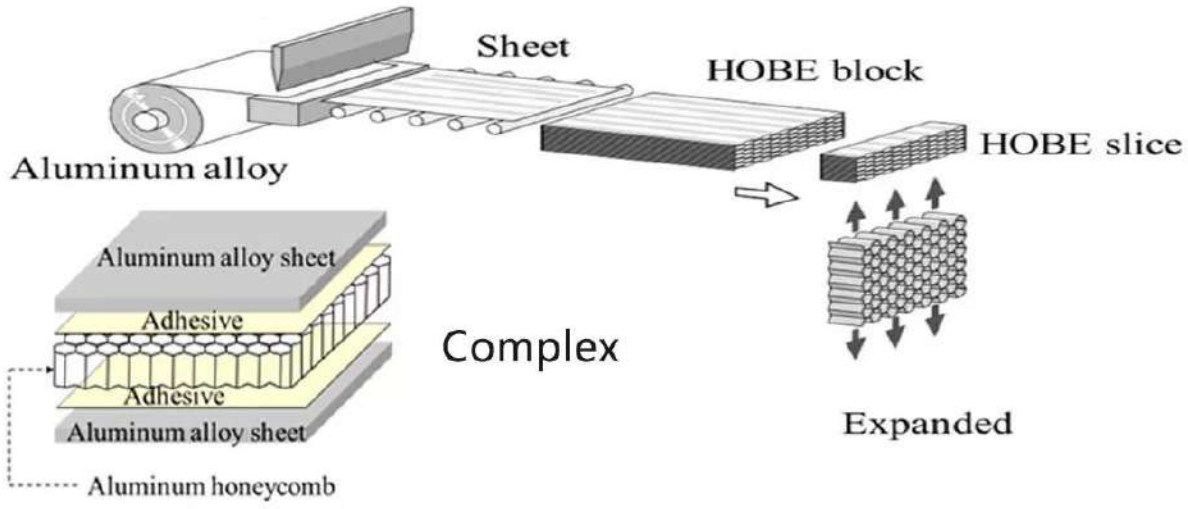

Figure 2.7: Expansion honeycomb core manufacturing method [4]

2. Corrugation Method

The steps of corrugation method are:
1)Aluminum honeycomb manufacturing begins life as a roll of foil with the required thickness.
2) Foil is passed through a corrugated roller (toothed rollers), creating a corrugated sheet.
3) Adhesive is applied to the flat sections of this sheet.
4) Finally, the flat sections of corrugated sheets are then bonded and held together until the adhesive is cured, but also they can be brazed or resistance welded to form a honeycomb core.

This method is preferred for high density cores which cannot be expanded due to thick and strong metallic sheets; therefore it is typically performed for honeycomb cores with a smaller size than those made through the expansion process.
The corrugation process for honeycomb core manufacturing is depicted in figure 2.8.

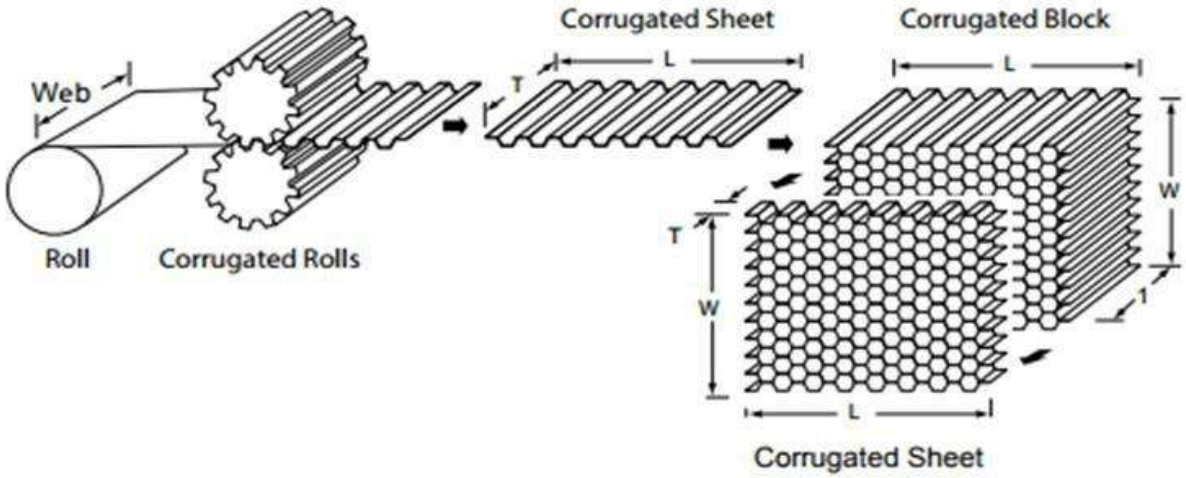

Figure 2.8: Corrugation honeycomb core manufacturing method [4]

2.2.1 Cell features and properties

Some basic terms that are frequently used for honeycomb structures are the following:

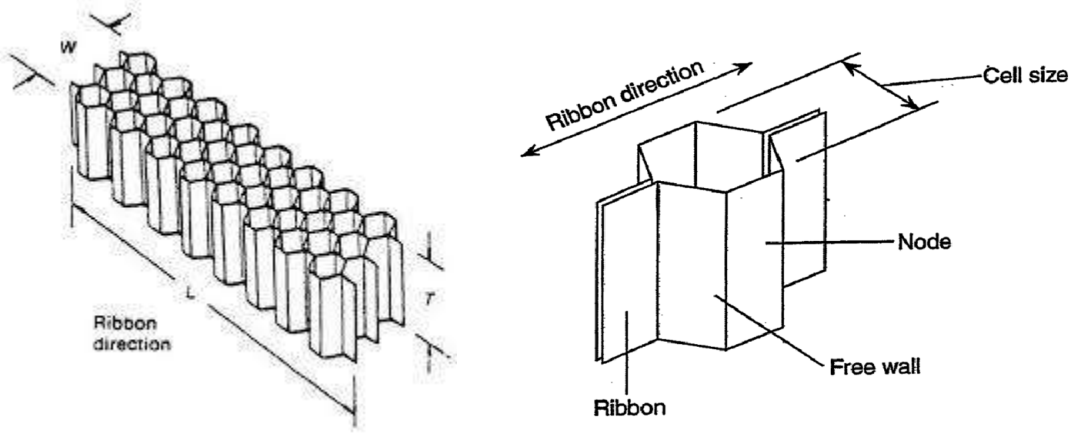

Figure 2.9: Honeycomb features and terminology [4]

- Honeycomb density: weight of one cubic meter of core expressed in kilograms (kg/m^3)
- Cell: a single honeycomb unit
- Cell size: distance between two opposite sides of hexagonal cell

- Ribbon: the flat sheet material constituting the honeycomb
- Node: the bonded portion of adjacent ribbon sheets
- Free wall: cell wall sections of single bonded sheets
- Foil thickness: thickness of free wall
- L direction: the core ribbon direction
- W direction: the core expansion direction
- T direction: the core direction parallel with cell openings
- Honeycomb Before Expansion (HOBE): the solid block of bonded sheets

The mechanical properties of honeycomb are a) stabilized and bare compressive strength, b) stabilized compressive modulus L and W direction, depending on the core's thickness. In the case of energy absorption, application crush strength is considered 50% of bare compressive strength. The change in thickness does not alter the compressive properties and shear modulus, however shear strength decreases with increase in thickness. Table 1 and Table 2 depict Typical mechanical properties for honeycomb core made of aluminum alloys.

Core		Compression		L shear		W shear	
	Density (pcf)	Strength (psi)	Modulus (ksi)	Strength (psi)	Modulus (ksi)	Strength (psi)	Modulus (ksi)
5052 Al	1	55	10	45	12	30	7
5056 Al	1	60	15	55	15	35	7

Table 1: Mechanical properties for honeycomb core made of aluminum alloys 5052, 5056 [4]

Materials	**Aluminium**		
Core	ECM		
Size of the cell (mm)	9.6	6.4	3.2
Densities (Kg/m^3)	55	82	130
Shear strength (L direction) (MPa)	1.48	2.4	5.47
Shear modulus (L direction) (MPa)	253	430	523
Shear strength (W direction) (MPa)	0.88	1.4	3.36
Shear modulus (W direction) (MPa)	170	220	311
Compressive strength (MPa)	2.75	4.5	11.55

Table 2: Mechanical properties for honeycomb core made of aluminum ECM alloys [5]

2.3 Applications

As previously mentioned, sandwich composites with honeycomb core structure are presented in many technological applications that require the combination of satisfactory rigidity and light structure. At this point of this study, it is worth mentioning some examples of aerospace, civil, transportation, automotive applications that use the sandwich composites with honeycomb core.

Rail Sectors

For more than 30 years aluminum honeycomb core material is provided at the rail industry being suitable for coverings, antiskid surfaces, interior panel partitions, doors, floors and furniture. Also in Hitachi Class 800 train project, which has maximum operating speed at 201 km/h (maximum design speed: 225 km/h), aluminum honeycomb was used in the chassis.

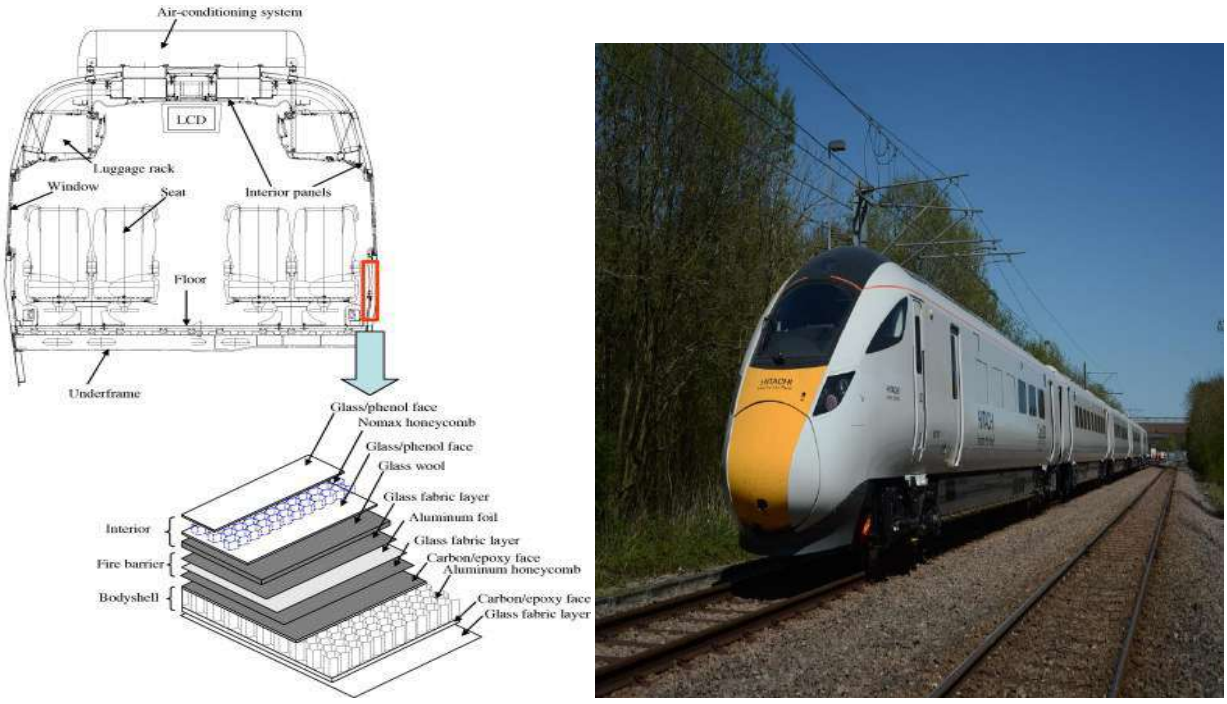

Figure 2.10: a) Train body made of sandwich material, b) Hitachi class 800 train project. [6]

Automotive Sectors

For the reduce of weight but mainly for energy absorption aluminum honeycombs are used in the field of automotive industry. Due to the ability of absorbing forces over a large area and the ability of high strength compared to its weight, it is a great material for energy absorption applications. The cells of the honeycomb are compressed to the point of being folded into one another, when the impact occurs, and the requiring energy for this to happen is equal to the energy which is getting absorbed. This is an efficient method of preventing damage. Also, Negative Stiffness Honeycomb (NHS) structure, shown in figure 2.11, has been developed by Correa et al. [7], which can provide repetitive protection from multiple impacts by recovering its original shape each time after impact. As it can be reused after collision and repeatedly absorb energy, NHS structure has a very high potential in future vehicle applications.

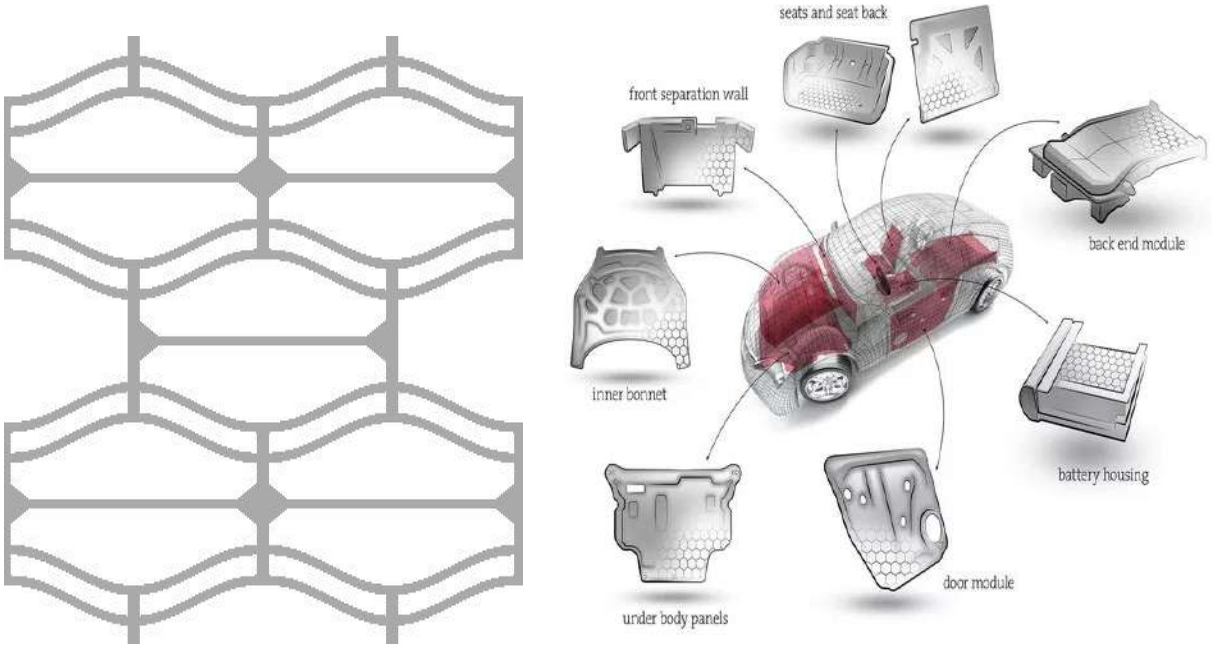

Figure 2.11: a) NSH Structure, b) Body parts of vehicles with hexagonal honeycomb structures [7]

Aerospace Sectors

Finding ways for mass reduction is always a challenge for the Design Engineer. In the Aerospace industry a typical example of this can be found, where every extra kilogram of structural mass cost the Airline operator a huge amount each year. The first use of Honeycomb cores was on aircraft in the 1940s in order to achieve a reduced weight and increased payload and flight distance. They were incorporated into the aircraft design to replace the heavier conventional sheet and stringer or beam support approach, and their incorporation into sandwich panels has been a basic structural concept in the industry since the 1950s. From 2000 till now, the integrity and reliability of honeycomb cores are of vital importance for virtually every aircraft. Some examples of using honeycomb composites in Aerospace industry are shown below in figures 2.12, 2.13.

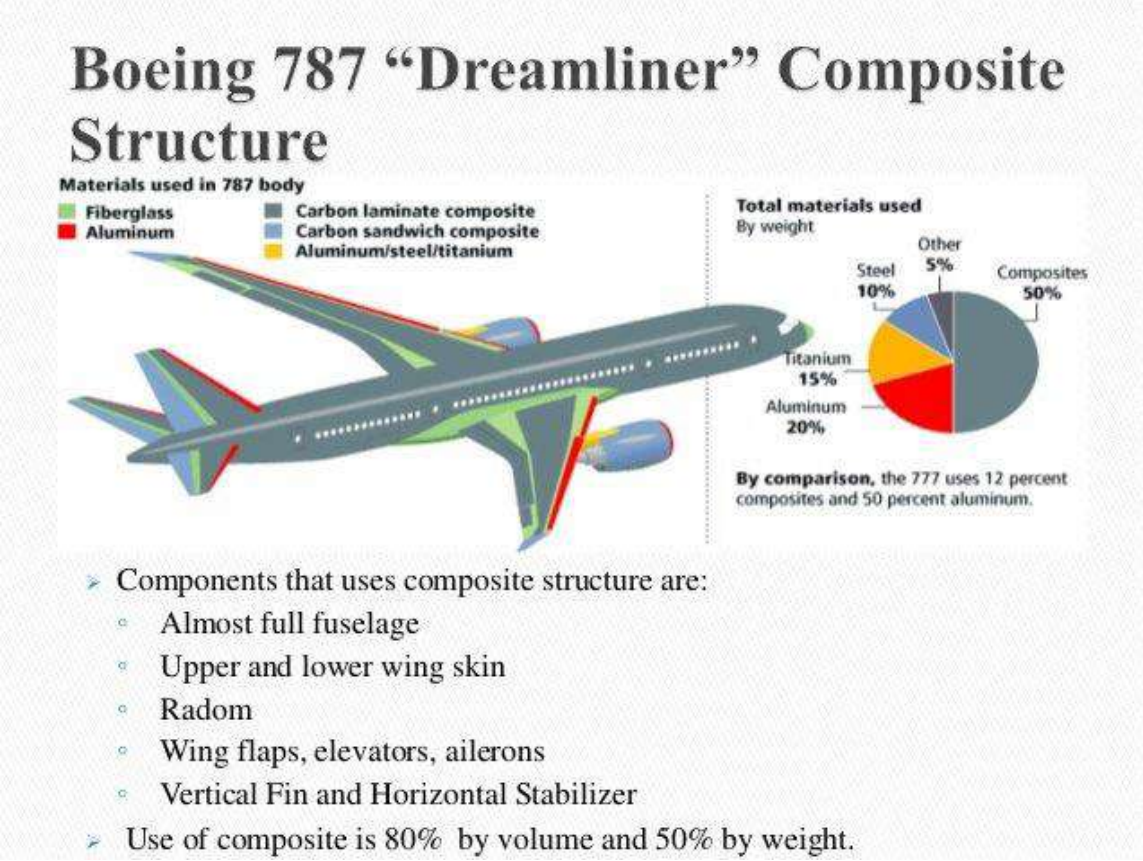

Figure 2.12: Sandwich and composite structures in Boeing 787 [8]

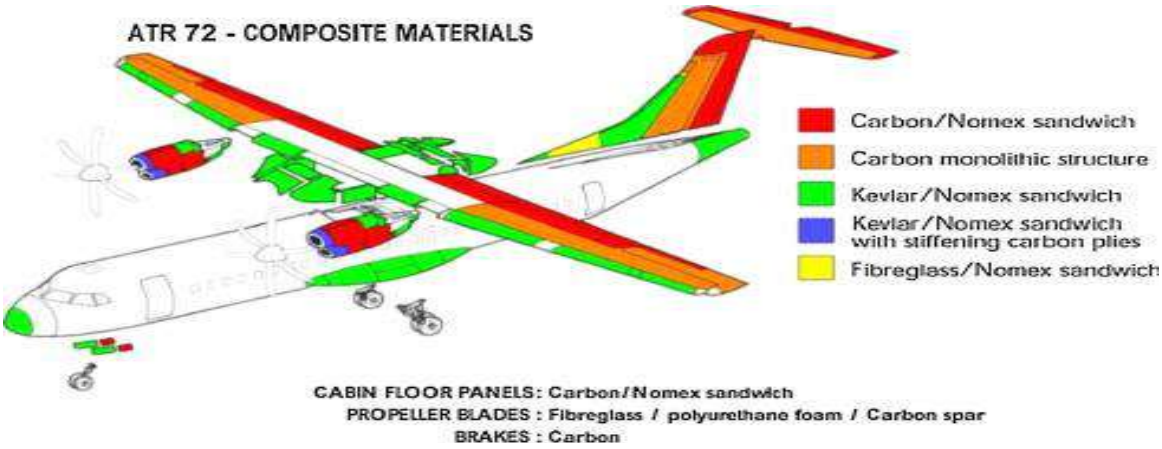

Figure 2.13: ATR 72 composite materials [8]

Civil Sectors

Innovative materials and new techniques are more dominant not only in the aerospace and automotive industries but also in the building industry [9]. Typical example is that in bridge construction. One of the most used group of new materials in bridge design is fiber-reinforced polymer (FPR). A strong and rigid composite material can be created when the different physical and chemical properties, exhibited from the fibers and the matrix are combined together. The production of a wide range of solid and hollow structures with a constant cross section can be applied as bridge beams, deck panels, granting systems, handrails, and so forth. Also, FPRs and other composites provide a greater degree of freedom than other common materials like steel and concrete.

Figure 2.14: Bridge structures that are made of sandwich materials like FPRs and Aluminum

a) Pontresina, Switzerland; b) Lleida, Spain; c) Kolding, Denmark [9]

2.4 Mechanical Behavior of Honeycomb cores – Bibliographic review

Mechanical behavior of cellular type honeycomb structures is being studied thoroughly in the last years in international literature. Some of these researches are presented below:

The scholars Shi-Dong et al. [10] performed shear experiments cellular structures in order to study how this material deforms and fails. They used hexagonal structure Honeycomb of aluminum 5056. It was discovered that the deformation is categorized into four stages:

1) Elastic deformation of the walls
2) Plastic deformation of the walls
3) Failure of the sloping walls and;
4) Detachment of the honeycomb core.

Bianchi Gabriel et al. [11] performed static and shear fatigue experiments as well in hexagonal cell structures. It was attempted to model the structure in a computing environment and it was found that there is no linear correlation between shear strength and imposed load. In fatigue experiments it was concluded that the load direction L has a longer lifespan than in the W direction.

Hodge et al. [12] examined the shear strength of cellular structures with thickness of 35mm. This study was performed in three ways: with percussion, bending and pure shear experiment. It was observed that as the percussive energy was increased the strength of the structure was decreasing. Finally, it was found that the shear strength of bending tests was greater than in the net shear tests.

Liu et al. [13] approached the shear problem in such detail as well as experimentally. The results of the analytical process coincide with the results of the experimental process. It was found out that the measure of shear strength in the horizontal direction is 1.667 times higher than the longitudinal.

Francois Cote et al. [14] constructed and tested shear strength in honeycomb square structures. It has been observed that this structure has isotropic behavior. There was also a difference in

shear strength when the dimensions of the cell changed so it was concluded that the behavior of the structure is correlated to its dimension ratio.

Yang et al. [15] examined the strength of honeycomb structures under compression conditions. The conclusion was that in fully crushing conditions the material can be considered elastic perfect – plastic, while in partial crushing conditions the behavior is considered elastic – plastic and the material hardens after each repetition.

Solmaz et al. [16] studied the behavior of honeycomb material in bending and crushing conditions. It was observed that when the thickness of the outer tile is increased the bending strength is increased as well. Also, when the load exceeded a certain value, there was detachment of the honeycomb core from the walls of the plates.

Wahl Laurent et al. [17] examined the types of hexagonal failures in honeycomb structures. The first type of failure was through shear stresses and the second through a recess in the walls of the core. Pre-existing recess causes bending effects and in the walls of the core that have no initial damage during load enforcement.

2.5 Shear Stress in thin-walled cells

It is well known that the behavior of honeycombs is not linear under high strains due to geometric and material nonlinearities of cell walls [18, 19, 20]. The investigation of the response of honeycombs subjected to in-plane shear along vertical cell walls direction is minimal, therefore at this point of the current study it is important to present, in a brief way, the mathematical equations and simultaneously, the proper method of how this problem of six sided cells can be approached for study, according to Youming Chen et al. [21].

Figure 2.15 presents the structure of a honeycomb. The determination of the global (macro) response of the honeycomb can be done by the analysis of deformation of a unit cell. Since the behavior of honeycombs at the horizontal X (or L) direction differs from that at the vertical Y (or W) direction, it is possible to be studied separately.

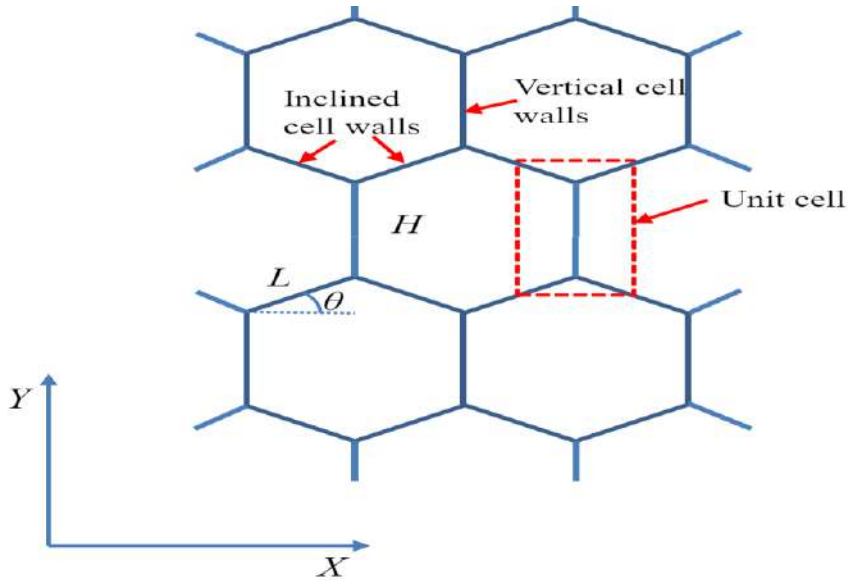

Figure 2.15: Schematic of a honeycomb structure [21]

2.5.1 In plane shear along the horizontal (X) direction

Figure 2.16 depicts the undeformed and deformed configurations of a unit cell under shear along X direction. Due to the unit cells geometrical symmetry about point D, the force applied on the unit cell has also a symmetrical behavior about point D:

$$u_A = -u_G \qquad u_E = -u_C$$

Where u_A, u_G, u_C and u_E are the displacements of points A, G, C and E, respectively. Furthermore, due to the lack of bending moment at points A, G, C and E, the distance between points A and C and distance between points E and G are constant, i.e.,

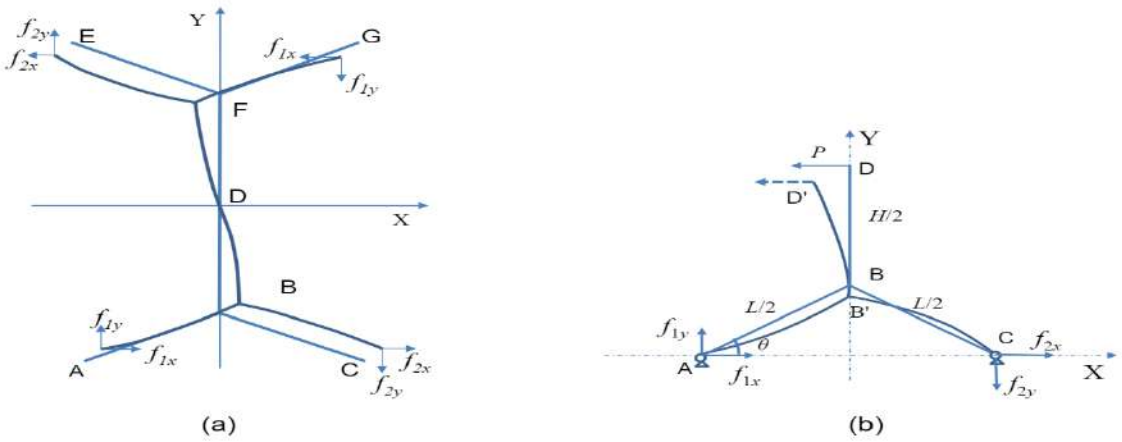

Figure 2.16: (a) Undeformed and deformed configurations of a unit cell under shear along X direction; (b) Boundary conditions of the half unit cell

$$u_A = u_C \qquad u_E = u_G$$

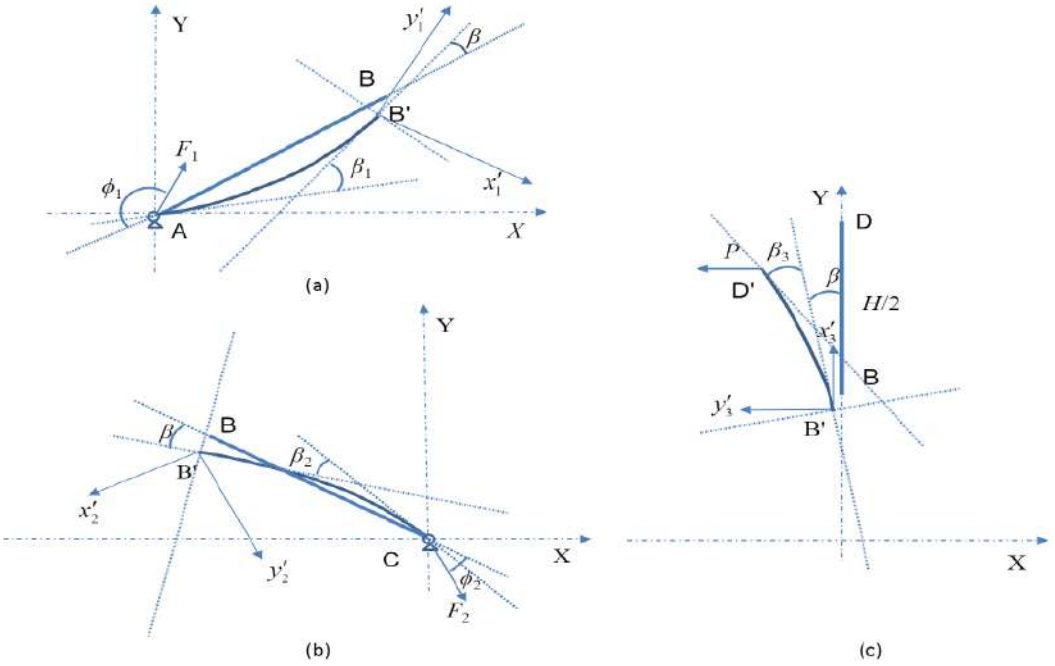

Figure 2.17: Deformation of cell walls (a) AB, (b) CB and (c) DB under shear along X direction

As a result of geometry's and load's symmetrical behavior, there's only need for half of the unit cell to be analyzed, as shown in figure 2.16 (b). Points A and C can be assumed to be simple supported. For the initiation of the analysis, a division takes place to three cell walls into individual entities and their deflection can be studied individually as shown in figure 2.17.

From beam theory [22, 23] the equations being conducted are:

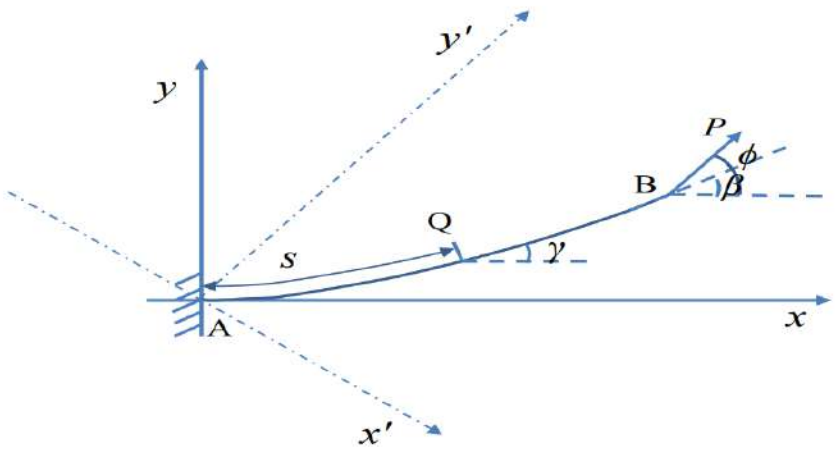

Figure 2.18: Cantilevered beam subjected to a force at free end

$$l = \frac{1}{k}\int_{\eta_0}^{\pi/2} \frac{d\eta}{\sqrt{1-\sin^2\eta\cos^2(\frac{\phi-\beta}{2})}} \qquad (1)$$

Where,

$$\eta_0 = \sin^{-1}[\frac{\cos(\phi/2)}{\cos(\frac{\phi-\beta}{2})}] \quad \text{and} \quad k = \sqrt{\frac{P}{E_s I}}$$

and,

l: length of the beam

E_s: Young's modulus of material of the beam

I: second moment of area of the cross-section of the beam

ϕ: the angle between the direction of the force (P) and horizontal (x) axis

β: rotation angle at the free end

Equation (1) has the form of an elliptical integral of the first kind, so it can be written as:

$$l = \frac{1}{k}[F(m) - F(m,\eta_0)] \qquad (2)$$

where,

F: is the symbol of the elliptical integral of the first kind and,

$$m = \cos^2(\frac{\phi-\beta}{2})$$

The calculation of the rotation angle at the free end can be made through Eq. (1). Additionally, the bending moment at the fixed end and the projections of the deformed beam on x' and y' axes:

$$M_A = E_s I\left(\frac{d\gamma}{ds}\right)_{|\gamma=0} = \sqrt{2}E_s Ik\sqrt{\cos(\phi-\beta)-\cos\phi} \quad (3)$$

$$\bar{x}' = \frac{\sqrt{2}}{k}\sqrt{\cos(\phi-\beta)-\cos\phi} \quad (4)$$

$$\bar{y}' = \frac{1}{k}[F(m)-F(\eta_0,m)]-\frac{2}{k}[E(m)-E(\eta_0,m)] \quad (5)$$

where,
E: is the symbol of the elliptical integral of second kind.

The parameters of the equations that are going be presented below (as shown in figure 2.17) are:

- F_1 : Force acting on point A
- F_2 : Force acting on point C
- P: Force acting on point D
- t: thickness
- b: honeycomb thickness
- L, H: cell wall lengths
- β: rotation angle of point B
- β_1: rotation angle of cell walls AB at point A
- β_2: rotation angle of cell walls CB at point C
- β_3: rotation angle of cell walls DB at point D
- ϕ_1: angle between F_1 and undeformed cell wall AB
- ϕ_2: angle between F_2 and undeformed cell wall CB
- θ: inclination angle
- $\overline{X}_{AB}$: projection of deformed wall AB on X axis
- $\overline{X}_{CB}$: projection of deformed wall CB on X axis
- $\overline{Y}_{AB}$: projection of deformed wall AB on Y axis
- $\overline{Y}_{CB}$: projection of deformed wall CB on Y axis

The following eight equations were developed by the application of equations (2) and (3), according to Lan and Hu [24].

$$\frac{L}{2}=\frac{1}{k_i}[F(m_i)-F(\eta_i,m_i)]\ (i=1,2) \tag{8a}$$

$$\frac{H}{2}=\frac{1}{k_3}[F(m_3)-F(\eta_3,m_3)] \tag{8b}$$

$$F_1\sin(\phi_1-\theta)-F_2\sin(\phi_2+\theta)=0 \tag{9}$$

$$-F_1\cos(\phi_1-\theta)+F_2\cos(\phi_2+\theta)=P \tag{10}$$

$$\begin{aligned}&k_1\sqrt{\cos(\phi_1+\beta-\beta_1)-\cos(\phi_1+\beta)}+k_2\sqrt{\cos(\phi_2+\beta-\beta_2)-\cos(\phi_2+\beta)}\\&=k_3\sqrt{\cos(\pi/2-\beta-\beta_3)-\cos(\pi/2-\beta)}\end{aligned} \tag{11}$$

$$|\bar{Y}_{AB}|=|\bar{Y}_{CB}| \tag{12}$$

$$|\bar{X}_{AB}|+|\bar{X}_{CB}|=L\cos\theta \tag{13}$$

Where,

$$\frac{1}{k_i}=\sqrt{\frac{E_sI}{F_i}},\ m_i=\cos^2\left(\frac{\phi_i+\beta-\beta_i}{2}\right),\ \eta_i=\sin^{-1}\left[\frac{\cos\left(\frac{\phi_i+\beta}{2}\right)}{\cos\left(\frac{\phi_i+\beta-\beta_i}{2}\right)}\right]\ (i=1,2)$$

$$\frac{1}{k_3}=\sqrt{\frac{E_sI}{P}},\ m_3=\cos^2\left(\frac{\pi/2-\beta-\beta_3}{2}\right),\ \eta_3=\sin^{-1}\left[\frac{\cos\left(\frac{\pi/2-\beta}{2}\right)}{\cos\left(\frac{\pi/2-\beta-\beta_3}{2}\right)}\right]$$

By using the incremental method, for a given shear force P, the solution of these nonlinear equations can be determined, and then the displacement of point D can be calculated as:

$$\Delta X=\left(\frac{L}{2}\cos\theta-\bar{X}_{AB}\right)+\bar{y}_3 \tag{16}$$

$$\Delta Y=\frac{H}{2}+\frac{L}{2}\sin\theta-(\bar{Y}_{AB}+\bar{x}_3) \tag{17}$$

and the global shear stress and strain of the honeycomb are:

$$\tau=\frac{P}{2Lb\cos\theta} \tag{18}$$

$$\gamma_{XY} = \tan^{-1}\left(\frac{\Delta X}{\frac{H}{2}+\frac{L}{2}\sin\theta}\right) \qquad (19)$$

For regular honeycombs, H=L and θ=30°. An analytical solution cannot be achieved despite the reduction of parameters in the analysis to give a plain relationship between shear stress and shear strain. Therefore, a shear stress parameter that is non-dimensional is presented:

$$\alpha = \frac{\tau L^3}{E_s t^3} \qquad (50)$$

Solutions for F_1, F_2, β, β_1, β_2, β_3, ϕ_1 and ϕ_2 can be obtained for several E_s, L, t, b and P values. By examining the solutions, it is observed that they are functions of only the non-dimensional shear stress parameter α. Additionally, ΔX, ΔY and γ_{XY} are functions of α as well. A comparison of the solutions from the equation system in contrast to the results from the FEM (finite element method) analysis was made in order to create a relationship between shear stress and shear strain as it is depicted in figures 2.19 and 2.20.

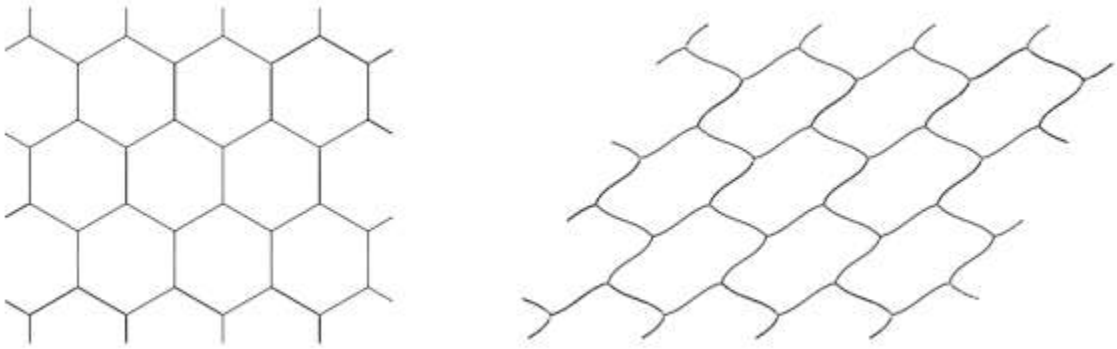

Figure 2.19: (a) Geometry of the finite element model, (b) Configuration of a deformed honeycomb under in-plane shear along X direction

Table 3: Geometric parameters of tested honeycombs

	E_s (MPa)	H (mm)	L (mm)	θ (°)	$t_{inclined}$ (mm)	$t_{vertical}$ (mm)
Honeycomb-1	2320	10	10	30	0.1	0.1
Honeycomb-2	2320	10	10	30	0.1	0.2
Honeycomb-3	2320	10	10	40	0.1	0.1
Honeycomb-4	2320	10	12	30	0.1	0.1

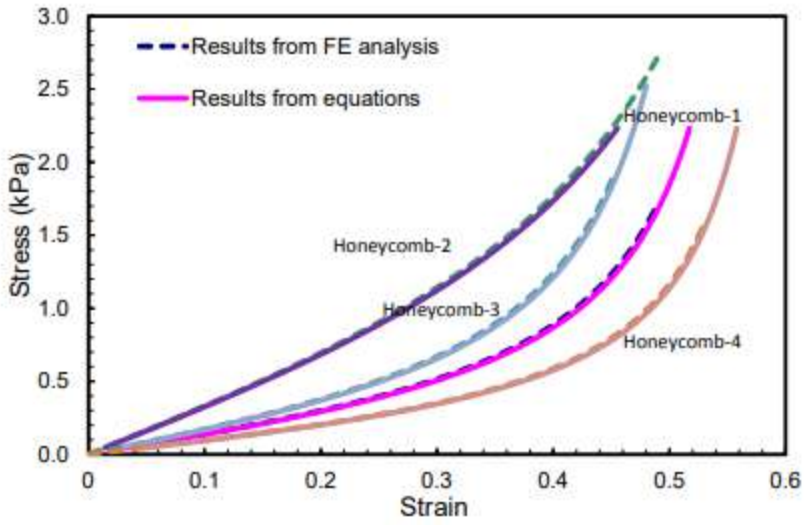

Figure 2.20: Comparison of the stress-strain curves of honeycombs along X direction from Finite Element Method analysis and from the developed equations (8a) -(13)

By curve fitting, it was obtained that:

$$\gamma_{XY} \approx 0.483(e^{0.0898\alpha} - e^{-4.158\alpha}) \qquad (51)$$

which, describes the universal stress-strain curve of all regular honeycombs with cell walls of uniform thickness subjected to in-plane shear along the horizontal X (or L) direction and:

$$\gamma_{XY} \approx 0.795(e^{-0.1024\alpha} - e^{-1.139\alpha}) \qquad (58)$$

for regular honeycombs with vertical walls of double thickness.

In a similar way the in-plane shear along Y direction was developed and it was obtained that:

$$\gamma_{YX} \approx 0.328(e^{0.1225\alpha} - e^{-6.169\alpha}) \qquad (62)$$

which, describes the universal stress-strain curve of all regular honeycombs with cell walls of uniform thickness subjected to in-plane shear along the horizontal Y (or W) direction and also:

$$\gamma_{XY} \approx 0.486(e^{-0.2119\alpha} - e^{-1.907\alpha}) \qquad (65)$$

for regular honeycombs with vertical walls of double thickness.

The expressions for predicting the shear stress-strain of honeycombs are really important for new investigational studies. From these expressions it can be derived that by doubling the thickness of cell walls of honeycombs, along the vertical (Y) direction the shear

strength does not improve significantly and along the horizontal (X) direction the shear strength is increased almost twice.

Chapter 3. EXPERIMENTAL STUDY

3.1 Material of honeycomb's core

In this present work, the type of honeycomb used is PAMG-XR1 5052. PAMG-XR1 5052 honeycomb is made of aluminum and meets all the requirements (aluminum core materials for sandwich type construction) of the specification AMS C7438 Rev A. The aluminum material was received in large plates by the Institute of Structural Mechanics and Lightweight Constructions (Institut für Strukturmechanik und Leichtbau) of the Department of Mechanical Engineering of the University of Aachen (RWTH Aachen). These large plates were cut into thin sheets in the dimensions that served the requirements for the shear experiments. The honeycomb type aluminum specimens were constructed by electro-discharge machining method, which was selected as suitable for cutting thin walls. The dimensions of the honeycomb's core are L= 120 mm of length (X direction), W=50 mm of width (Y direction) and b=10 mm of honeycomb's thickness (T direction). The cutting process of these specimens took place at University of Patras at the Machine shop - Support of Research Activities – ΜΥΕΔ. Also, the core has a hexagonal structure with length of the inclined cell walls: H=3mm, thickness of the walls: t=0.0254mm and cell size: c=4.8mm, as shown in figure 3.1. In table 4 there are presented some additional features about PAMG-XR1 5052 honeycomb [25].

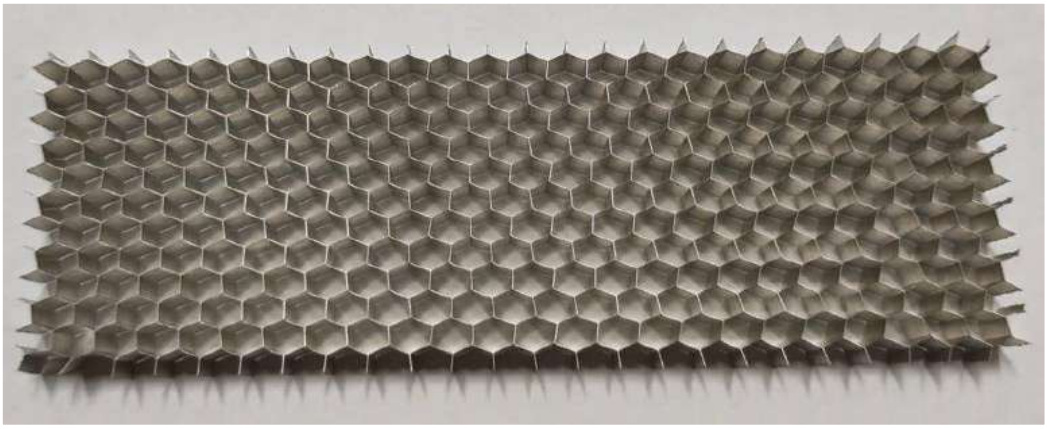

Figure 3.1: Specimen of honeycomb's core

PAMG-XR1 5052 Mechanical Properties																			
CELL SIZE		NOMINAL DENSITY		BARE COMPRESSIVE STRENGTH				PLATE SHEAR STRENGTH "L" DIRECTION				PLATE SHEAR MODULUS "L" DIRECTION		PLATE SHEAR STRENGTH "W" DIRECTION				PLATE SHEAR MODULUS "W" DIRECTION	
				Typical		Minimum		Typical		Minimum		Typical		Typical		Minimum		Typical	
in	mm	lb/Ft³	Kg/m³	psi	Mpa	psi	Mpa	psi	Mpa	psi	Mpa	ksi	Gpa	psi	Mpa	psi	Mpa	ksi	Gpa
5/32	4.8	3.8	61	436	3.01	300	2.07	210	1.45	215	1.48	58	0.40	175	1.21	125	0.86	32	0.22

Table 4: Features and mechanical properties of PAMG-XR1 5052 [25]

3.2 Apparatus of shear experiment

The design of the apparatus for shear tests (Figure 3.2,3.3) was made according to ASTM C273 Standard Test Method for Shear Properties of Sandwich Core Materials [26,27]. Following the specification pattern, the width of the specimen must be at least 50 mm and its length at least 12 times its thickness. The joints of the apparatus are simple supports (Figure 3.4) are needed for placing the specimen in the tensile machine and they serve into performing the shear experiments. Thus, their existence contributes into differentiating the experiment from a simple tensile strength to a pure shear experiment, and this happens because the direction of where the tensile force is exerted must passes through the diagonal of the honeycomb core, as shown in figure 3.4.

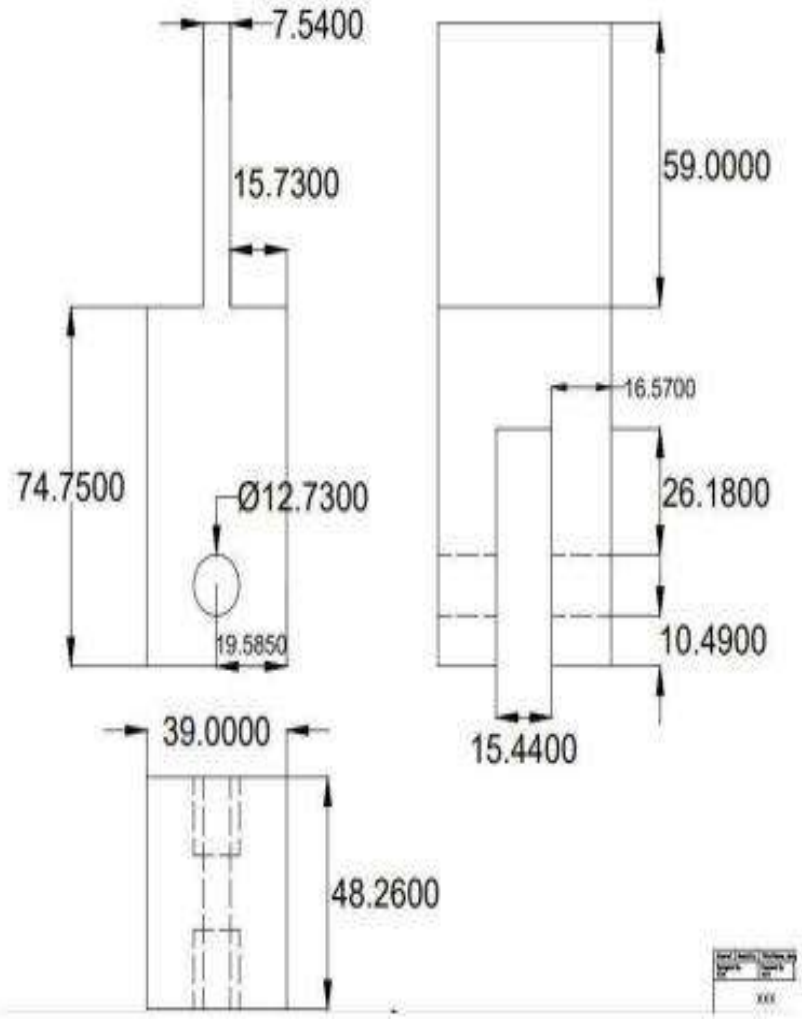

Figure 3.2: Apparatus base design

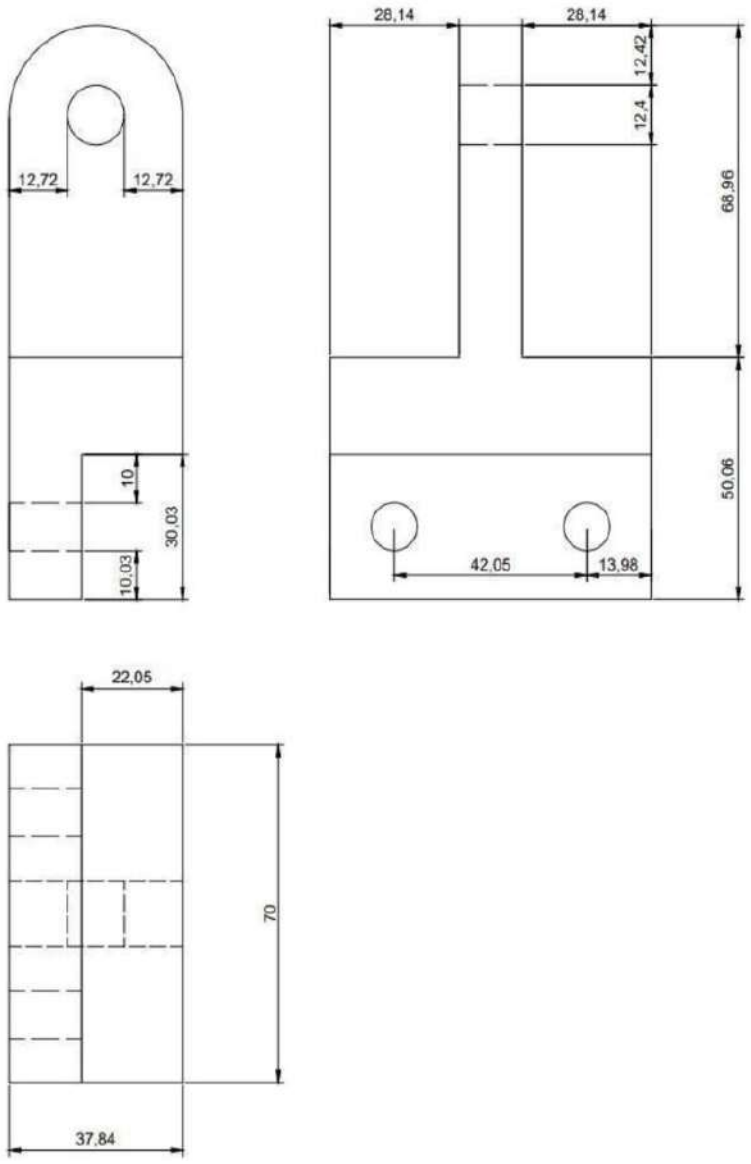

Figure 3.3: Apparatus joint design

For pure shear tests the angle of the diagonal needs to have a very small value so that it is as parallel as possible to the axial direction, as shown in the figure below.

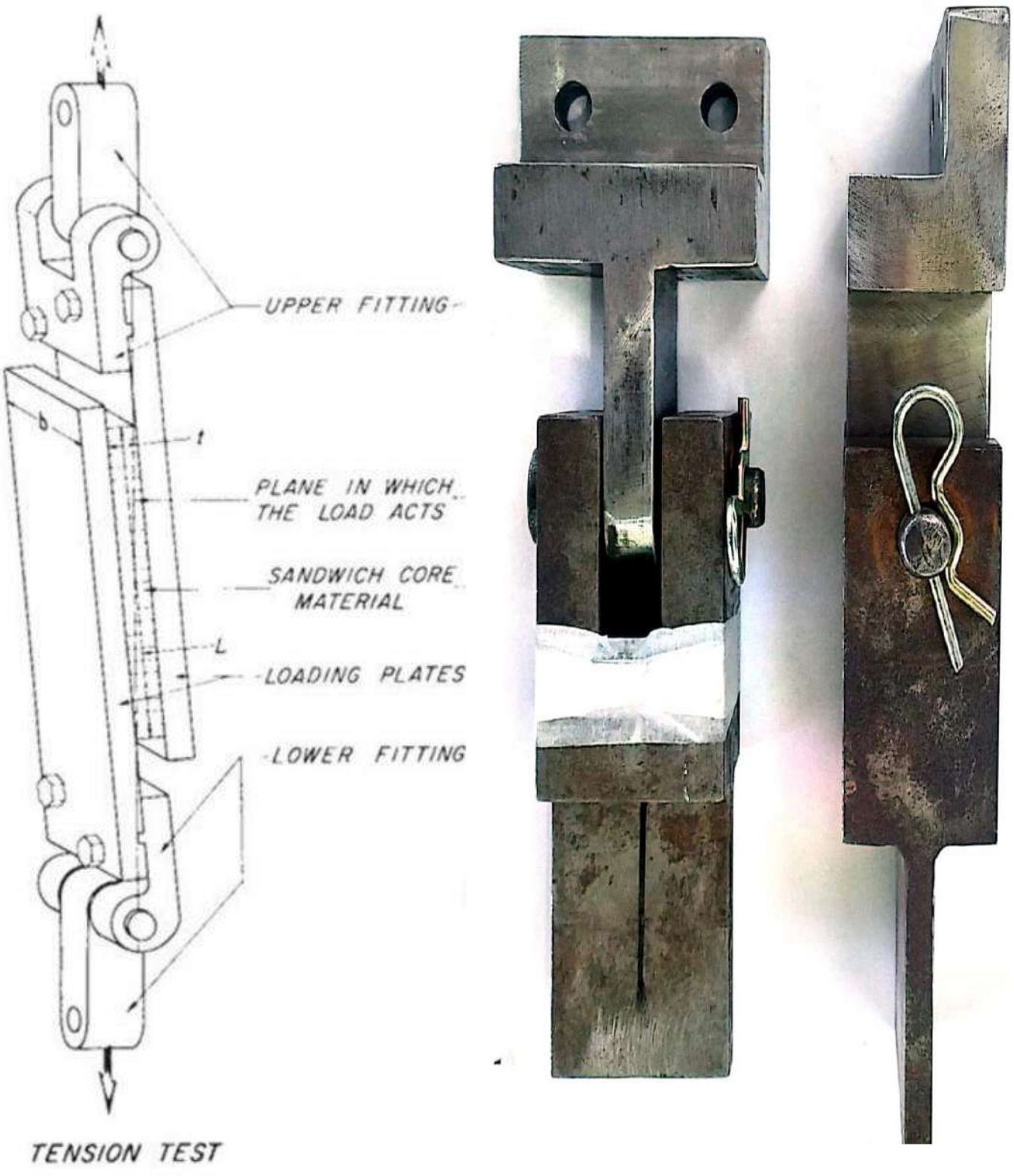

Figure 3.4: Proposed apparatus for performing shear tests according to the model in honeycomb cores

3.3 Plate design

3.3.1 Material Selection and dimensions

Another important section for this experimental procedure to take place is the material selection and the dimensions of the plates for the sandwich composite. The material used for the plates was of 5000 series aluminum and more specifically 5052-H32 (H32 means that it has been strain hardened to a quarter of hard temper and that it is thermally stabilized). This choice was made for two reasons:

1) The specification states that effective bonding can be done between aluminum surfaces and;
2) To avoid any problems that may appear from the bonding of different metals in the oven.

Since the honeycomb sandwich structure was made from the same material when it will be put in the oven, due to the same degree of thermal expansion, the cells and plates will expand or contract at the same degree. This will result in no loosening of the clamps that are applied in the honeycomb sandwich and also not forming thermal residual stresses. Finally, the mechanical properties of aluminum 5052- H32 were decisive, as they concur with the requirements of the experiment. Listed below in Tables 5, 6 there are presented the composition of this specific material and some of its mechanical and thermal properties.

Alloy	Si	Fe	Cu	Mn	Mg	Cr	Ni	Zn	Ti	Zr	Other	Al
5052	0.25	0.4	0.1	0.1	2.2-2.8	0.15-0.35	-	0.1	-	-	0.05	Remainder

Table 5: Composition of aluminum material 5052-H32 [28]

Monotonic properties	
Yield strength	193 MPa
Ultimate strength	228 MPa
Modulus of elasticity	70.3 GPa
Elastic Poisson's ratio	0.33
Density	2.68 g/mm3
Cyclic properties	
Material constant of S-N curve, C	1348 MPa
Slope of S-N curve, b	-0.17

Specific heat	963	J/(kg.°C)
Thermal conductivity	144	W/(m.C)

Temperature. °C	Coefficient of expansion, oC^{-1}	Young's modulus E, GPa
25		69.85
100	$2.38x10^{-5}$	67.02
150		65.14
200	$2.48x10^{-5}$	63.26
250		61.38
300	$2.63x10^{-5}$	

Table 6: Mechanical and thermal properties of aluminum material 5052-H32[28]

The geometry and the design of the plates was made according to the constraints set by the apparatus. In previous study, it was found out that plates with thickness of 5mm appeared unwanted bending deformations at honeycomb. So, for the experiments of this study, plates of 10mm were used, as shown in figure 3.5.

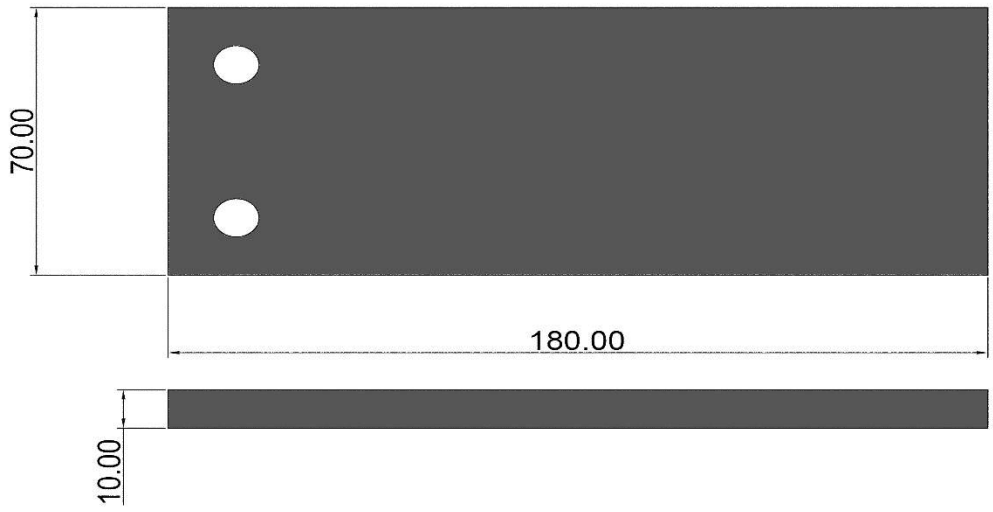

Figure 3.5: Aluminum plates geometry and dimensions

3.4 Adhesive Selection

A problem that could appear by selecting a non-suitable adhesive, is that the it can prevent the walls from deforming and furthermore alter the shear phenomenon. So, to avoid any possible problems that could come up, in the previous study [30] and on this study as well, experiments were made with the HexBond 609 adhesive of the HEXCEL company [29]. HexBond 609 is delivered by the manufacturer in film form and it is consisted of the main epoxy adhesive containing fibers along its length and thickness (Figure 3.5), in order to ensure a uniform thickness over the entire surface of the adhesive, and two protective layers on top and bottom to prevent its alteration. It was selected due to the two following main applications:

1) Aluminum to Aluminum bonding
2) Sandwich bonding with a variety of skins and cores.

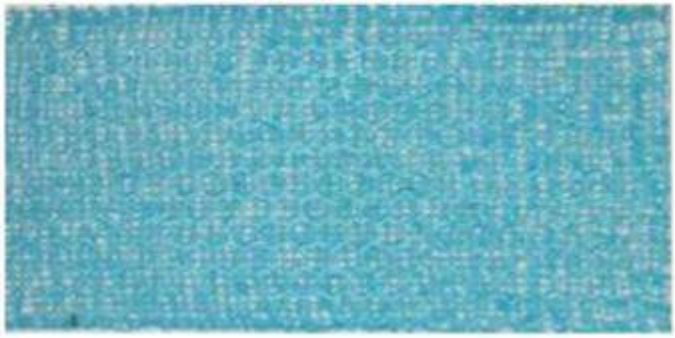

Figure 3.5: Hexbond 609 adhesive structure (fibers morphology)

On top it is placed a layer of polyethylene that does not let the adhesive interact with the environment and at the bottom there is a protective paper. It is also important to mention that the adhesive's storage life is: 18 months at -18°C (shelf life) and 90 days at 19 – 27°C (out life). So, it is recommended to be maintained in refrigeration for more duration of its life at -18°C. In table 7 there are presented some of HexBond 609 mechanical properties.

Test	Environmental Conditioning	Test Temperature °C	HexBond™ 609 200g/m² Supported	HexBond™ 609 300g/m² Supported	HexBond™ 609U 300g/m² Unsupported
Lap Shear Strength (MPa)	None	22 50 80 100	31 31	33 31 24 15	43
	70°C 95% RH (1000 hrs.)	22 80		24 3	
Bell Peel (N/25mm)	None	22 50 80 100	102	76 110 114 136	75
	70°C 95% RH (1000 hrs.)	22 80		71 50	
Climbing Drum Peel (Lower skin) (N/76mm)	None	22 50 80 100	141	193 250 250 288	308
Flatwise Tensile (MPa)	None	22	4.5	7	6

Table 7: Mechanical properties of Hexbond 609 epoxy adhesive [29]

3.5 Equipment and heat treatment for successful bonding

The manufacturer of Hexbond 609 specifies that for optimum properties the adhesive should be cured at 120±5°C for 60 minutes (alternative cure cycles are given in Table 8). Also, a cure pressure of around 350 kPa and heat up rate of approximately 5°C per minute is recommended during cure.

Temperature (°C)	180	170	160	150	140	130	120	110	100
Time (min)	5	7	8	10	20	30	60	120	240

below 100°C incomplete cure

Table 8: Alternative cure cycles

After the application of the adhesive on the aluminum plates and the placement of the honeycomb core, one plate is placed centered on the other so that they are parallel to each other without any deviations in all directions. Then the sandwich specimen is placed at a vice and before getting into the mechanical convection oven (Figure 3.8), it needs a constant pressure of 350 kPa. Because of the restrictions that came up from the dimensions of the oven it was

explored and discovered that by applying four clamps (Figure 3.7) alternately and symmetrically, succeeding 0.4mm of compressive displacement (that is always getting measured with a caliper) uniformly in the specimen [28], as shown in figure 3.6, there was a successful bonding with the pressure reaching the limits set by the manufacturer.

Figure 3.7: Modified clamps for applying pressure at honeycomb specimen and fitting in the mechanical convection oven

Figure 3.6: Method of tightening the specimen with clamps

Figure 3.8: Mechanical convection oven at room temperature before the thermal process begins

Figure 3.9: Thermal process for successful bonding at honeycomb specimen

The adhesive specification states that the clamp assembly must enter the oven at room temperature and the curing time starts to be taken into consideration (60 minutes), only when the temperature of the oven reaches 120 °C. Once the required time is up, the specimen is put out of the oven and it is left until it reaches room temperature again. An important detail is that the clamps should not been removed from the specimen until it reaches room temperature. Earlier removals of pressure can lead to incomplete curing or complete bonding failure.

Further details about the application of clamps method, step-by-step process of bonding and preparing the specimens for experiments can be found in the previous thesis work of the students that worked at the materials laboratory of the University of Thessaly: “Experimental investigation of mechanical behavior under shear loading in cellular aluminum cells “[30].

3.6 System Setup for shear stress tests

In this section the equipment used for shear stress tests will be presented. For the experiments, that took place at the Laboratory of Mechanics and Strength of Materials of the Department of Mechanical Engineering of University of Thessaly, the compression/tensile machine model that was used is the MTS 810 Material Test System (Figure 3.10).

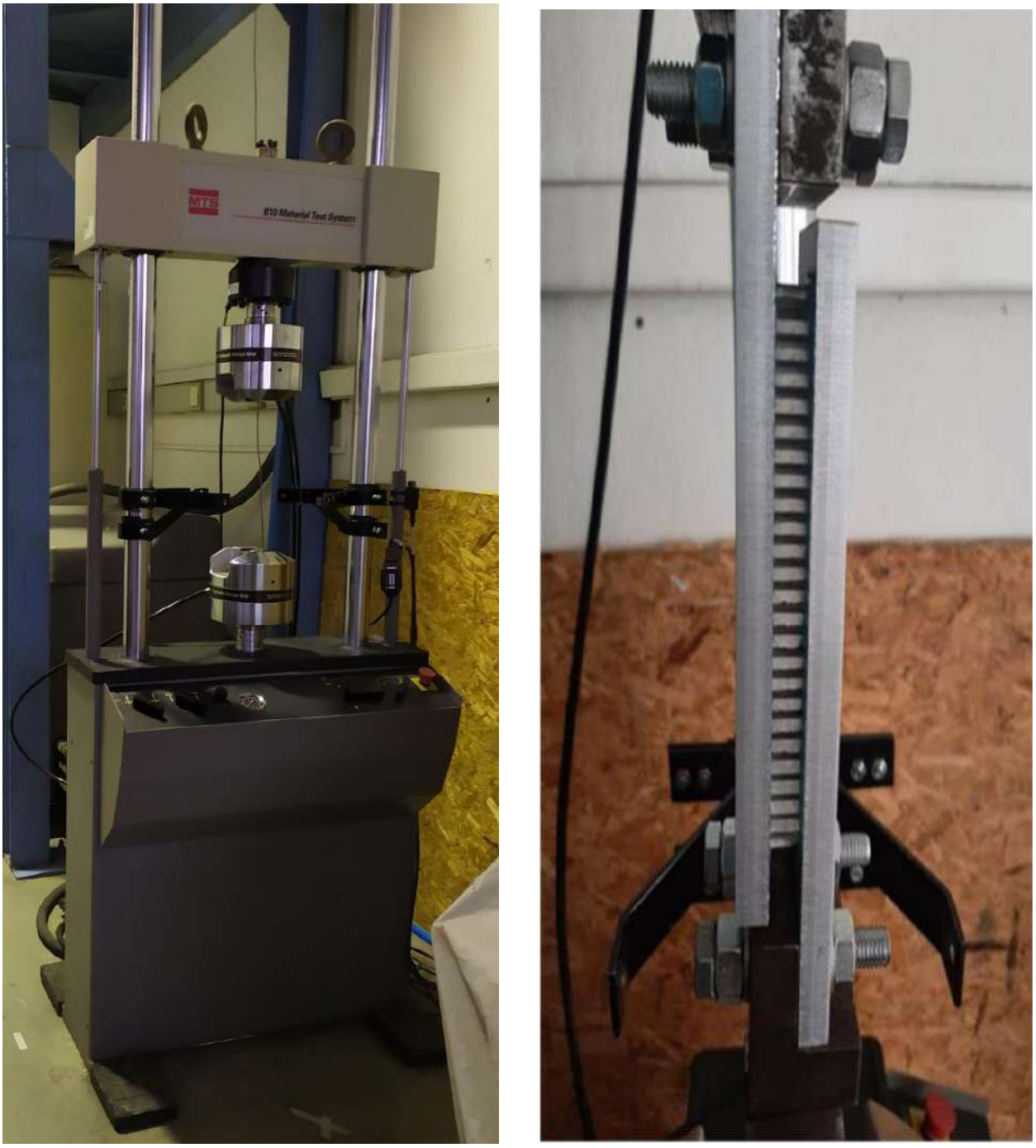

Figure 3.10: (a) MTS 810 Material Test System, (b) Specimen placed upon the MTS system

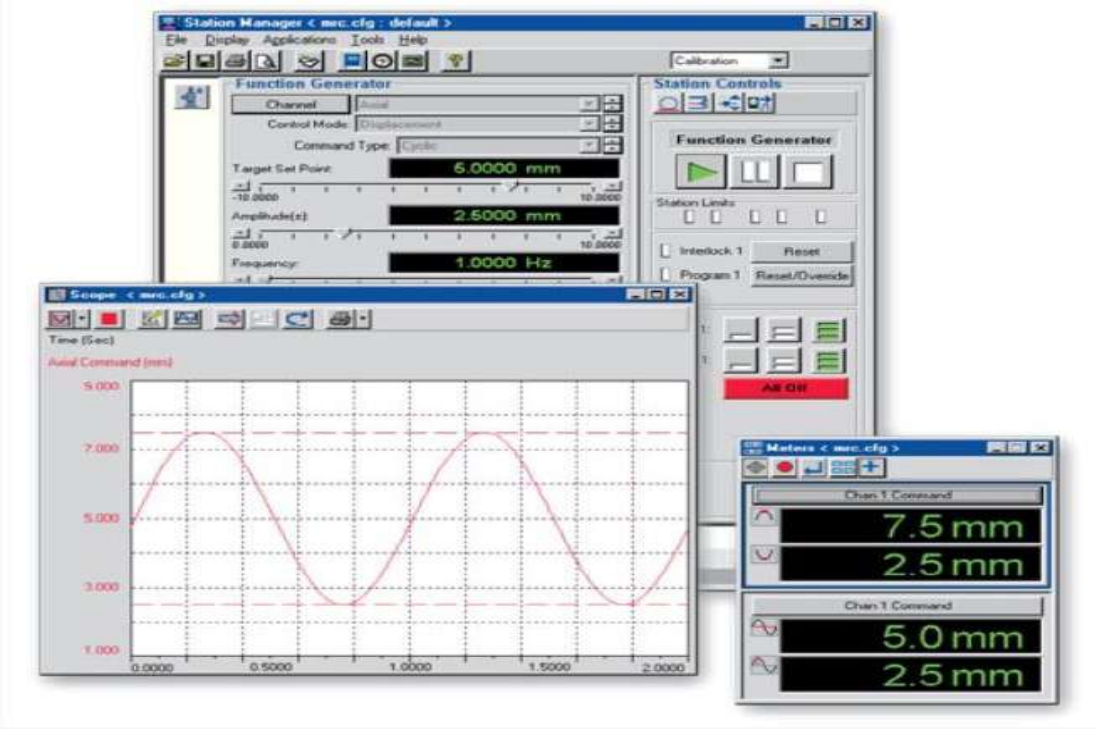

Figure 3.11: Example of controller's display at computer screen

Apart from the MTS system, for more information and details about the experiments that are going to be described in chapter 4, Spark optical emission camera RTSS was used (figure 3.12) by LIMESS company [31].

Figure 3.12: Spark optical emission camera RTSS [30]

The RTSS Video extensometer measures the longitudinal and transversal strain during material tests (e.g., tension, compression tests).

In order to provide results from the RTSS camera, two points must be defined in the test specimen with the desired distance (depending on the situation). The camera locates and tracks these points and the distance of them constantly throughout the experiment, recording the data of longitudinal strain for each force value. These points are located with the help of two led lights, which are in the camera kit, and are installed near the desired study area. The manual suggests that for the right functioning of the camera these two points have to be located upon two adhesive stickers that are placed on the specimen with a black line drawn on them, as shown in figures 3.13,3.14,3.15.

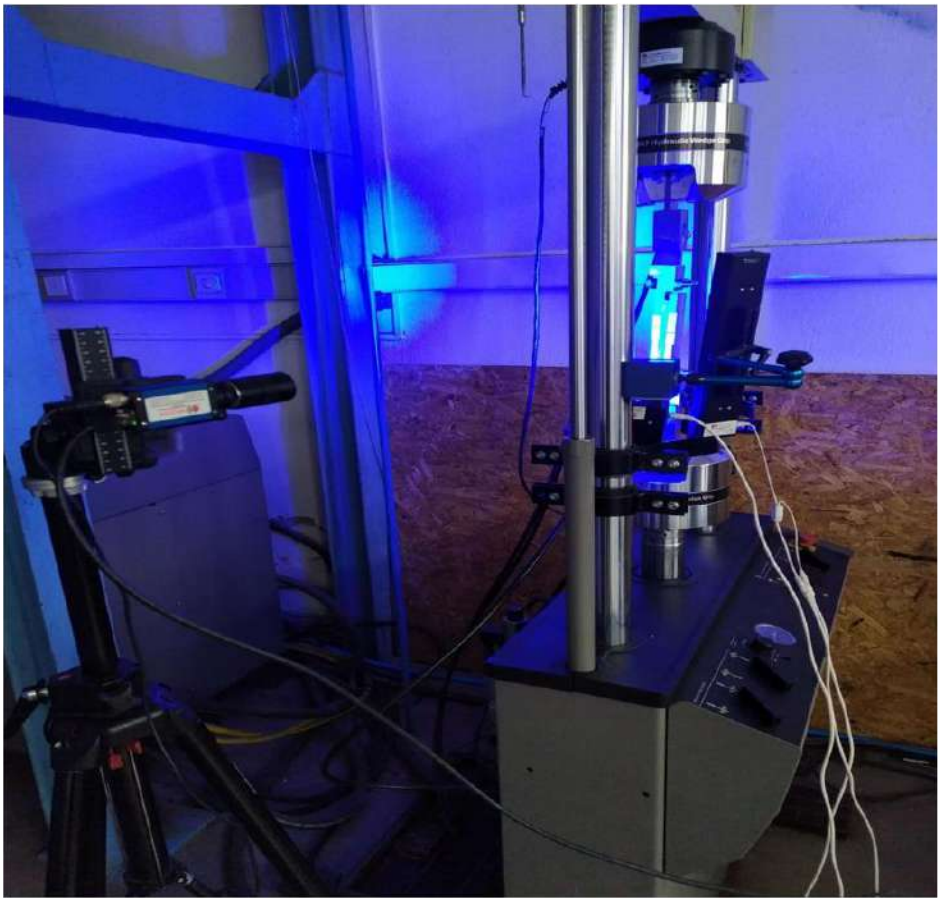

Figure 3.13: System setup - Material Test System 810 & camera RTSS installation

Figure 3.14: Adhesive stickers placed in the middle of the aluminum plates, so the desired points can be detected by the camera

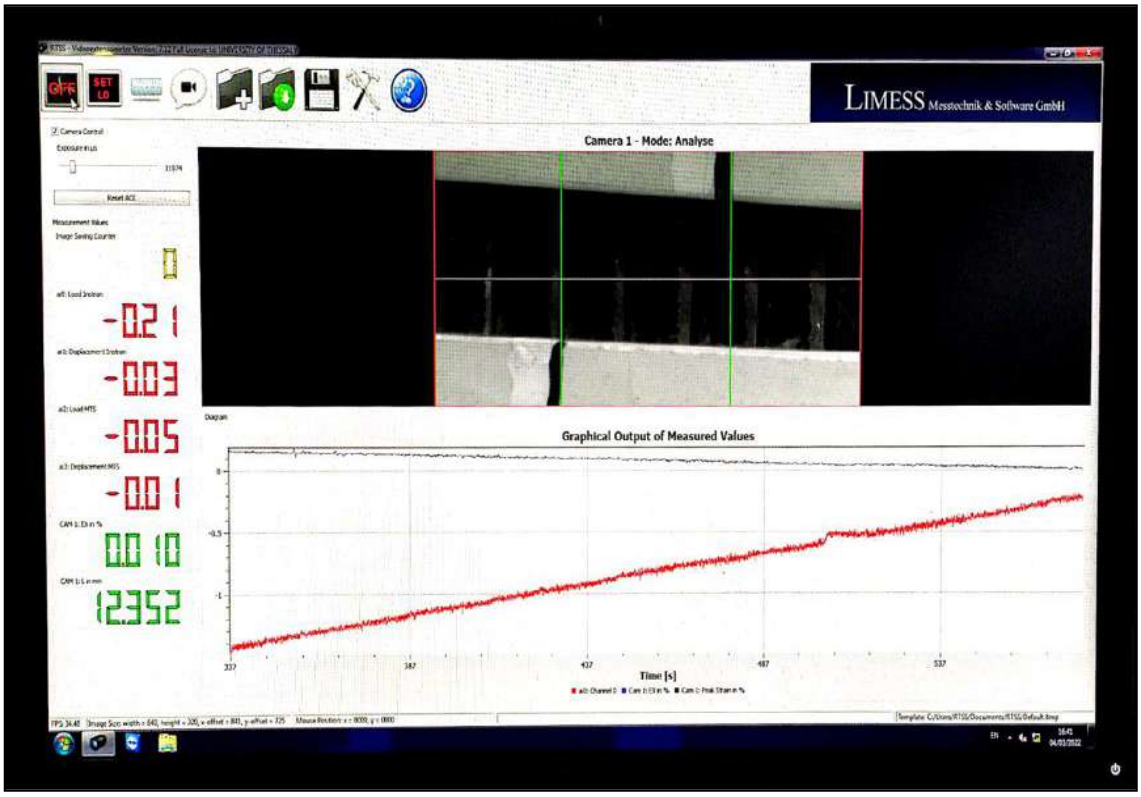

Figure 3.15: LIMESS software display at computer screen

The reason of use of the RTSS video-extensometer is that by having the results that it can provide, alongside with the benefits (contact less, high precision etc.), a more comprehensive view about the specimen's mechanical behavior. Also, it was a determining factor that helped to explain some phenomenon that appeared during the tests and furthermore, to conclude more safely if the specimen was subjected to plastic deformation or not, as discussed in chapter 4. The longitudinal strain is measured from the fraction of the different displacements of the green lines, figure 3.14, with the initial distance L_0 depending on the value of the force in each loading and unloading.. After the first experiment with the RTSS camera it was noticed that the detected green lines, upon the stickers, indicated small displacements at zero force value. This effect is not desirable because the results that were given were not 100% accurate and reliable, as there were some deviations from the true behavior of the specimen. Thus, a new way of detecting the lines was found in which the lines were formed with a mechanical pencil directly on the aluminum plates, as shown in figure 3.15. Finally, it is worth mentioning that trying to detect directly points – lines inside the honeycomb's core specimen, due to the physics of the experiment the results do not provide any noteworthy information.

Figure 3.16: (a) Drawn lines for detection with adhesive stickers and black marker,

(b) Forming lines for detection with mechanical pencil

Chapter 4. EXPERIMENTAL RESULTS

In this section, the shear experiments and their results are presented. The force from the MTS 810 system is passed on through the bonded aluminum plates, to the honeycomb core, that are contingent on opposing compressive or tensile displacements which result in the shear force on the sandwich core. As mentioned in section 3.2, the line of action of the load goes through the diagonally opposite corners of the sandwich, in order to minimize the effects from secondary stresses. All tests were conducted at room temperature in force control at a speed of 5 N/s.

More specifically, the diagrams of Force – Displacement and Force – Strain were recorded by the MTS and RTSS camera for 1000, 1500, 2000, 2500, 3000, 3500 N of force for loading-unloading and loading-unloading tests of 3,5 and 10 cycles. From these diagrams the values of displacement, angular deformation, axial shear stress for both honeycomb and aluminum plates, shear modulus [32] and stiffness at each experiment can be derived.

4.1 Force-Displacement & Force-Strain diagrams

Test 1 - 1000 N

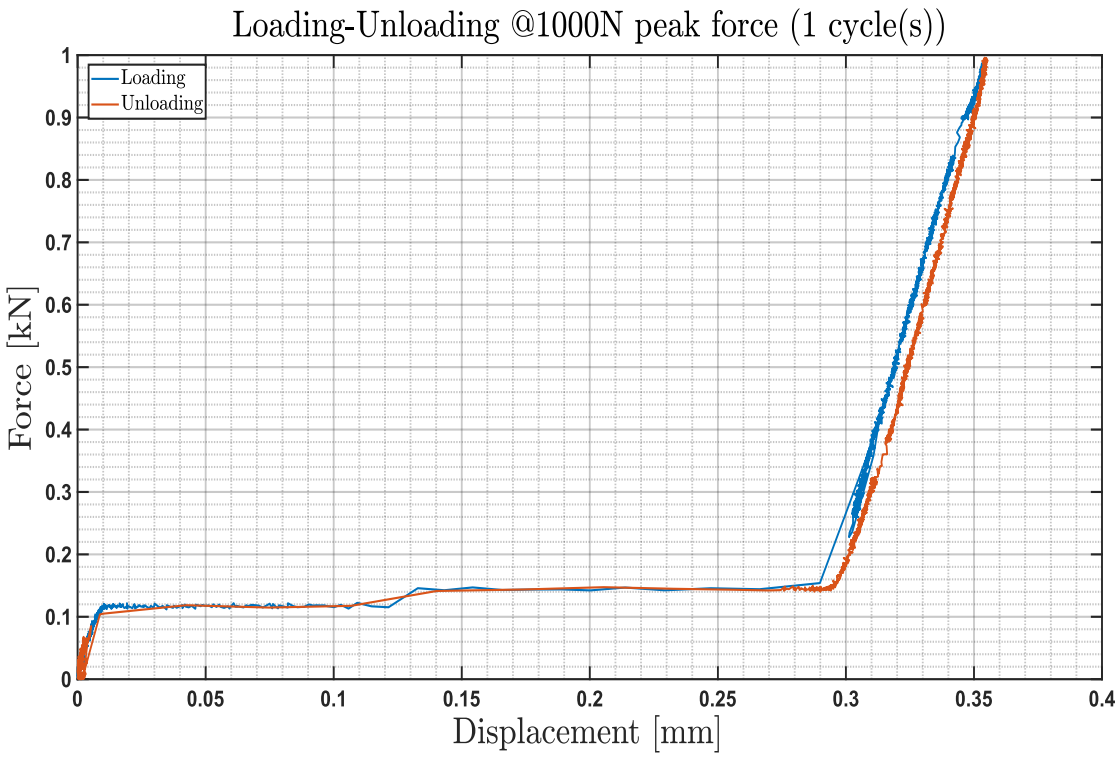

Plot 1(a): Force – Displacement, test 1 - 1000N peak force

Plot 1(a), shows the Force – Displacement diagram of shear stress of the specimen at 1000N peak force. At a first glance, it is noticeable that there is a linear behavior until the point of (Force, Displacement) = (114.7 N, 0.0092 mm) - (point 1), and from point 1 until the point of (Force, Displacement) = (154 N, 0.2899 mm) – (point 1'), there is a rapid increase of the displacement with relatively low load increase. This phenomenon was observed in all experiments where the force load was in the range of 110 – 150 N and it was increased or decreased, depending on the stage of the test (loading or unloading). This behavior of the material was concerning, because the factors that can contribute to this are many and complex (e.g., Hexbond 609 adhesive, between the aluminum plates and the core of honeycomb). However, after consultation and considering more experiments, it was found out that it is a no-resistance travel of the actuator, attributed to the margins of the apparatus imposed by the mechanical fasteners and connections in the system. Therefore, this behavior is observed until the specimen is fully 'stretched' on the system and then the data recorded (after point 1') is used to determine its behavior. For that reason, in the calculations used below the space until point 1' and after point 2 is excluded. Also, after the rapid increase of displacement it is distinct a hysteresis loop that creates an area between the loading and unloading path. From plot 1(a) it is derived:

Maximum displacement: x_{max} = 0.3554 mm

Actual maximum displacement: x_{actual} = 0.3554 – 0.3036 => x_{actual} = 0.0518 mm

Global shear stress of the honeycomb at maximum load: $\tau = \frac{P}{2Lbcos(\theta)}$ => $\tau = \frac{1(kN)}{2*3(mm)*10(mm)*\cos(30)}$ => τ_{max} = 19.245 MPa

Maximum shear stress of the aluminum plates: $\tau = \frac{P}{L,plate\ W,plate}$ => $\tau = \frac{1(kN)}{180(mm)*70(mm)}$ =>

=> $\tau_{plates,\ max}$ = 0.0794 MPa

Area of hysteresis loop: W = 0.002687 J.

The difference between the values of shear stress of the aluminum plates and shear stress of the honeycomb occurs, due to the fact that the aluminum plates are consisted of a solid, monolithic

material, while the honeycomb is not solid as it is composed of a geometric sequence of aluminum hollow cells. So, when the force is transmitted from the MTS to the specimen it is reasonable and consequent that the plates receive significantly less shear stress than the honeycomb. Additionally, the area of hysteresis loop is schemed in diagrams of Force-Displacement and by calculating it, the measurement unit of it is: kN × mm = J. This fact implies that this area is created due to an energy activity that is taking place during the procedure. In this thesis work it wasn't explored why and how this phenomenon is caused, but an assumption could be that it is caused due to: elastic buckling of the aluminum cells or from viscoelastic behavior of adhesive at the interface between the aluminum plates and honeycomb core.

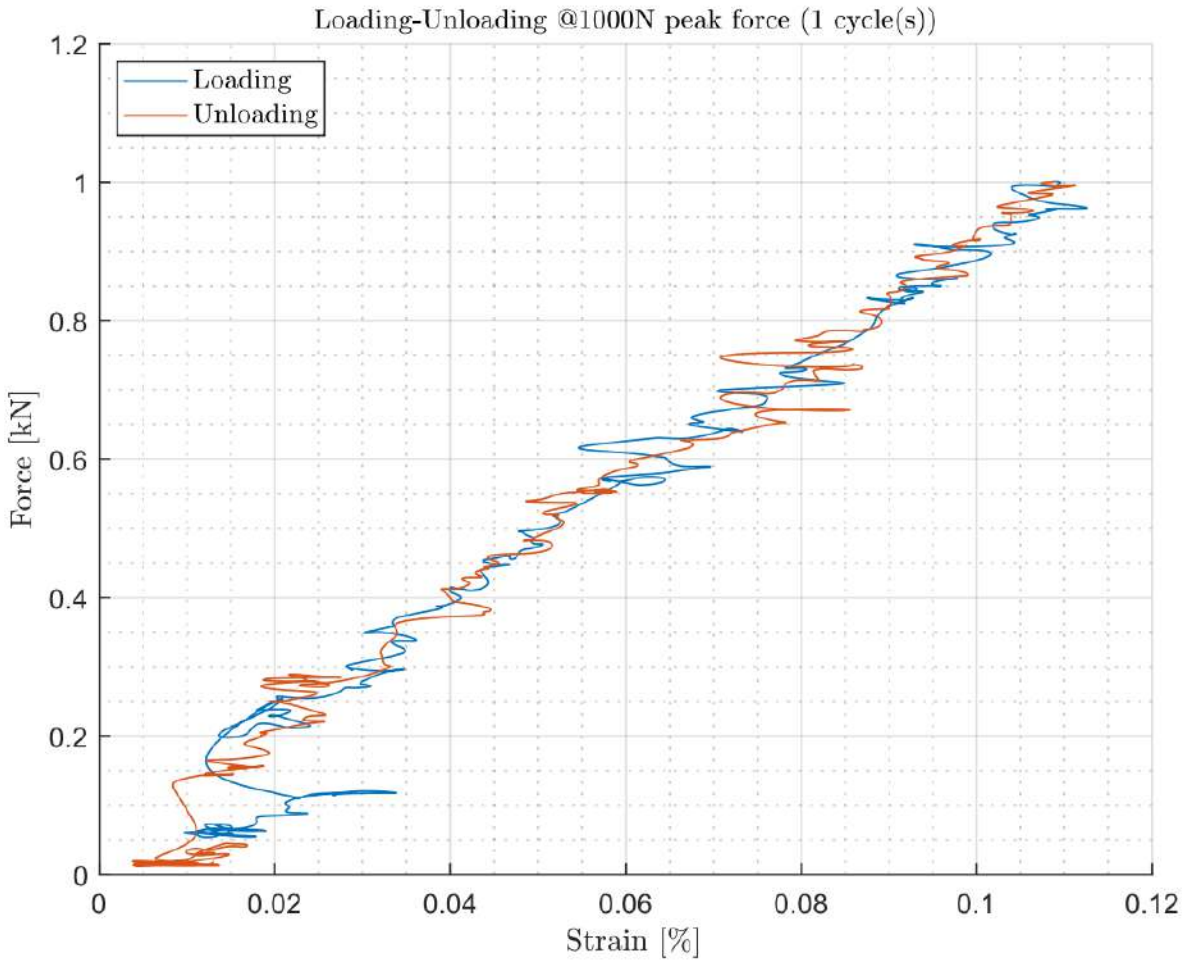

Plot 1(b): Force – Strain, test 1 - 1000N peak force

Plot 1(b), shows the Force – Axial strain diagram of shear stress of the specimen at 1000N peak force. It is clearly visible that the behavior of the honeycomb specimen is linear and the loading and unloading paths are coinciding. Also:

Maximum axial strain: ε_{max} =0.11 %

Shear Modulus: $G = \frac{\Delta\tau}{\Delta\varepsilon}$ => G= $\frac{\tau max - \tau 1'}{\varepsilon max - \varepsilon 1'} = \frac{\tau max - \tau 1'}{\varepsilon max}$ = 139.96 MPa, $\tau_{1'}$= 0.2/2Lbcosθ = 3.849 MPa

Final Strain: $\varepsilon_{end} = \varepsilon_{start} = 0$.

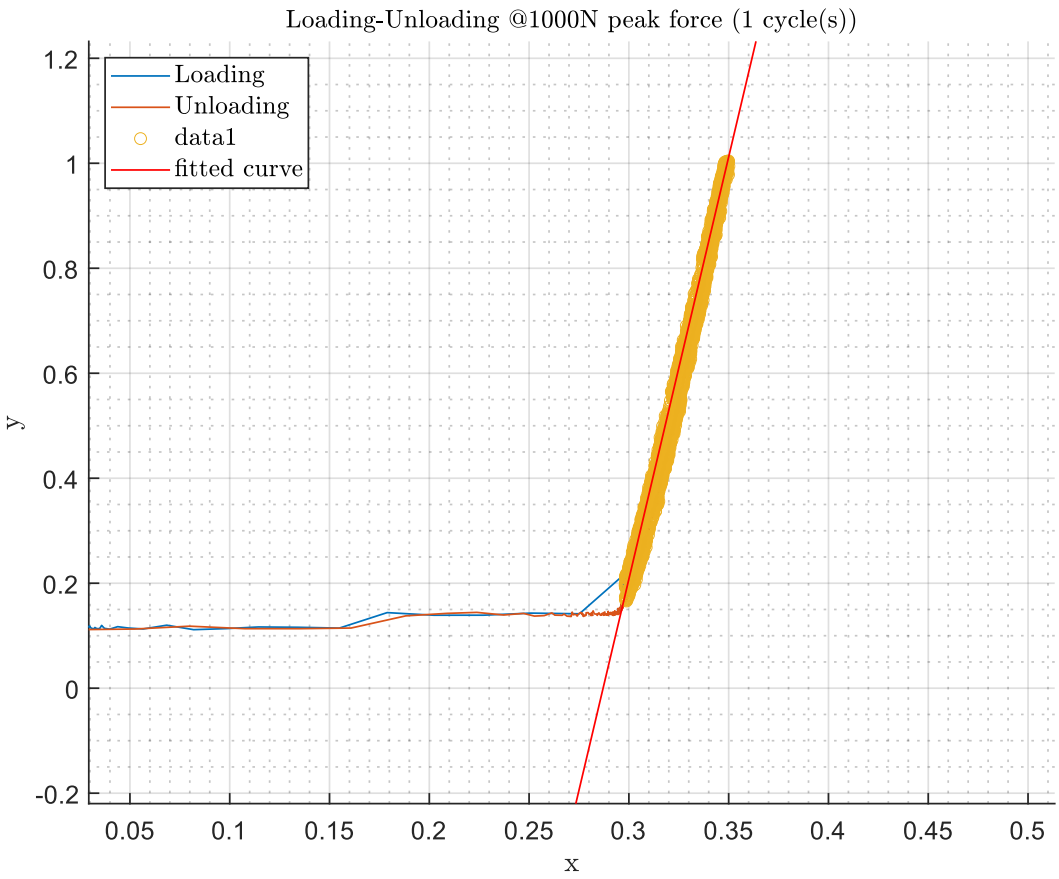

Plot 1(c): Force – Displacement fitted curve diagram at 1000 N peak force

Where, x axis interprets the displacement values in mm and y axis interprets the force values in kN.

By fitting a curve into the Force – Displacement diagram (plot 1(c)), information about the angle of incline and stiffness of the specimen can be obtained in each test, with the following way

Stiffness: $S = \frac{\Delta P}{\Delta X}$ => S = $\frac{1.0021-0.196332}{0.3554-0.30541}$ => S = 16.1 kN/mm

Angle of incline: $tan^{-1}(S) = \varphi$ => $\varphi = 86.444^{o}$.

Test 2 - 1500 N

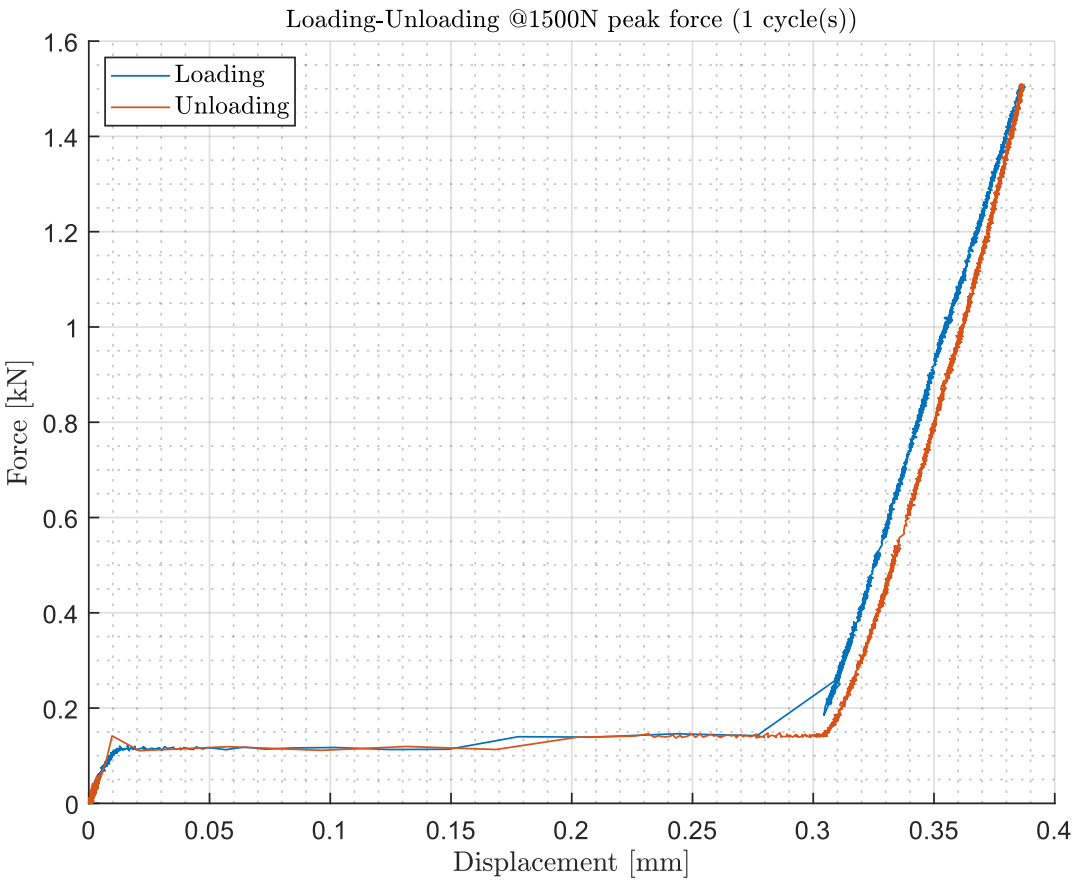

Plot 2(a): Force – Displacement, test 2 - 1500N peak force

From plot 2(a), it is noticeable that the area created by the hysteresis loop at 1500N is greater than the area at 1000N and it will be shown in subsequent tests that, as the load increases the hysteresis loop grows larger. Similarly with Test 1, from plot 2(a) it is derived:

Maximum displacement: x_{max} = 0.3843 mm

Actual maximum displacement: x_{actual} = 0.3843 – 0.3038 => x_{actual} = 0.0805 mm

Global shear stress of the honeycomb at maximum load: τ_{max} = 28.868 MPa

Maximum shear stress of the aluminum plates: $\tau_{plates,\ max}$ = 0.119 MPa

Area of hysteresis loop: W = 0.008062 Joule.

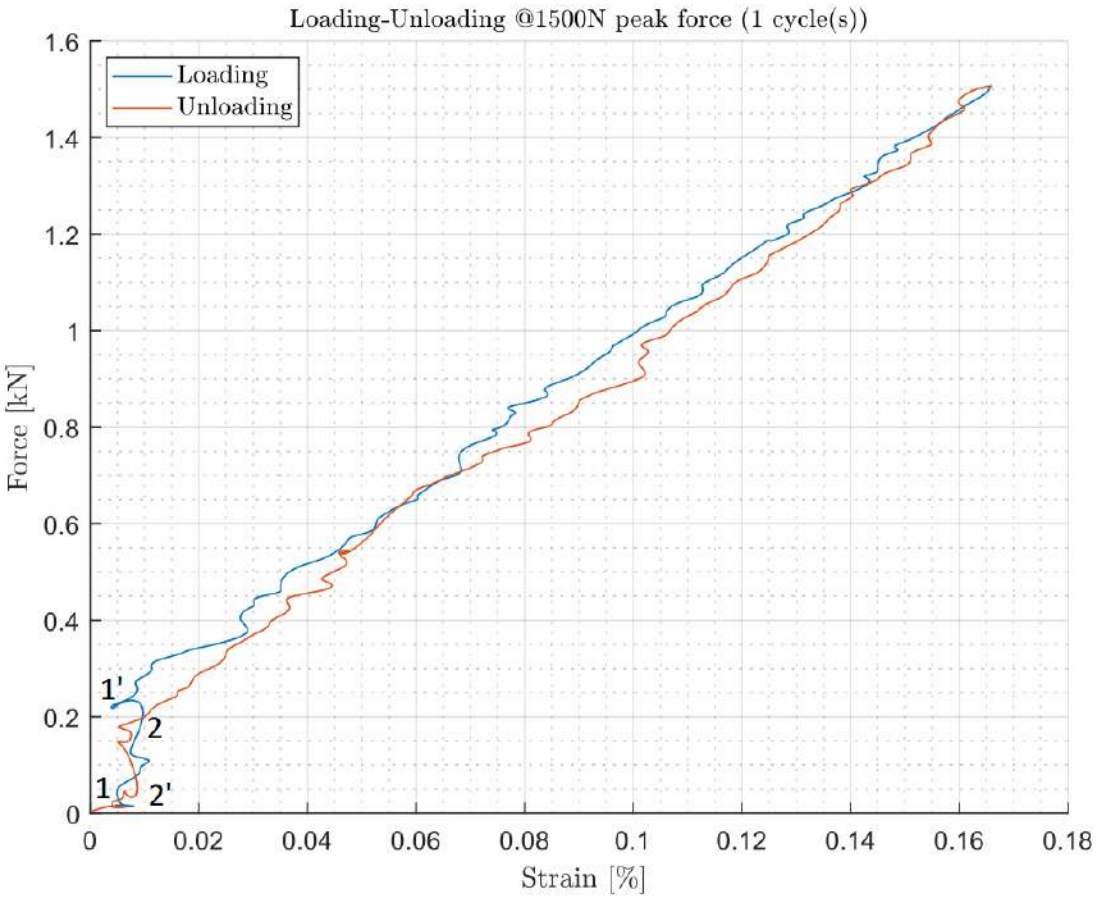

Plot 2(b): Force – Strain, test 2 - 1500N peak force

From plot 2(b) it is visible that at 1500N peak force of the honeycomb specimen has a linear behavior of force – strain and it is clearly visible that at paths 1-1’ and 2-2’ there is an increase in

force about 180-200N but zero increase in strain, which confirms this no- resistance travel as mentioned before, due to the margins of the apparatus in the system.

Maximum axial strain: ε_{max} =0.17 %

Shear Modulus: G=146.61 MPa

Final Strain: $\varepsilon_{end} = \varepsilon_{start} = 0$.

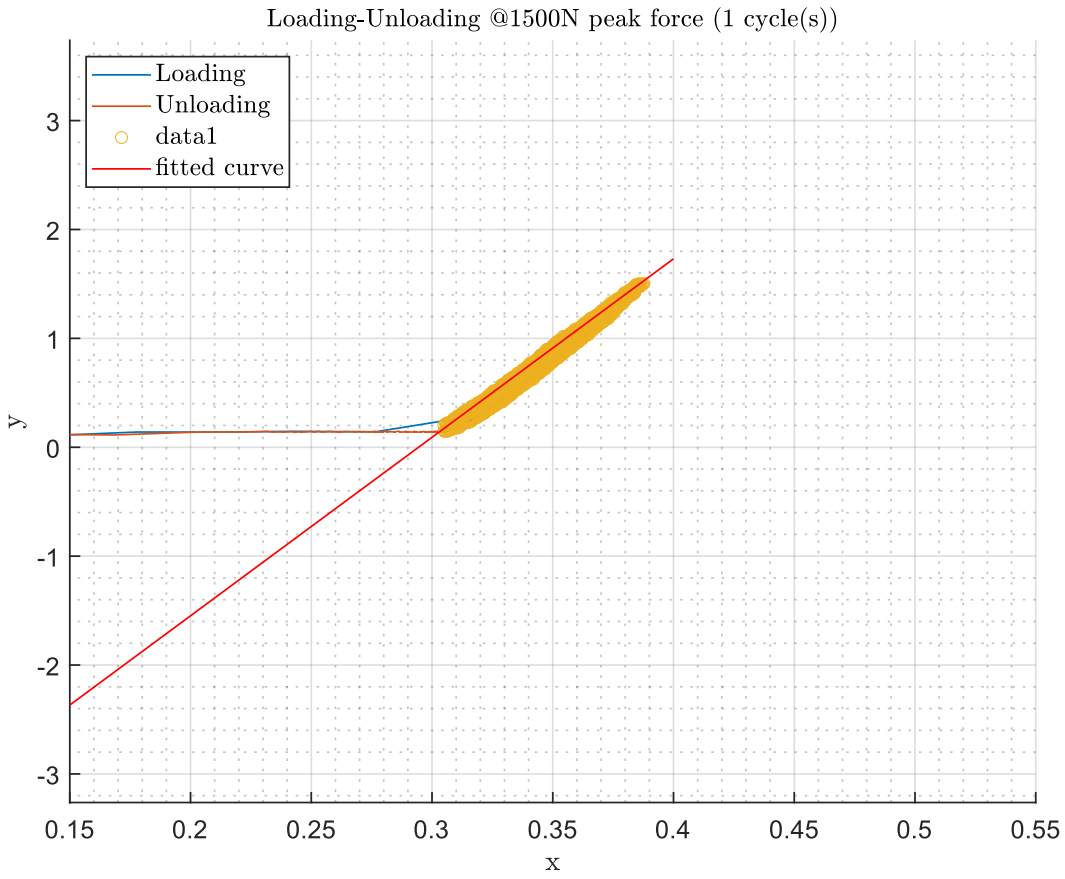

Plot 2(c): Force – Displacement fitted curve diagram at 1500 N peak force

Where, x axis interprets the displacement values in mm and y axis interprets the force values in kN.

Stiffness: S = 16.416 kN/mm

Angle of incline: $\phi = 86.515^{o}$.

Test 3 - 2000 N

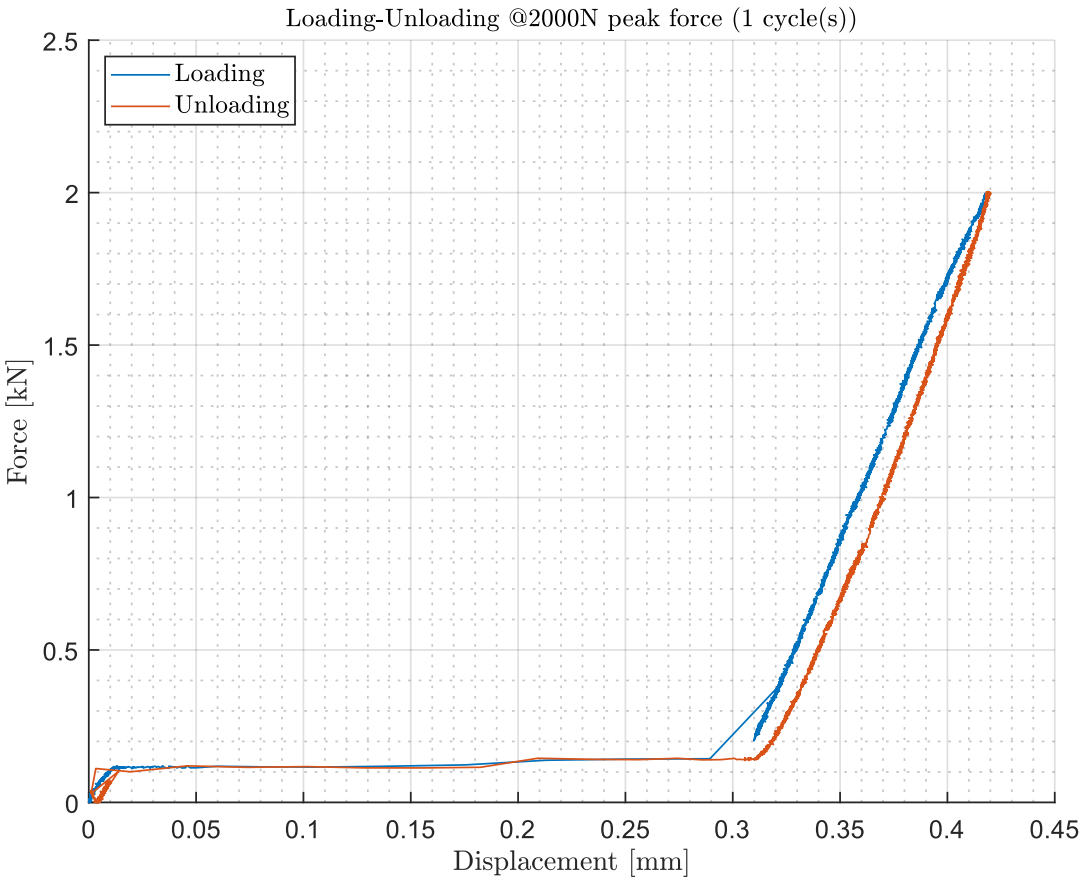

Plot 3(a): Force – Displacement, test 3 - 2000N peak force

Maximum displacement: $x_{max} = 0.4194$ mm

Actual maximum displacement: $x_{actual} = 0.4194 - 0.3099 \Rightarrow x_{actual} = 0.1095$ mm

Global shear stress of the honeycomb at maximum load: $\tau_{max} = 38.49$ MPa

Maximum shear stress of the aluminum plates: $\tau_{plates,\,max} = 0.159$ MPa

Area of hysteresis loop: W = 0.01663 Joule.

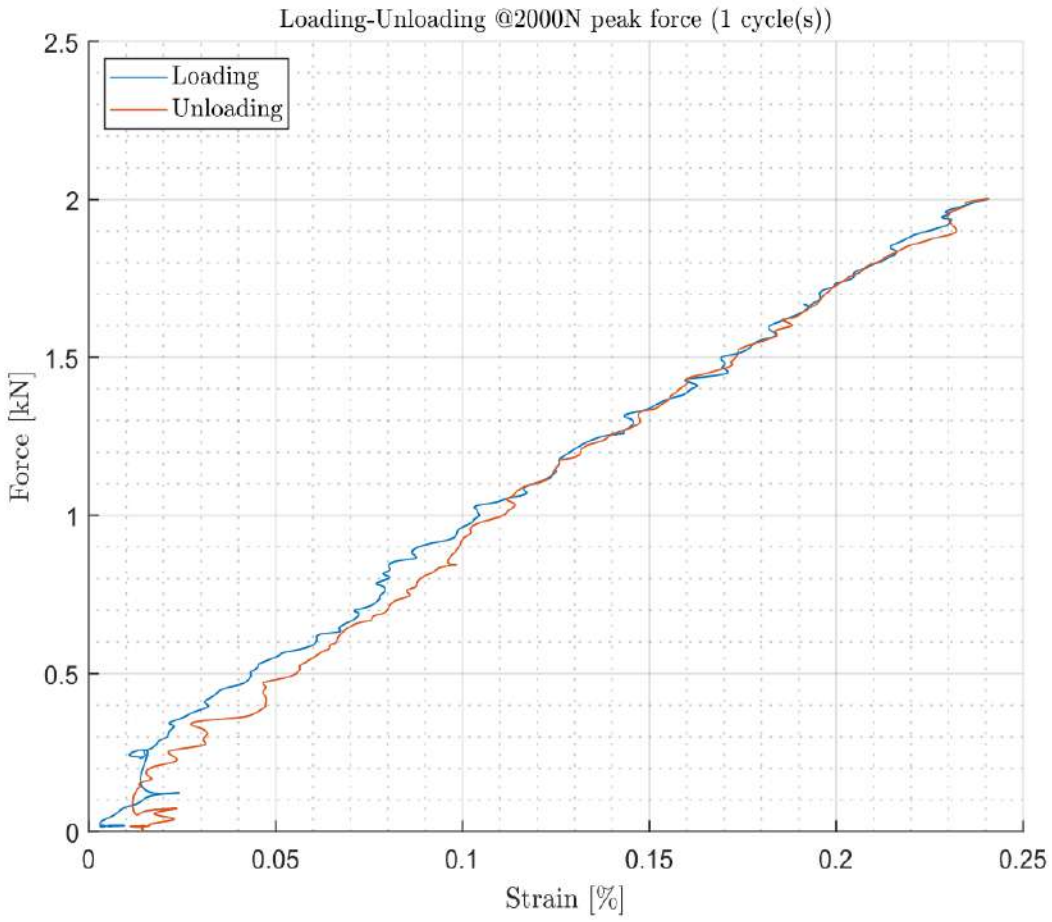

Plot 3(b): Force – Strain, test 3 - 2000N peak force

Maximum axial strain: $\varepsilon_{max} = 0.2408$ %

Shear Modulus: G= 139.863 MPa

Final Strain: $\varepsilon_{end} = 0$.

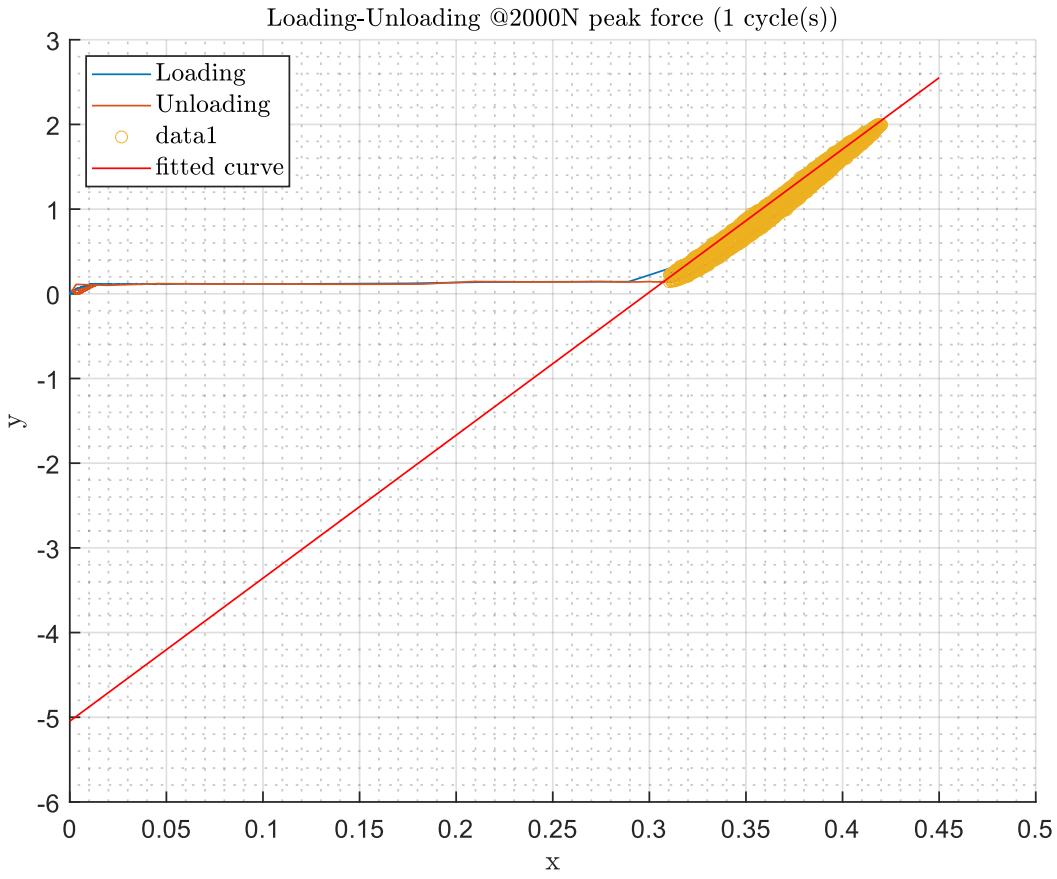

Plot 3(c): Force – Displacement fitted curve diagram at 2000 N peak force

Where, x axis interprets the displacement values in mm and y axis interprets the force values in kN.

Stiffness: S = 16.962 kN/mm

Angle of incline: $\phi = 86.626^{o}$.

Test 4 - 2500 N

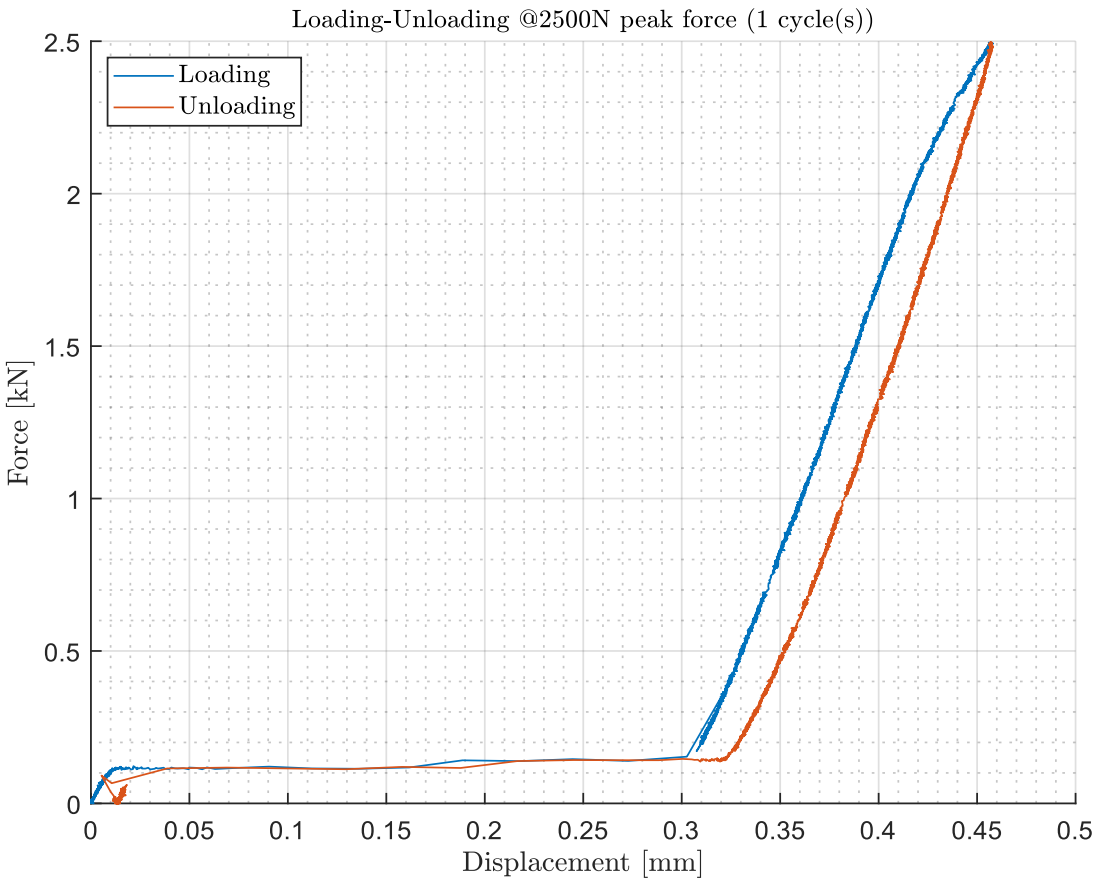

Plot 4(a): Force – Displacement, test 4 - 2500N peak force

Maximum displacement: x_{max} = 0.4573 mm

Actual maximum displacement: x_{actual} = 0.4573 – 0.3092 => x_{actual} = 0.1481 mm

Global shear stress of the honeycomb at maximum load: τ_{max} = 48.11 MPa

Maximum shear stress of the aluminum plates: $\tau_{plates,\ max}$ = 0.198 MPa

Area of hysteresis loop: W = 0.04479Joule.

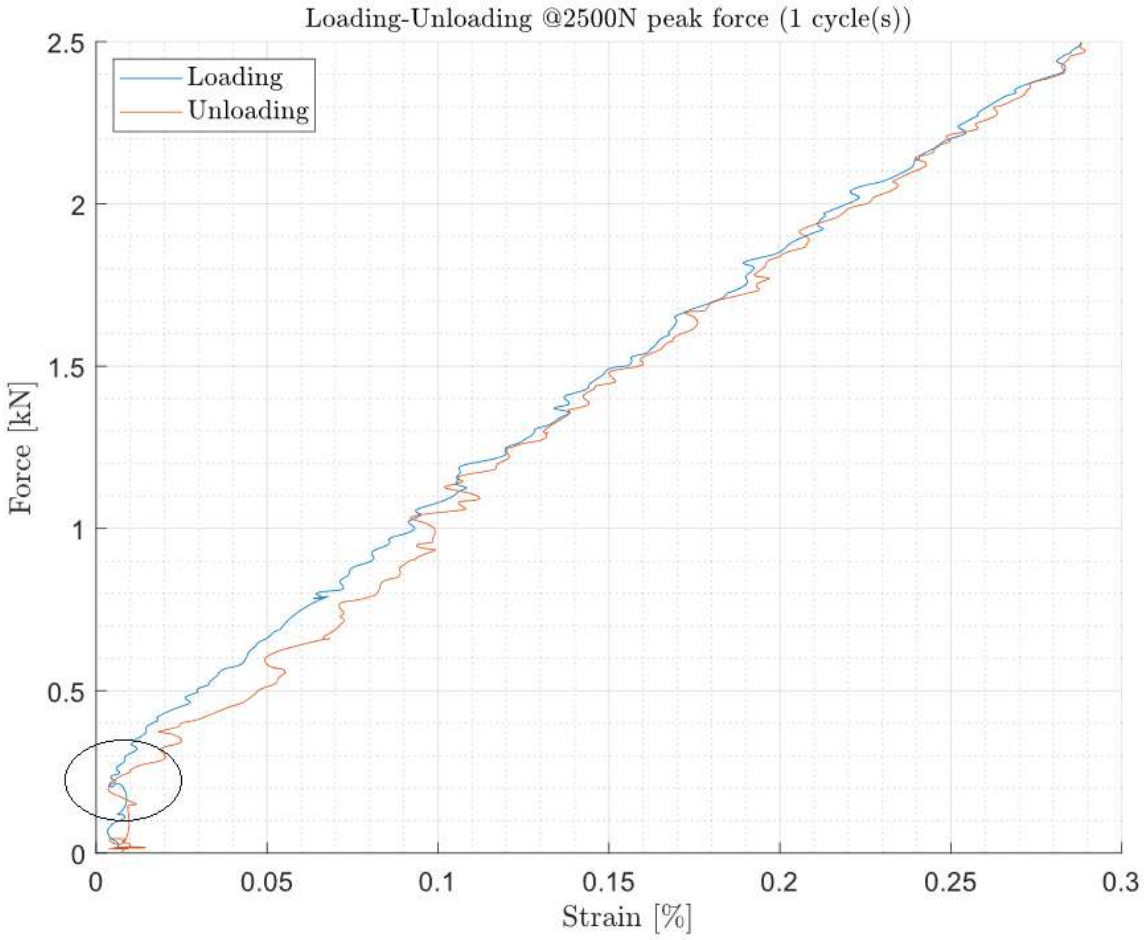

Plot 4(b): Force – Strain, test 4 - 2500N peak force

As the data at of points 1-1' and 2-2' are excluded the final strain is measured by the distance of the points of the loading and unloading path, being in the center of the cycle of plot 4(b). In this case and in the previous cases as well, this distance is zero which means that the value of the 'final' strain is zero. From Material Science theory, it is concluded that the specimen has not been subjected into plastic deformation.

Maximum axial strain: ε_{max} =0.2894 %

Shear Modulus: G= 146.303 MPa

Final Strain: ε_{end} = 0.

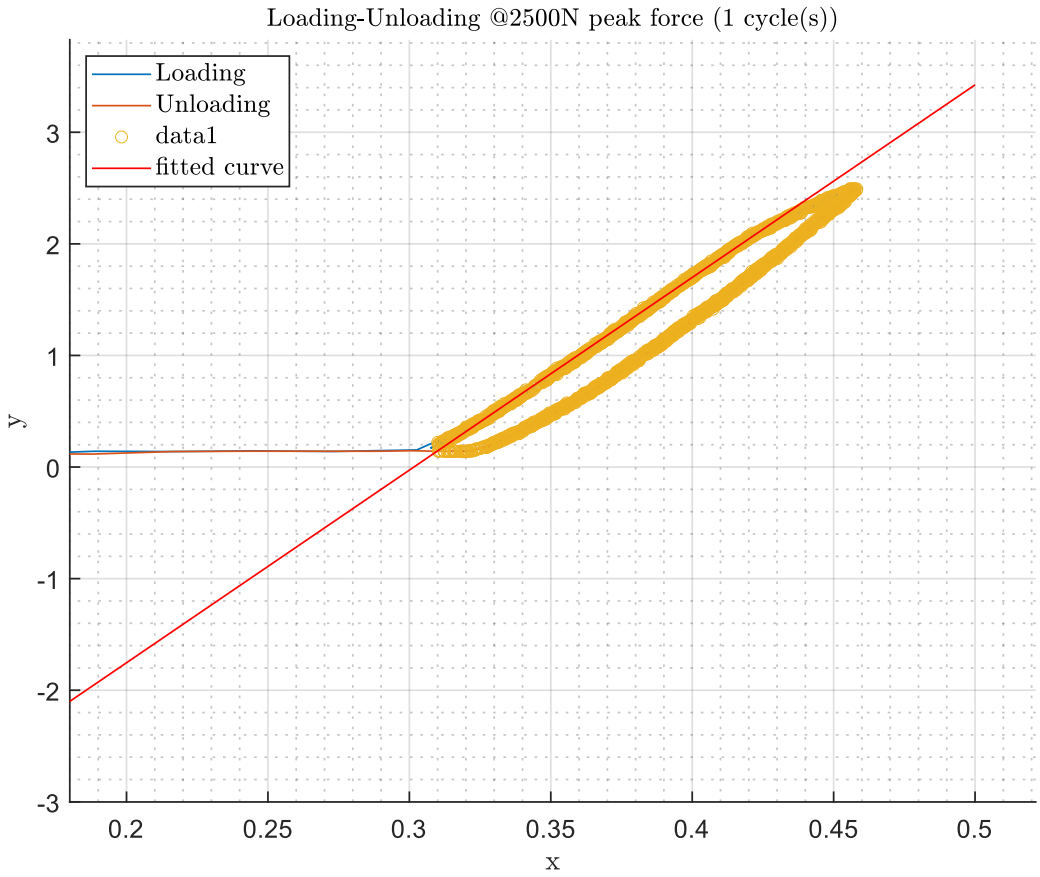

Plot 4(c): Force – Displacement fitted curve diagram at 2500 N peak force

Where, x axis interprets the displacement values in mm and y axis interprets the force values in kN.

Stiffness: S = 17.2499 kN/mm

Angle of incline: ϕ = 86.682

Test 5 - 3000 N

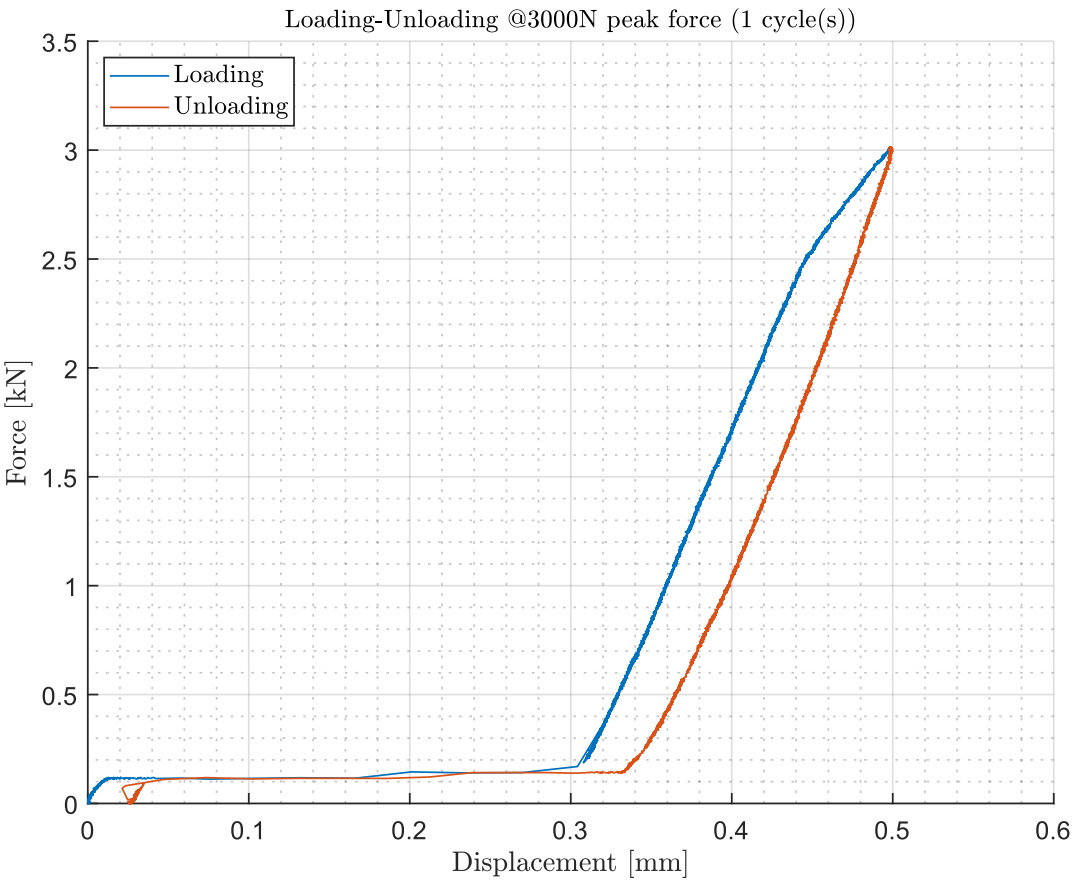

Plot 5(a): Force – Displacement, test 5 - 3000N peak force

Maximum displacement: x_{max} = 0.5 mm

Actual maximum displacement: x_{actual} = 0.5 – 0.3078 => x_{actual} = 0.1822 mm

Global shear stress of the honeycomb at maximum load: τ_{max} = 57.735 MPa

Maximum shear stress of the aluminum plates: $\tau_{plates,\ max}$ = 0.238 MPa

Area of hysteresis loop: W = 0.09456 Joule.

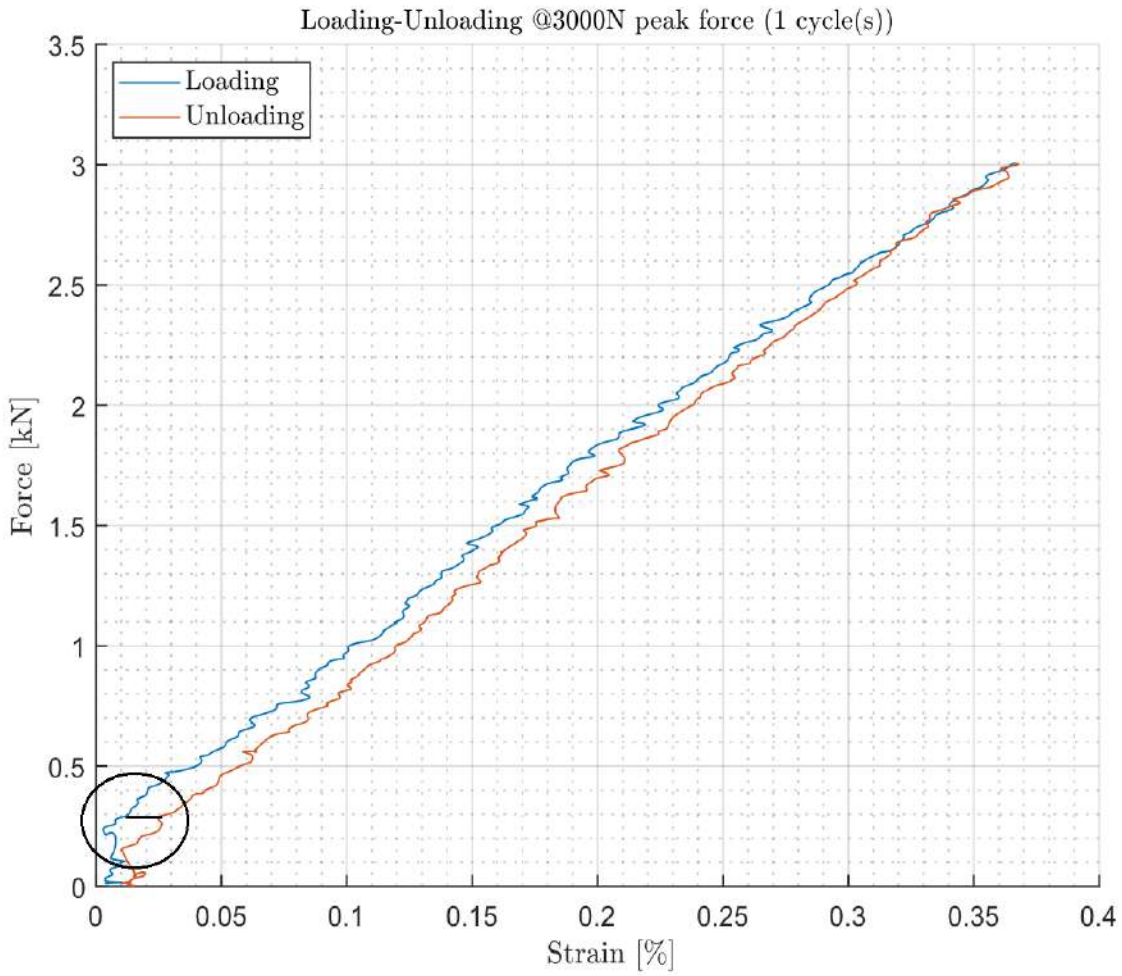

Plot 5(b): Force – Strain, test 5 - 3000N peak force

In this case of 3000 N peak force, unlike previous tests, it is observable that the path of unloading and the path of loading are not coincided and most importantly at the 'final' stage the value of strain is not zero but 0.0166%. From this information it can be concluded that the specimen has been subjected into plastic deformation (plastic buckling of the walls of the honeycomb's core).

Maximum axial strain: ε_{max} =0.3687 %

Shear Modulus: G=140.41 MPa

Final Strain: ε_{end} = 0.0166 %.

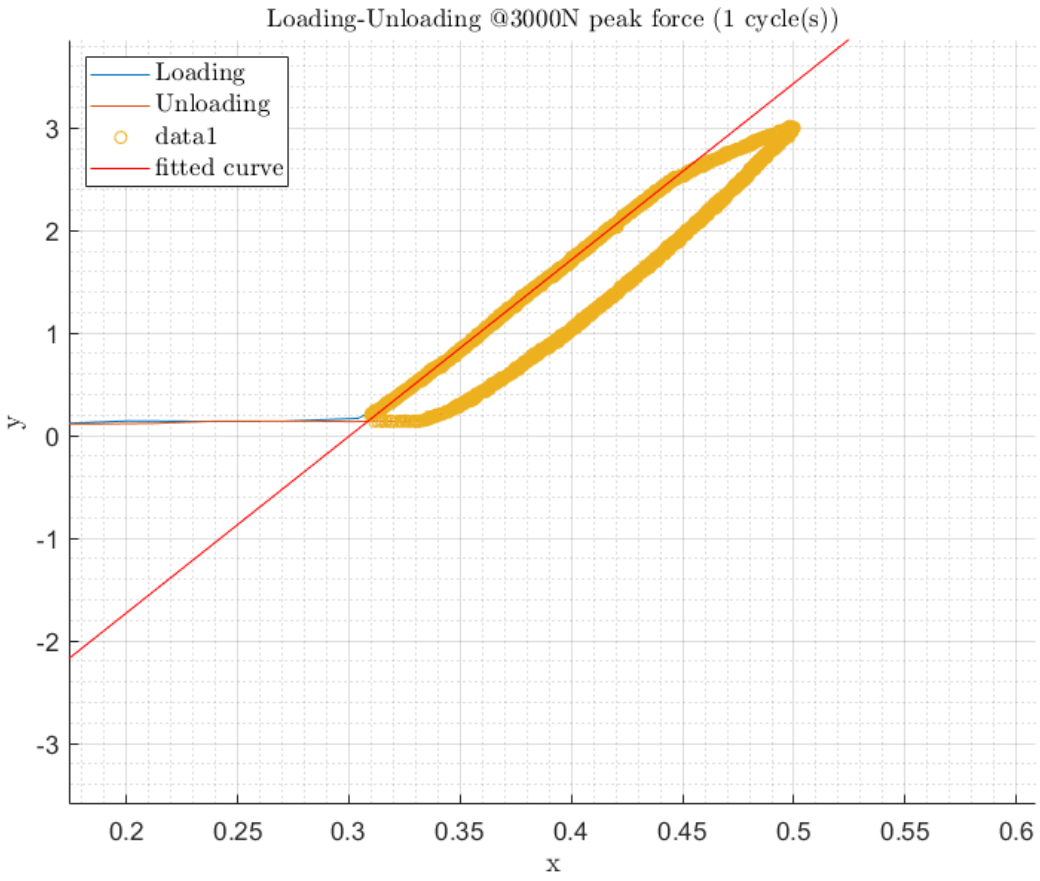

Plot 5(c): Force – Displacement fitted curve diagram at 3000 N peak force

Where, x axis interprets the displacement values in mm and y axis interprets the force values in kN.

From plot 5(c), it observable that there is a non-linear correlation of force-displacement as at the load of 2.5kN there is a change of inclination in the diagram.

Stiffness: S = 17.252 kN/mm

Angle of incline: ϕ = 86.6825°.

Test 6 - 3500 N

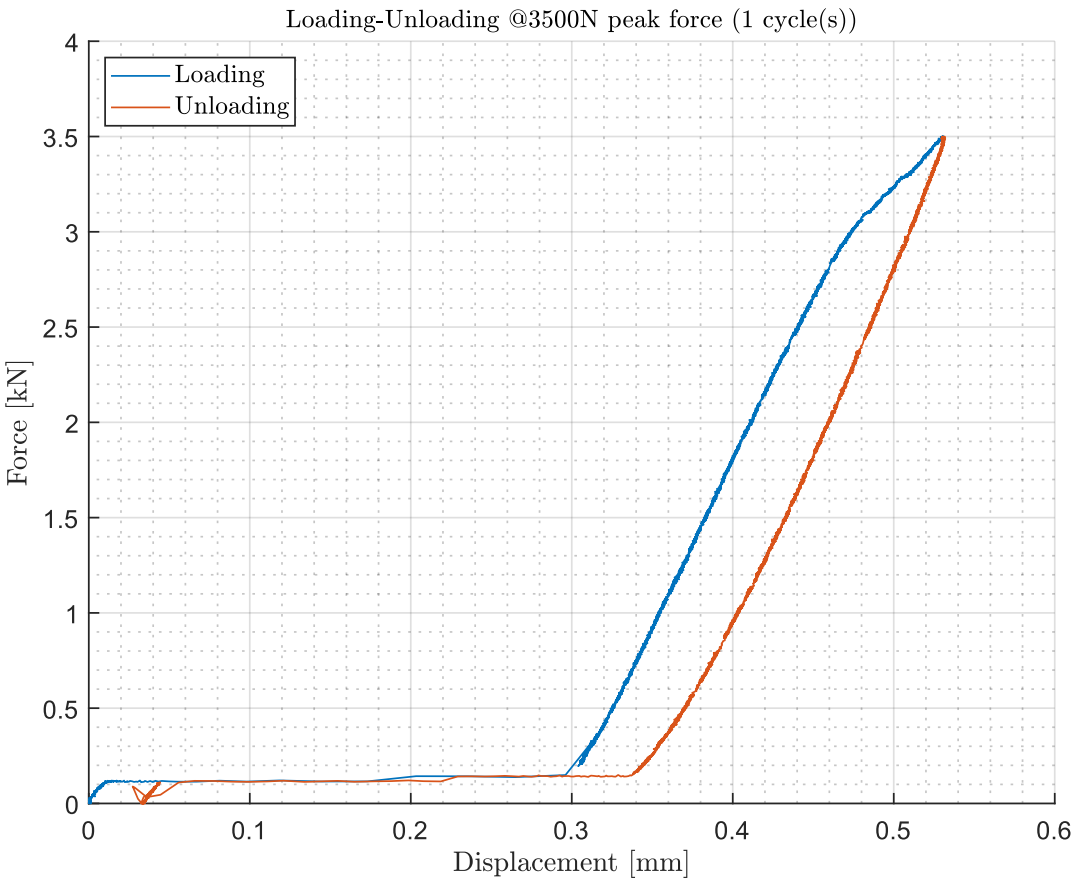

Plot 6(a): Force – Displacement, test 6 - 3500N peak force

Maximum displacement: x_{max} = 0.5316 mm

Actual maximum displacement: x_{actual} = 0.5316 – 0.3039 => x_{actual} = 0.2277 mm

Global shear stress of the honeycomb at maximum load: τ_{max} = 67.358 MPa

Maximum shear stress of the aluminum plates: $\tau_{plates,\ max}$ = 0.278 MPa

Area of hysteresis loop: W = 0.1408 Joule.

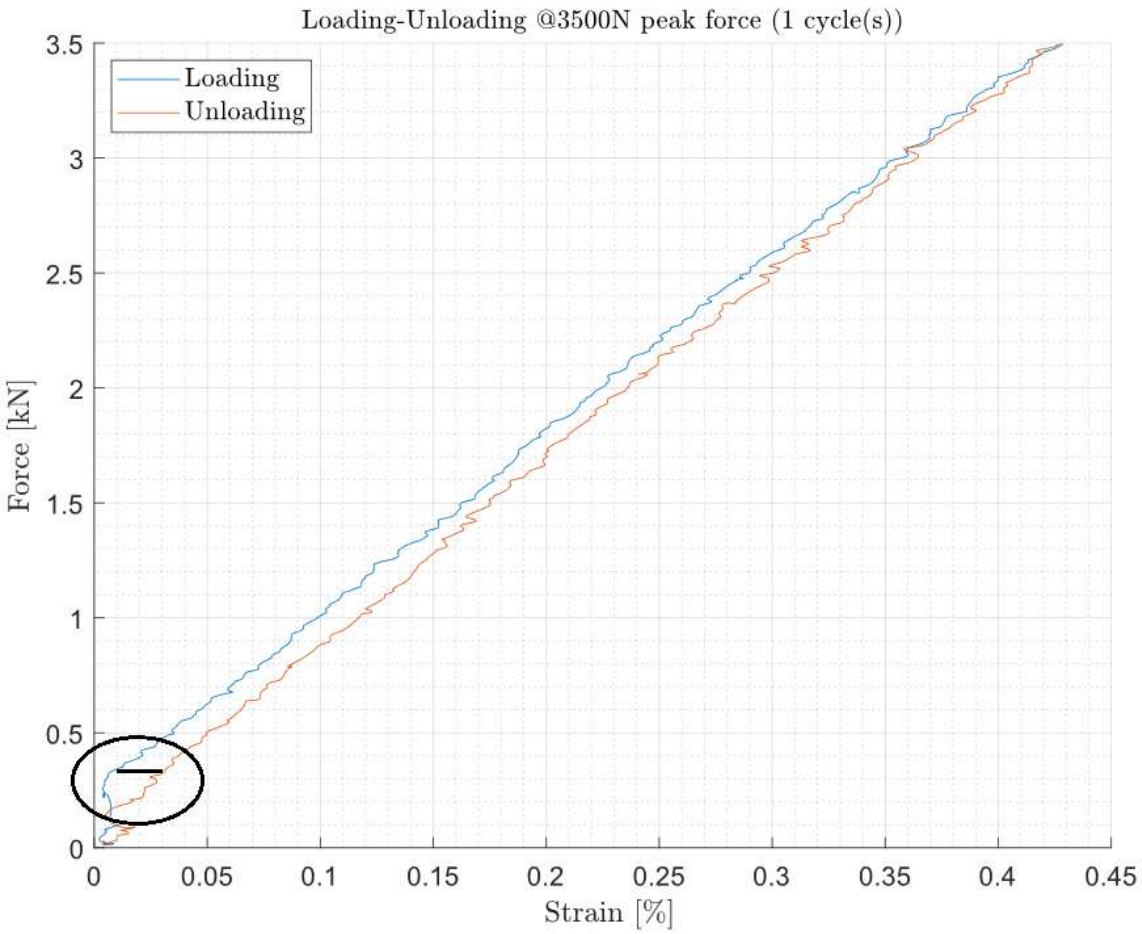

Plot 6(b): Force – Strain, test 6 - 3500N peak force

Maximum axial strain: ε_{max} =0.4275 %

Shear Modulus: G= 143.61 MPa

Final Strain: ε_{end} = 0.0181 %.

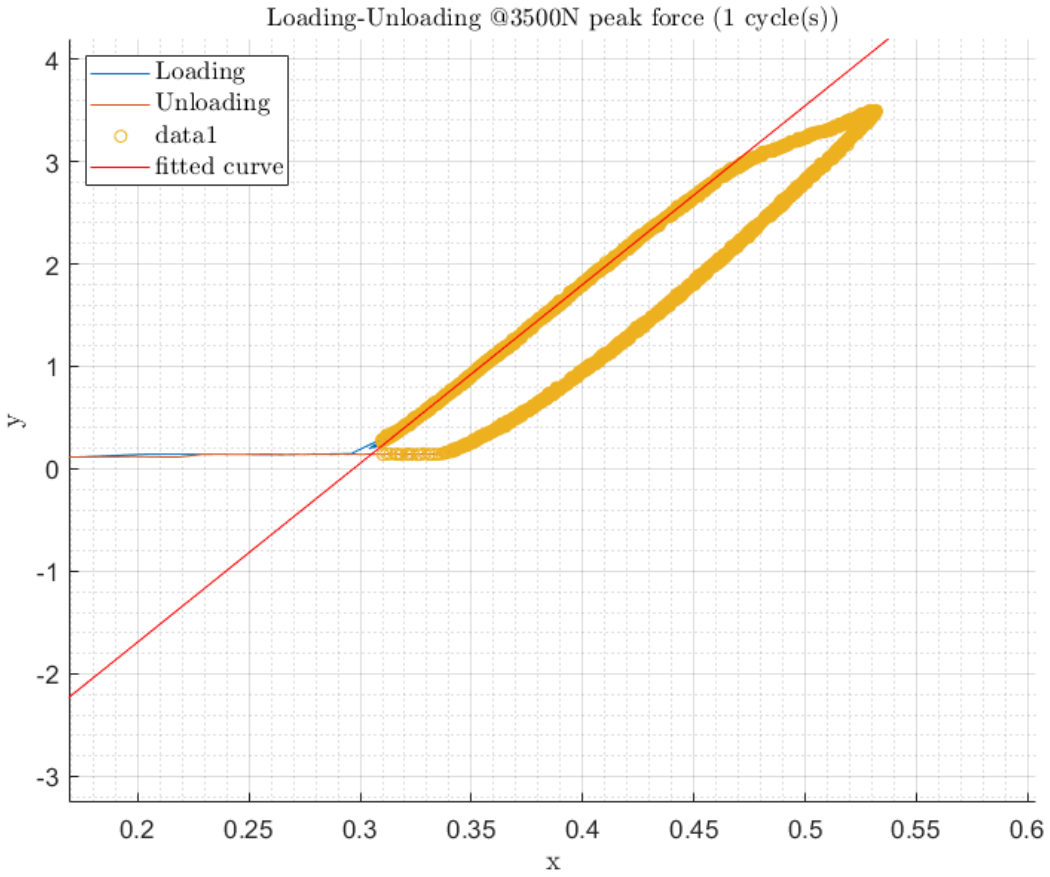

Plot 6(c): Force – Displacement fitted curve diagram at 3500 N peak force

Where, x axis interprets the displacement values in mm and y axis interprets the force values in kN.

At this case, similarly to plot 5(c), it observable that there is a non-linear correlation of force-displacement as at the load of 3kN there is a change of inclination in the diagram.

Stiffness: S = 17.35 kN/mm

Angle of incline: $\phi = 86.7^{o}$.

4.1.1 Summary of the experimental results

The following tables depict a summary of the experimental results derived from the plots: Force – Displacement and Force – Axial Strain in each measurement. More specifically, the values of the displacement, actual displacement, angular deformation, shear stress of honeycomb, shear stress of aluminum plates are the maximum values at the peak force in each test

TEST	Maximum Load	Displacement	Actual Displacement	Maximum strain	Final strain
	P [N]	xmax [mm]	xactual [mm]	εmax [%]	εend [%]
1	1000	0.3554	0.0518	0.11	0
2	1500	0.3843	0.0805	0.17	0
3	2000	0.4194	0.1095	0.2408	0
4	2500	0.4573	0.1481	0.2894	0
5	3000	0.5	0.1822	0.3687	0.0166
6	3500	0.5316	0.2277	0.4275	0.0181

Table 9: Final experimental results associated with the specimen's displacement – Load

TEST	Maximum Load	Shear Stress of honeycomb	Shear Stress of aluminum plates	Shear modulus	Area of hysteresis loop	Stiffness
	P [N]	τmax [MPa]	τ plates, max [Mpa]	G [Mpa]	W [J]	S[kN/mm]
1	1000	19.245	0.0794	139.96	0.002687	16.1
2	1500	28.868	0.119	146.61	0.008062	16.416
3	2000	38.49	0.159	139.863	0.01663	16.962
4	2500	48.11	0.198	146.303	0.04479	17.25
5	3000	57.735	0.238	140.41	0.09456	17.252
6	3500	67.358	0.278	143.61	0.1408	17.35

Table 10: Final experimental results associated with the specimen's shear stresses, modulus, area of hysteresis loop and stiffness

From tables 9,10 it is noticeable that as the force is getting increased the displacement, axial strain, shear stress of honeycomb and shear stress of aluminum plates is also increased, as expected. The interesting observation is that in the experiments where the value of the peak load

was equal or greater than 2000N, at the end of the unloading path where the force had zero value, the final displacement and final strain had non zero values, which implies that the specimens were subjected in to plastic deformation.

4.2 Quality control & comparison of behavior between UTH and RWTH's specimen

In consultation with Professor Kermanidis and Professor Dafnis, who is in charge of the laboratory of the Department of Mechanical Engineering at RWTH University for experiments on honeycomb structures, Mr. Dafnis and his students prepared some honeycomb specimens that were ready for tests. Their way of curing the specimens, which is when a specimen is put at the mechanical convection oven, a fixed barium object is placed upon it in order to create a uniform pressure on the entire surface, is different than the one that is applied on the process presented on this study. Hence, it was important to conduct the same tests with these two 'different' specimens to determine if the adhesive bonding is reliable and furthermore, to perform a quality control. The plots are presented below:

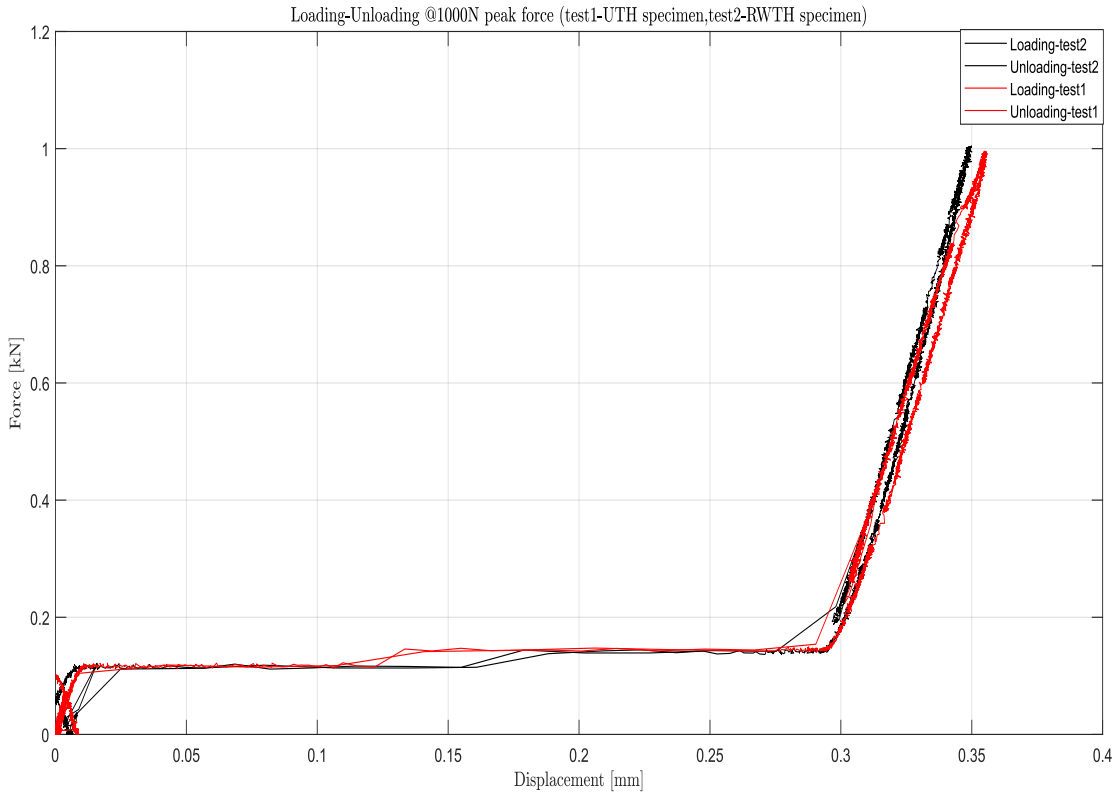

Plot 7: Force – Displacement comparison diagram at 1000N peak force

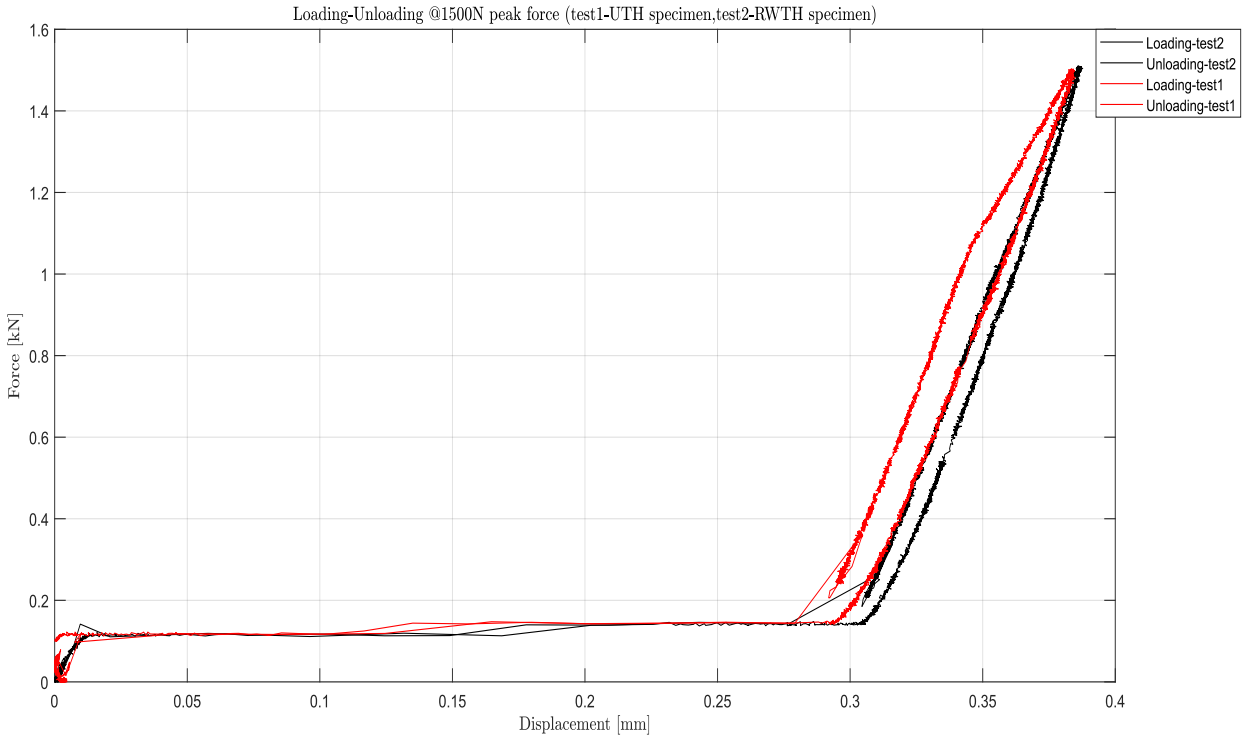

Plot 8: Force – Displacement comparison diagram at 1500N peak force

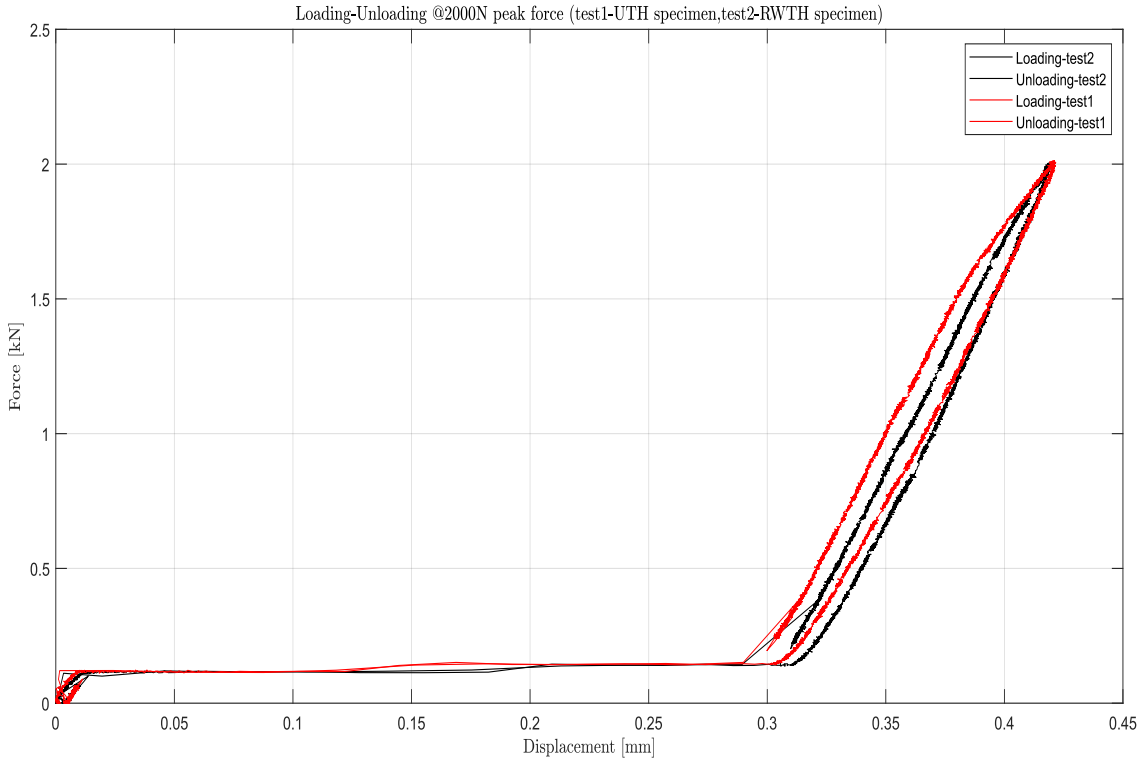

Plot 9: Force – Displacement comparison diagram at 2000N peak force

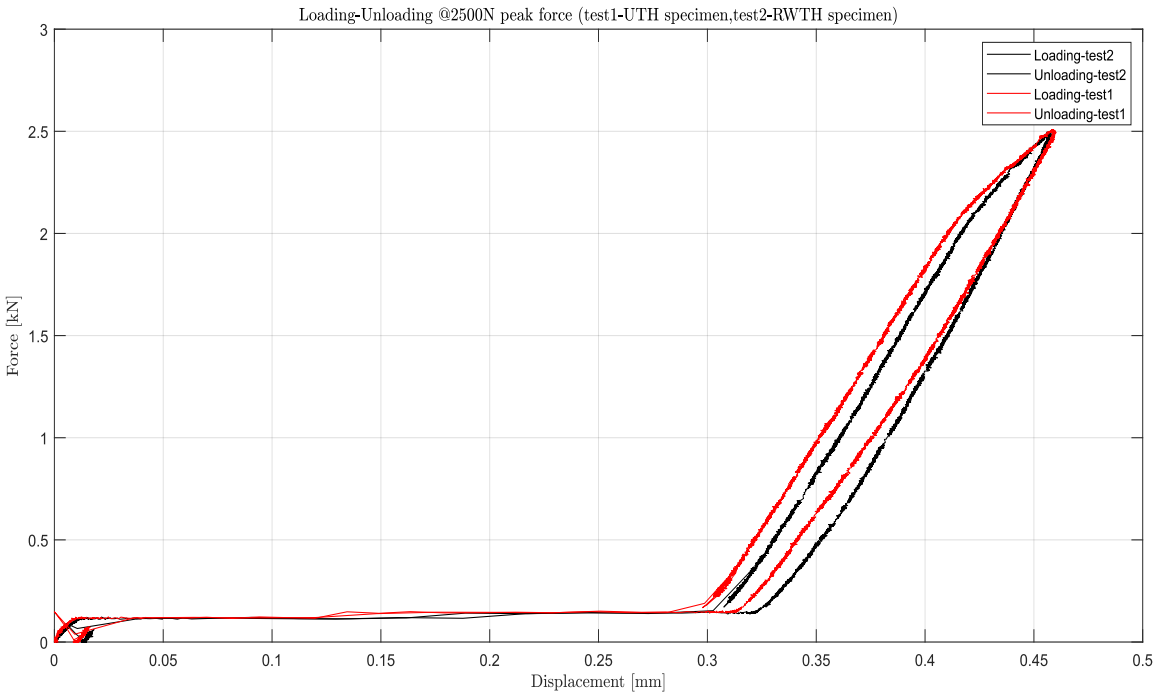

Plot 10: Force – Displacement comparison diagram at 2500N peak force

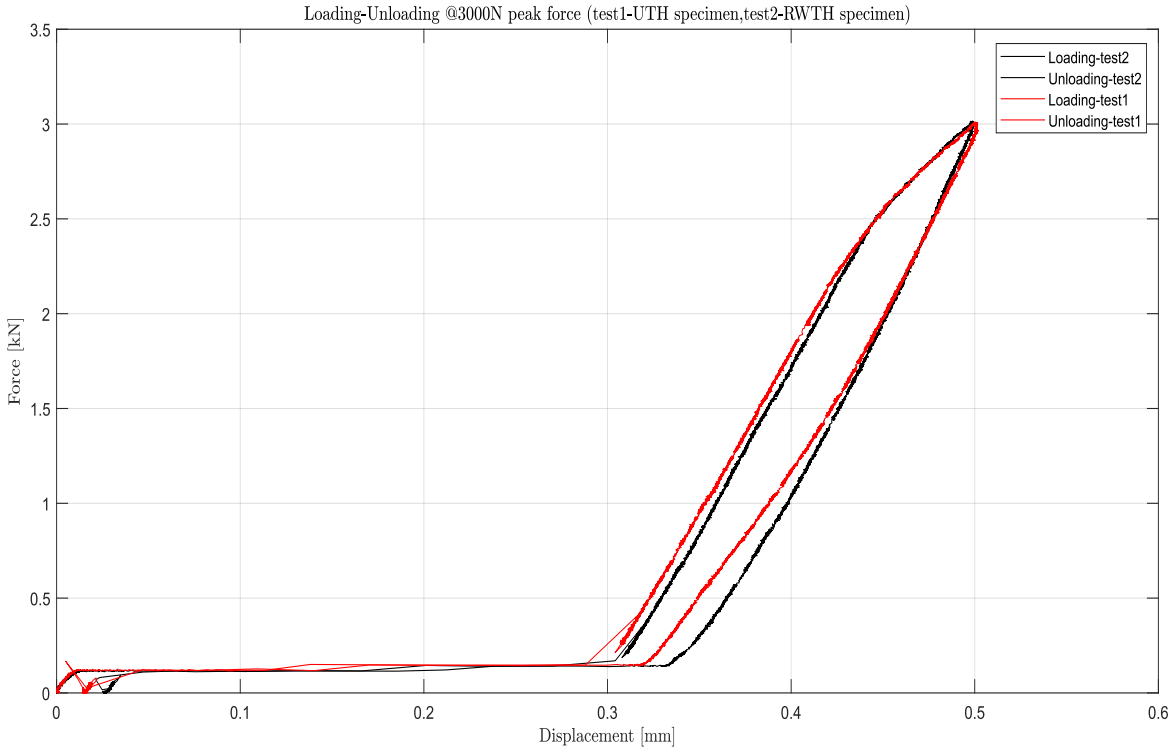

Plot 11: Force – Displacement comparison diagram at 3000N peak force

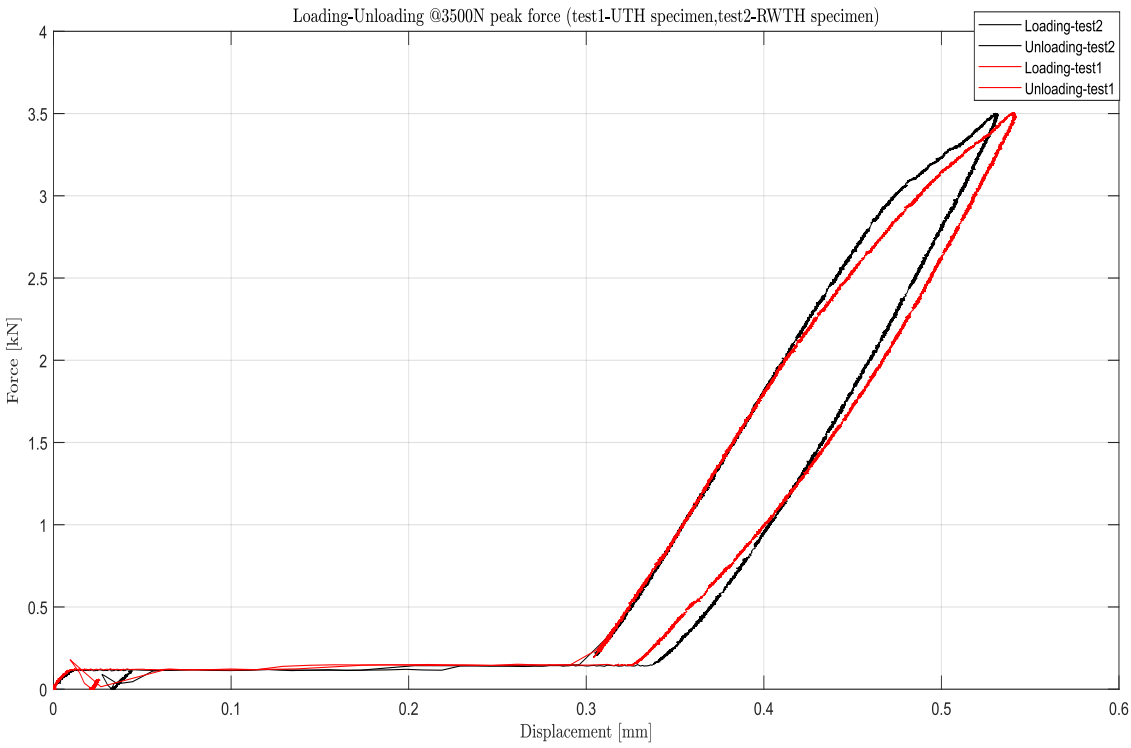

Plot 12: Force – Displacement comparison diagram at 3500N peak force

From the presented comparison plots, it can be derived that the RWTH's specimen behavior is almost identical to the UTH's specimen at every loading-unloading test, so it can be concluded that the way of adhesive bonding and curing the specimen, by the method of applying the four clamps upon it, is successful, reliable and sufficient.

4.3 Examples of repetitive loading-unloading tests (at 3,5,10 cycles)

The figures presented below are some examples of fatigue tests of honeycomb specimen at:

- 1500 N peak force – 5 cycles (Force – Axial strain plot)
- 2000 N peak force – 10 cycles (Force - Displacement plot)
- 25000 N peak force – 3 cycles (Force - Displacement plot)

It is important to mention that these tests were conducted with force value above the range of 110 – 150 N in order to avoid the rapid horizontal phenomenon, as discussed in chapter 4.1.

<u>test 1 (5 cycles @ 1500 N)</u>

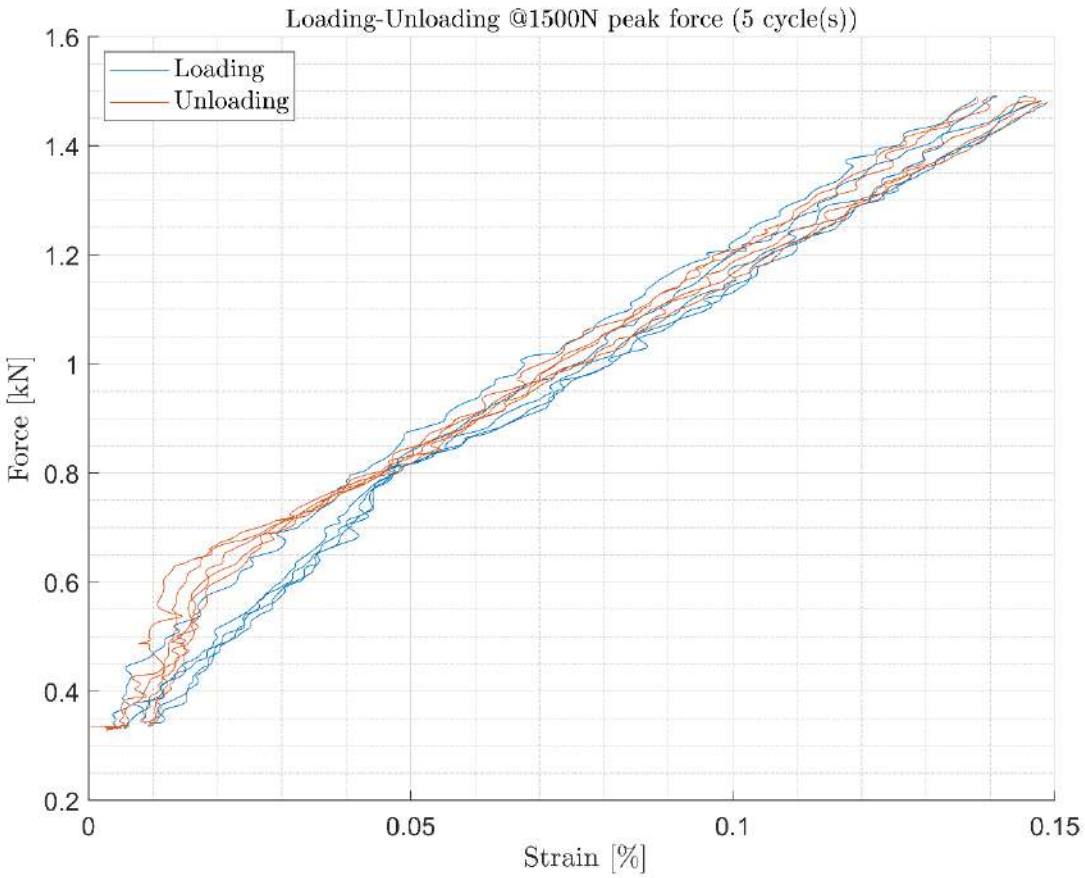

Plot 13: Force – Strain diagram for 5 cycles at 1500 N

From plot 13, it is noticeable that in these 5 cycles of loading and unloading at 1500 N, in each cycle: $\varepsilon_{start} = \varepsilon_{end}$, and especially, $\varepsilon_{1,\,start} = \varepsilon_{final} \approx 0$. This data and behavior of the material were expected, since from plot 2(a) and plot 2(b) it was observed that the specimen at the load of 1500 N is not being subjected at plastic deformation.

test 2 (10 cycles @ 2000 N)

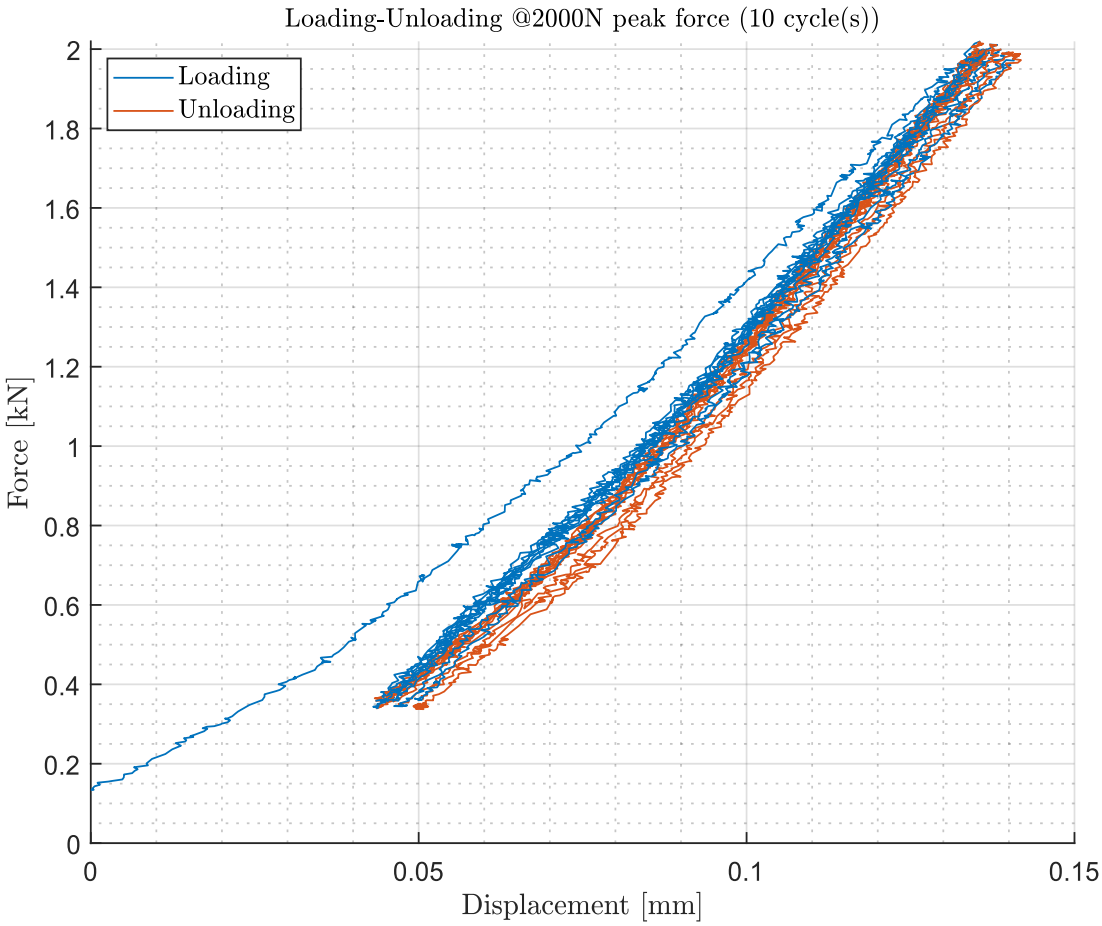

Plot 14: Force – Displacement diagram for 10 cycles at 2000 N

Cycle	i	1	2	3	4	5	6	7	8	9	10
Final displacement	xend [mm]	0.04312	0.04342	0.04353	0.0445	0.04543	0.04552	0.04604	0.04759	0.05057	0.05077

Table 11: Numerical data for the final displacement at the end of each cycle for plot 14

From plot 14, it is observed that in each cycle: $x_{start} \neq x_{end}$ and also it is clearly seen that x_{end} is increasing by each cycle. From table 11, the average value of this rate increase of the displacement is calculated as: 0.00085 mm/cycle.

Test 3 (3 cycles @ 2500 N)

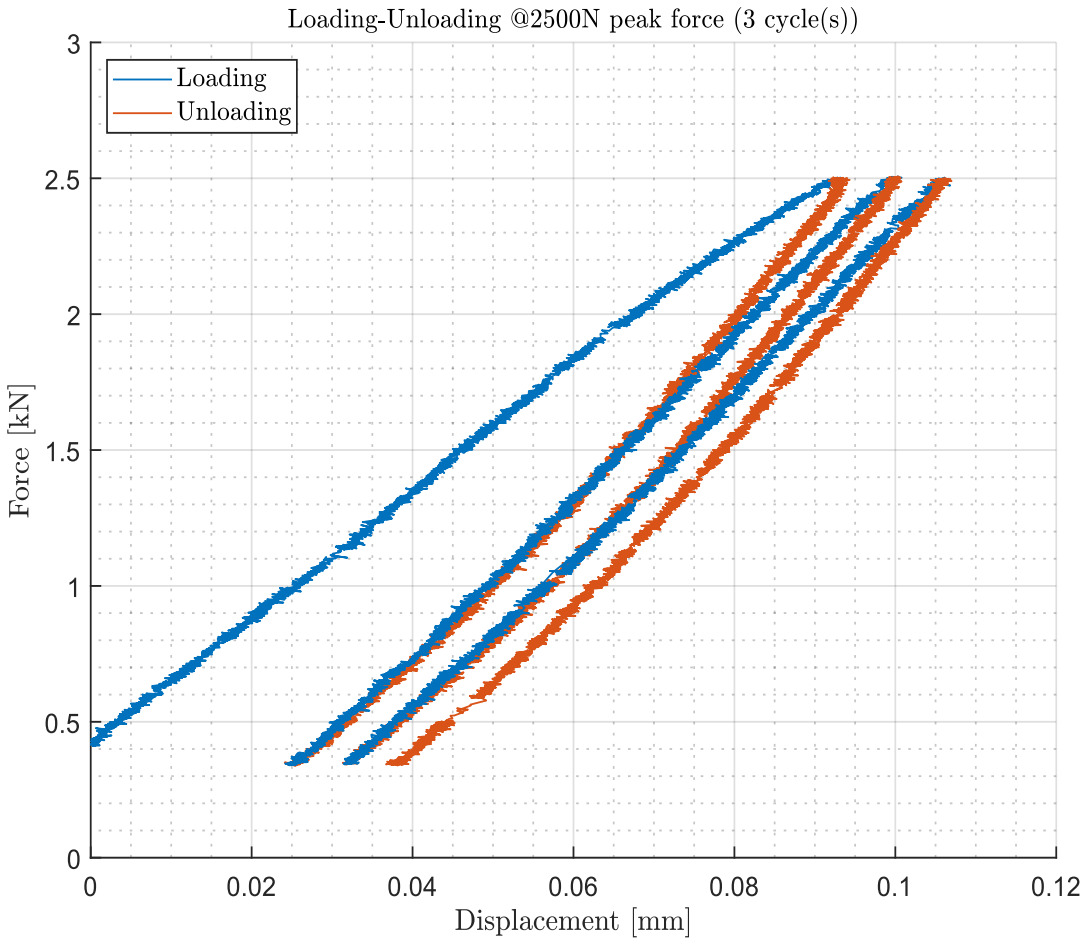

Plot 15: Force – Displacement diagram for 3 cycles at 2500 N

	i	1	2	3

Cycle				
Final displacement	xend [mm]	0.0255	0.0324	0.0395

Table 12: Numerical data for the final displacement at the end of each cycle for plot 15

Similarly, as test 2, it is more easily noticed that the final displacement of each cycle is getting increased with a greater rate than the one in plot 14, as it is expected due to the bigger peak force. From table 12, the average value of this rate increase of the displacement is calculated as: 0.0070 mm/cycle.

Chapter 5. CONCLUSIONS

In this study, the behavior of aluminum hexagonal honeycomb sandwich structure was examined, under loading-unloading and fatigue tests. The required necessary equipment for creating a specimen ready for shear tests, under the ASTM C273 specification, was presented as well as the thermal process for successful adhesive bonding. In contrast to previous theses, at the laboratory of engineering and materials of the University of Thessaly, which have been associated with honeycomb material experiments, apart from the MTS (hydraulic press system), the video-extensometer RTSS (contactless strain sensor for material testing) was also installed and utilized in the experiments conducted. The video-extensometer proved to be very useful, as through the direct measurement of the deformation on the specimen, provided information about the longitudinal strain and furthermore information about its behavior.

From the loading-unloading diagrams it was derived that at the first tests with 1000 and 1500 N peak force, the specimen showed a linear elastic behavior as the final strain and displacement had zero value ($\varepsilon_{start} = \varepsilon_{final} = 0$, $x_{start} = x_{final} = 0$). When the peak force had a value of 2000N or greater, it was noticed that the final strain and displacement did not have a zero value. Furthermore, in each increase of the load, these final values were increasing, as expected. According to material science it was concluded that the specimen was subjected to plastic deformation. Additionally, an interesting phenomenon that was observed during the tests is that in each test (from test 1 to test 6 and fatigue tests as well) there was an area of hysteresis loop created. This area is schemed in diagrams of Force-Displacement and by calculating it, the measurement units of it are: kN × mm = J. This fact implies that this area is created due to an energy activity that is taking place during the procedure.

The optimal way of making a successful bonding at the honeycomb specimen, between the honeycomb core and aluminum plates, is to perform a uniform pressure at the entire surface of the top aluminum plate with a fixed barium, once the specimen is getting into the mechanical convection oven. Due to size limitations of the mechanical convection oven used in this study, for the heat treatment, the pressure performed on the specimen is done by four clamps applying pressure until there is a 0.4mm of compressive displacement uniformly at the specimen. In consultation with RWTH university, a specimen with the optimal way of bonding was given for experiments. So, it was necessary to perform the same loading-unloading tests, in order to clarify if the way of bonding presented in this thesis was reliable. After quality and quantity control of the plots (chapter 4.2), it was concluded that the deviations shown in the diagrams are really small, therefore they can be considered negligible, and the method of bonding with applying four clamps is successful, reliable and sufficient.

Finally, some repetitive loading- unloading tests at 1500,2000 and 2500 N were conducted at 5,3,10 cycles respectively. At the case of 1500 N – 5 cycles, from the diagram of Force [kN] – Axial Strain [%], it was clear that the specimen had a linear elastic behavior ($\varepsilon_{1,\,start}$ =

$\varepsilon_{final} \approx 0$), as expected. In the tests though of 2000 N – 3 cycles and 2500 N – 10 cycles, from the diagrams of Force [kN] – Displacement [mm], it was observed that the specimen was subjected to plastic deformation and the increase rate of displacement by each cycle was calculated at both tests.

The main conclusions derived from this study are presented below:

- Shear tests were conducted for study of the behavior of honeycomb core of aluminum 5052 according to ASTM standard C273.

- From the Force-Displacement diagrams, the behavior of honeycomb specimen showed inelastic behavior at peak forces equal or greater than 3000N.

- Installation of video-extensometer RTSS, that provided direct optical images of the specimen and helped to establish the conclusions about honeycomb's plastic behavior.

- It has been confirmed that the method of applying four clamps on the specimen for adhesive bonding and curing in the mechanical convection oven is reliable, effective and successful.

- Finally, some repetitive loading-unloading shear tests were conducted that gave information about honeycomb's behavior at 1500,2000 and 2500N of peak force.

Below, there are some suggestions for future studies in continuity of this thesis results:

Suggestions for future improvements:

- Loading - unloading tests from 4000 - 5500 N peak force (which is close to the critical force value of specimen's failure) in order to collect data about the behavior of the specimen.
- Fatigue tests until failure from 2000 – 5500 N peak force.
- Fatigue tests with displacement control at different rates of mm/s (or N/s for force control).
- Experimental investigation of the hysteresis loop area in order to find out why and how this phenomenon is caused (e.g., elastic/plastic buckling of the core's walls? due to the apparatus system? etc.)
- Use of FEM (finite element method), recreating the test in computational resources.

Using the RTSS video-extensometer camera to capture video and images of specimen's deformation is highly recommended in each test, since it can provide really useful information and data.

Chapter 6. REFERENCES

[1] The Fibre Reinforced Plastic & Composite Technology Resource Centre (2010, December 12). Sandwich Composite and Core Material. Retrieved from http://www.fibre-reinforced-plastic.com/2010/12/sandwich-composite-and-core-material.html

[2] AKTAY, Levent; JOHNSON, Alastair F.; KRÖPLIN, Bernd-H. Numerical modelling of honeycomb core crush behaviour. Engineering Fracture Mechanics, 2008, 75.9: 2616-2630. DOI: https://doi.org/10.1016/j.engfracmech.2007.03.008

[3] Ju Wang, Rahul Rai: Classification of Bio-Inspired Periodic Cubic Cellular Materials Based on Compressive Deformation Behaviors of 3D Printed Parts and FE Simulations. DOI: 10.1115/DETC2016-59729

[4] Shubham V. Rupani, Shivang S. Jani, G.D.Acharya: Design, Modelling and Manufacturing aspects of Honeycomb Sandwich Structures: A Review. DOI: 10.1712/ijsdr.17013

[5] Boubekeur Moahammed Bilel Mertani, Boualem Keskes, Mostapha Tarfaoui: Numerical study on the compressive behaviour of an aluminium honeycomb core DOI:10.17222/mit.2018.028

[6] Corex Honeycomb: BS EN ISO 1716:2018**:** Aluminium honeycomb core material for the rail sector https://corex-honeycomb.com/applications/rail/

[7] O.Ganilova, J. Low: Application of smart honeycomb structures for automotive passive safety. DOI: 10.1177/0954407017708916

[8] Nermin M. Aly: A review on utilization of textile composites in transportation towards sustainability DOI:10.1088/1757-899X/254/4/042002

[9] J.Smits: Architectural engineering of FRP bridges
DOI:10.2749/222137814814067383

[10] Pan, S. D., Wu, L. Z., Sun, Y. G., Zhou, Z. G., & Qu, J. L. (2006). Longitudinal shear strength and failure process of honeycomb cores. Composite Structures, 72(1), 42-46. DOI:10.1016/j.compstruct.2004.10.011

[11] BIANCHI, Gabriel; AGLIETTI, Guglielmo S.; RICHARDSON, Guy. Static and fatigue behaviour of hexagonal honeycomb cores under in-plane shear loads. Applied Composite Materials,honeycomb sandwich structure. Journal of Reinforced Plastics and Composites,2021. DOI: 10.1007/s10443-010-9184-5

[12] HODGE, A. J.; NETTLES, Alan T. A novel method of testing the shear strength of thick honeycomb composites. 1991. https://www.researchgate.net/publication/24325864_A_novel_method_of_testing_the_shear_strength_of_thick_honeycomb_composites

[13] LIU, Yue; LIU, Wei; GAO, Weicheng. Out-of-plane shear property analysis of Nomex honeycomb sandwich structure. Journal of Reinforced Plastics and Composites, 2021, 40.3-4: 165-175. https://doi.org/10.1177/0731684420943285

[14] COTE, François; DESHPANDE, Vikram; FLECK, Norman. The shear response of metallic square honeycombs. Journal of Mechanics of Materials and Structures, 2006, 1.7: 1281-1299. DOI: 10.2140/jomms.2006.1.1281

[15] YANG, Mijia; QIAO, Pizhong. Quasi-static crushing behavior of aluminum honeycomb materials. Journal of Sandwich Structures & Materials, 2008, 10.2: 133-160. DOI: https://doi.org/10.1177/1099636207078647

[16] SOLMAZ, Murat Yavuz; TOPKAYA, Tolga. The Flexural Fatigue Behavior of Honeycomb Sandwich Composites Following Low Velocity Impacts. Applied Sciences, 2020, 10.20: 7262. DOI: https://doi.org/10.3390/app10207262

[17] Wahl, L., Maas, S., Waldmann, D., Zürbes, A., & Frères, P. (2014). Fatigue in the core of aluminum honeycomb panels: Lifetime prediction compared with fatigue tests. International Journal of Damage Mechanics, 23(5), 661-683. https://doi.org/10.1177/1056789513505892

[18] L. J. Gibson and M. F. Ashby, Cellular solids: structure and properties, 2nd ed. Cambridge; New York: Cambridge University Press, 1997. https://doi.org/10.1017/CBO9781139878326

[19] H. X. Zhu and N. Mills, "The in-plane non-linear compression of regular honeycombs," International Journal of Solids and Structures, vol. 37, pp. 1931-1949, 2000. DOI: 10.1016/S0020-7683(98)00324-2

[20] W. Warren, A. Kraynik, and C. Stone, "A constitutive model for two-dimensional nonlinear elastic foams," Journal of the Mechanics and Physics of Solids, vol. 37, pp. 717-733, 1989. DOI: https://doi.org/10.1016/0022-5096(89)90015-X

[21] Youming Chen*, Raj Das and Mark Battley, Centre for Advanced Composite Materials, Department of Mechanical Engineering, University of Auckland, Auckland 1010, New Zealand
DOI: 10.1115/1.4032964

[22] S. P. Timoshenko and J. M. Gere, "Theory of elastic stability. 1961," ed: McGraw-Hill, New York, 1961. https://doi.org/10.1243/03093247V071044

[23] T. Beléndez, C. Neipp, and A. Beléndez, "Large and small deflections of a cantilever beam," European Journal of Physics, vol. 23, p. 371, 2002. DOI: 10.1088/0143-0807/23/3/317

[24] L.-H. Lan and M.-H. Fu, "Nonlinear constitutive relations of cellular materials," AIAA journal, vol. 47, pp. 264-270, 2009. DOI: 10.2514/1.39531

[25] PAMG-XR1 5052 Aluminum Honeycomb, Datasheet from PLASCORE 05.10.2021

https://www.plascore.com/honeycomb/honeycomb-cores/aluminum/pamg-xr1-5052-aluminum-honeycomb/

[26] Πειραματική μελέτη της επίδρασης του πάχους κόλλησης και του ύψους κυψελίδας στην συμπεριφορά κόπωσης με διάτμηση κυψελοειδών δομών από αλουμινιο, 2020, Ευάγγελος Ψηλός,pages 13-16

[27] Standard, A. S. T. M. (2013). Standard test method for shear properties of sandwich core materials. ASTM Int, 1-7, p2.

http://file.yizimg.com/86194/2009081802421443.PDF

[28] Aluminum 5052-H32, Datasheet from protolabs 05.10.2021

https://www.wanji-aluminium.com/products/aluminium_plate_sheet/5052_aluminum_plate_sheet.html

[29] HexBond 609 modified epoxy film adhesive, Datasheet from HEXCEL 05.10.2021

https://www.imatec.it/wp-content/uploads/2021/02/HexBond_609_DataSheet_eu.pdf

[30] Πειραματική διερεύνηση της μηχανικής συμπεριφοράς σε διάτμηση κυψελοειδών δομών αλουμινίου , Χρήστος Δόσης,Βατσάκης Γεώργιος,2021,pages: 28-34

http://hdl.handle.net/11615/57389

[30] LIMESS, Messtechnik & Software GmbH: RTSS - videoextensometer

https://www.limess.com/en/products/rtss-videoextensometer?gclid=CjwKCAjw5NqVBhAjEiwAeCa97X3vLGTD9er9v8Hg5Yp10VV45T507kKiq5Abuo6i9pnftxiMdqAOGRoCQ18QAvD_BwE

[32] Gabriel Bianchi & Guglielmo S. Aglietti & Guy Richardson: Static and Fatigue Behaviour of Hexagonal Honeycomb Cores under In-plane Shear Loads.

https://link.springer.com/article/10.1007/s10443-010-9184-5

[33] MATLAB code by Filippos Katsimalis.

Contact info: https://gr.linkedin.com/in/filippos-katsimalis

Chapter 7. APPENDIX

A significant effort has been made in to developing a MATLAB code [33] that can be used to read data (.dat files from MTS system) or texts (.txt files from RTSS camera) and instantly plot diagrams of Force [kN] – Displacement [mm] or Force [kN] – Axial Strain [%], depending on the type of the data file given. This code is developed for loading – unloading tests of one or more cycles and fatigue tests. Comments are self-explanatory:

```
clear
close all
clc

%% INPUT
filename=''; % name of file you want to plot (must contain the ".dat" or ".txt" format at the
end)
peak=; % peak value of loading in [kN]
cycles=; % number of cycles
fontsize=; % desired size of all text (11 is the default)
mult=; % desired multiplier of default figure width and height (larger means bigger figures)
dpi=; % dpi controls the image quality (larger means higher resolution and bigger size)

% length of window fot smoothing. small (large) values -> less (more) smoothing
% set "smooth_level=[]" for default length of window
smooth_level=1000;

% "prom" controls the sensitivity of finding maximum and minimum peaks in the data
% when greater smoothing is used, "prom" should be small (~.1)
% for noisy non-smoothed data, "prom" should be large (~1)
% usually, when an error occurs, changing this variable will fix the error
% also, change this variable if the number of peaks found is not correct
prom=.3;
%%

if contains(filename,'.dat')
    exp_data=import_exp_data_dat(filename);

    X=abs(exp_data(:,1)-exp_data(1,1));
    Y=abs(exp_data(:,2));

    x_label='Displacement [mm]';
    y_label='Force [kN]';

elseif contains(filename,'.txt')
    exp_data=import_exp_data_txt(filename);

    X=abs(exp_data(:,1));
    Y=abs(exp_data(:,2));

    % smooths data, control the degree of smoothing by defining the
    % "smooth_level" variable. Enter "doc smoothdata" for details.
    X=smoothdata(X,'gaussian',smooth_level);
    Y=smoothdata(Y,'gaussian',smooth_level);

    x_label='Axial Strain [\%]';
    y_label='Force [kN]';

else
    error('Make sure that the filename ends in ".dat" or ".txt"')
end
```

```
x=1:length(X);

l_max=islocalmax(Y,'MinProminence',prom);
i_max=find(l_max);

l_min=islocalmin(Y,'MinProminence',prom);
i_min=find(l_min);
i_min=[1;i_min;length(Y)];

ind=zeros(1,2*length(i_max)+1);
ind(2:2:end-1)=i_max;
ind(1:2:end)=i_min;

fig=figure;
hold on
m=0;
for k=1:length(ind)-1
    if logical(rem(k,2))
        color=[0 0.4470 0.7410];
        m=m+1;
        disp(['Coordinates of peak #',num2str(m),': x=',num2str(X(ind(k+1))),' [mm],
y=',num2str(Y(ind(k+1))),' [kN]']);
    else
        color=[0.8500 0.3250 0.0980];
    end

    plot(X(ind(k):ind(k+1)),Y(ind(k):ind(k+1)),'Color',color);

end

fig.Position=[50 50 560*mult 420*mult];

grid on
grid minor

xlabel(x_label,'Interpreter','latex','FontSize',fontsize);
ylabel(y_label,'Interpreter','latex','FontSize',fontsize);

%ylim([0 peak+.1]);

ax=gca;
ax.FontSize=fontsize;

legend('Loading','Unloading','Interpreter','latex','FontSize',fontsize,'location','northwest');

title(['Loading-Unloading @',num2str(peak*1000),'N peak force (',num2str(cycles),'
cycle(s))'],'Interpreter','latex','FontSize',fontsize);


%% Calculate the loop area and slope of loading curve
if contains(filename,'.dat') && cycles==1
    % --loop area--
    disp('Press any key to continue');
    pause
    corner_point=input('\n Enter corner point in [mm] \n'); % "corner_point" holds the
displacement value in [mm] where force starts to increase significantly,
    % it defines the left boundary of the polygon whose area is the work in [J]
    area_ind=X>=corner_point;
    area=polyarea(X(area_ind),Y(area_ind));
    fprintf(['\n The area of the loop is ',num2str(area),' Joule \n\n']);

    % --loading curve slope--
    % "end_point" holds the rightmost displacement value in [mm] used to calculate the
    % slope of the loading curve. The slope of the loading curve is
    % calculated as the slope of the best-fit line on data between
    % "corner_point" and "end_point" on the loading curve
    end_point=input('\n Enter end point in [mm] \n');

    load_ind=(corner_point<=X) & (X<=end_point);
    load_ind(ind(2)+1:end)=0;
```

```
    fit_data=fit(X(load_ind),Y(load_ind),'poly1');
    slope=atan(fit_data.p1);
    slope_d=atand(fit_data.p1);
    fprintf(['\n The slope of the loading curve is: ',num2str(slope),' [rad] =
',num2str(slope_d),' [deg] \n\n']);
end


%%

print(fig,extractBefore(filename,'.'),'-dpng',['-r',num2str(dpi)]);
print(fig,extractBefore(filename,'.'),'-dsvg');

% check that everything looks ok
plot(X(area_ind),Y(area_ind),'o');
plot(fit_data);
```

```
function exp_data=import_exp_data_dat(filename)
%% Setup the Import Options and import the data
opts = delimitedTextImportOptions("NumVariables", 2);

% Specify range and delimiter
opts.DataLines = [6, Inf];
opts.Delimiter = "\t";

% Specify column names and types
opts.VariableNames = ["AxialDisplacement", "AxialForce"];
opts.VariableTypes = ["double", "double"];

% Specify file level properties
opts.ImportErrorRule = "omitrow";
opts.MissingRule = "omitrow";
opts.ExtraColumnsRule = "ignore";
opts.EmptyLineRule = "read";

% Import the data
exp_data = readtable(filename, opts);

%% Convert to output type
exp_data = table2array(exp_data);

%% Clear temporary variables
clear opts
```

```
function exp_data=import_exp_data_txt(filename)
%% Setup the Import Options and import the data
opts = delimitedTextImportOptions("NumVariables", 18);

% Specify range and delimiter
opts.DataLines = [2, Inf];
opts.Delimiter = ",";

% Specify column names and types
opts.VariableNames = ["Var1", "Var2", "Var3", "Var4", "Var5", "Var6", "Var7", "PeakStrainin",
"Var9", "Var10", "Var11", "Var12", "Var13", "Var14", "ai0LoadInstron", "Var16", "Var17",
"Var18"];
opts.SelectedVariableNames = ["PeakStrainin", "ai0LoadInstron"];
opts.VariableTypes = ["string", "string", "string", "string", "string", "string", "string",
"double", "string", "string", "string", "string", "string", "string", "double", "string",
"string", "string"];

% Specify file level properties
opts.ImportErrorRule = "omitrow";
```

```
opts.MissingRule = "omitrow";
opts.ExtraColumnsRule = "ignore";
opts.EmptyLineRule = "read";

% Specify variable properties
opts = setvaropts(opts, ["Var1", "Var2", "Var3", "Var4", "Var5", "Var6", "Var7", "Var9", "Var10",
"Var11", "Var12", "Var13", "Var14", "Var16", "Var17", "Var18"], "WhitespaceRule", "preserve");
opts = setvaropts(opts, ["Var1", "Var2", "Var3", "Var4", "Var5", "Var6", "Var7", "Var9", "Var10",
"Var11", "Var12", "Var13", "Var14", "Var16", "Var17", "Var18"], "EmptyFieldRule", "auto");

% Import the data
exp_data = readtable(filename, opts);

%% Convert to output type
exp_data = table2array(exp_data);

%% Clear temporary variables
clear opts
```
